THE ROLE OF RYANODINE RECEPTORS IN A MOUSE MODEL OF ALZHEIMER DISEASE

BY

CHARLENE B. SUPNET

A Thesis
Submitted to the Graduate Faculty
in Partial Fulfillment of the Requirements
for the Degree of

DOCTOR OF PHILOSOPHY

Department of Biomedical Sciences
Faculty of Veterinary Medicine
University of Prince Edward Island

Your file Votre référence
ISBN: 978-0-494-64473-7
Our file Notre référence
ISBN: 978-0-494-64473-7

CONDITIONS FOR THE USE OF THE THESIS

The author has agreed that the Library, University of Prince Edward Island, may make this thesis freely available for inspection. Moreover, the author has agreed that permission for extensive copying of this thesis for scholarly purposes may be granted by the professor or professors who supervised the thesis work recorded herein or, in their absence, by the Chairman of the Department or the Dean of the Faculty in which the thesis work was done. It is understood that due recognition will be given to the author of this thesis and to the University of Prince Edward Island in any use of the material in this thesis. Copying or publication or any other use of the thesis for financial gain without approval by the University of Prince Edward Island and the author's written permission is prohibited.

Requests for permission to copy or to make any other use of material in this thesis in whole or in part should be addressed to:

Chair of the Department of Biomedical Sciences
Faculty of Veterinary Medicine

University of Prince Edward Island

Charlottetown, P.E.I.

Canada C1A 4P3

SIGNATURE PAGE

(iii) & (iv)

REMOVED

ABSTRACT

By the year 2020 approximately 1.5 million Canadians will suffer from a form of aging-related dementia, with the majority diagnosed with Alzheimer disease (AD). Current cost estimates suggest that by the year 2025 treatment for neurodegenerative disease will cost the Canadian health care system approximately 50 billion dollars per year. Thus, there is an urgent need for discovery of new therapeutic targets that will delay the onset or reduce the devastating consequences of AD.

The accumulation of amyloid-beta (Aβ) peptide and disruption of cytosolic calcium (Ca^{2+}) levels are pathological hallmarks of neuronal dysfunction in the AD brain. Studies outlined in this thesis focus on the ryanodine receptors (RyRs); how they regulate cytosolic Ca^{2+} levels and contribute to the dysfunction of AD neurons. RyR type 3 (RyR3) expression was up-regulated when exposed to Aβ fragment 1-42 (Aβ42) and in neurons from transgenic (Tg)CRND8 mice; a model of AD. Ca^{2+} imaging experiments demonstrated that RyR3 contributed to the increased cytosolic Ca^{2+} response of Tg to glutamate and ryanodine compared to neurons from nonTg littermates. However, Tg neurons were no more susceptible to AD-related stressors such as glutamate, hydrogen peroxide, staurosporine and *in vitro* aging. Instead, the suppression of RyR3 up-regulation in Tg neurons by short-interfering RNA sensitized Tg neurons to death after aging *in vitro* for 18 days. When TgCRND8 mice were crossed with RyR3 knock-out ($RyR3^{-/-}$) mice, they were sensitized to premature, spontaneous death possibly by severe seizure. TgCRND8/$RyR3^{-/-}$ showed increased susceptibility to more severe, pharmacologically-induced seizure compared to littermates. These data suggest a role for RyR3 in the maintenance of neuronal viability and suppression of hyperexcitability and death in TgCRND8 mice. Further research is required to detemine if RyR3 up-regulation is an optimal therapeutic target for the treatment of AD.

DEDICATION AND ACKNOWLEDGEMENTS

This work is dedicated to my late colleague and friend, Dr. Nick Shepel. I will never forget his enthusiastic support of my decision to pursue graduate studies and all paths less travelled. This thesis is a tribute to my memories of him.

I would first like to thank my supervisor, Dr. Michael Mayne, for his years of encouragement, unwaivering support and mentorship. I appreciate that he took a chance on me as a student, as I know that many others would not have. He recognized that there was a scientist in me even when I was unable to see it for myself. I have learned more than I had ever anticipated during my time in his lab and I will walk away from my spot on the bench knowing that anything is possible.

I would like to acknowledge my supervisory committee, Dr. Tarek Saleh (Chair), Dr. Kathy Gottschall-Pass, Dr. George Roberston and Dr. Jeff Zidichouski. Thank you for all of your encouragement and guidance throughout the graduate studies process, it has been a great pleasure to work with you. Thanks also to Dr. John Bradley for his support in Michael's absence and for his critical review of my thesis.

There have been many people involved at various stages of my thesis project and it would be impossible to acknowledge everyone here by name. I would like to thank all of the technical support staff of Michael's Winnipeg and Charlottetown labs for their expertise and contributions to my thesis work. Thanks to all past lab members and fellow graduate students for their technical help, scientific advice, good humor and moral support. I am so fortunate to have had the opportunity to work along-side so many amazing people.

Thank you to my family and friends in Winnipeg for all their love and support over the years. My pursuit of knowledge has taken me far from home but home has never been far from my mind. I inherited my work ethic from my parents and developed a thick skin to deal with Winnipeg winters, which inadvertently has been handy for dealing with reviewer's comments. In many ways my family and friends have contributed a great deal to my success and for that I am humbly grateful. A special thanks to Adam Scanlan for being my rock and my inspiration, you are a remarkable person.

Finally, I would like to thank the many funding agencies for my salary and travel support and for the operational costs of my work: the National Research Council of Canada, the Canadian Institutes for Health Research, the Alzheimer's Society of Canada, the Department of Biomedical Sciences, the Atlantic Veterinary College, the Manitoba Health Research Council and the Scottish Rite Charitable Foundation of Canada.

TABLE OF CONTENTS

LIST OF FIGURES AND TABLES

LIST OF ABBREVIATIONS

Aβ	amyloid-beta peptide
ACh	acetylcholine
AICD	APP intracellular domain
AD	Alzheimer disease
AHP	afterhyperpolarization
AMPAR	α-amino-3-hydroxy-5-methyl-4-isoxozolepropionic acid receptor
ANOVA	analysis of variance
APLP	amyloid precursor-like protien
APP	amyloid precursor protein
APOE4	apolipoprotein E ε4
ATP	adenine triphosphate
AUC	area under the curve
BACE	β-secretase-cleaved soluble amyloid precursor protein
BK	big or large conductance potassium channels
C83	carboxy-terminal fragment of APP consisting of 83 residues
C99	carboxy-terminal fragment of APP consisting of 99 residues
CA	cornu ammonis
Ca^{2+}	calcium
$[Ca^{2+}]_{cyto}$	cytosolic calcium concentration
cADPR	cyclic adenine diphosphate ribose
CaM	calmodulin
cAMP	cyclic AMP
CASQ	calsequestrin
CREB	cyclic AMP response element binding protein

$Ca_v1.1$	long-type voltage-gated calcium channels
CCD	central core disease
cdk5	cyclin-dependent kinase 5
CERAD	Consortium to Establish a Registry for Alzheimer Disease
ChEI	cholinesterase inhibitors
CICR	calcium-induced calcium release
CPK	creatine phosphokinase
CPVT	catecholaminergic polymorphic ventricular tachycardia
CT	computed tomography
DIV	days *in vitro*
DMSO	dimethyl sulfoxide
DHPR	dihydropyridine receptors
e16	embryonic day 16
ECC	excitation contraction coupling
ELISA	enzyme-linked immunosorbent assay
ER	endoplasmic reticulum
ERK	extracellular signal-regulated kinase
FAD	familial or early-onset Alzheimer disease
FBS	fetal bovine serum
FDA	United States Food and Drug Administration
FITC	fluorescein isothiocyanate
FKBP	FK-506 binding protein
FKBP12	12kDa FK-506 binding protein
GABA	γ-aminobutyric acid
GFAP	glial fibrillary acidic protein
GFP	green fluorescent protein

Glu	glutamate
GSK	glycogen synthase kinase
GSR	GeneSilencer siRNA transfection reagent
H_2O_2	hydrogen peroxide
hAPP	human amyloid precursor protein
HBSS	Hank's balanced salt solution
HF	heart failure
ICC	immunohistochemistry
i.p.	intraperitoneal
JNK	c-jun N-terminal kinase
JP	junctiphilin
I_{AHP}	afterhyperpolarization current
IP_3	inositol-1,4,5-triphosphate
IP_3R	inositol-1,4,5-triphosphate receptor
IP_3R1	inositol-1,4,5-triphosphate receptor, type1
I_{sAHP}	slow afterhyperpolarization currents
LTD	long-term depression
LTP	long-term potentiation
L-VGCC	long-type voltage-gated calcium channel
mAHP	medium afterhyperpolarizations
MAP-2	microtubule-associated protein-2
MAPK	mitogen-activated protein kinase
MCI	mild cognitive impairment
mEPSC	mini excitatory post-synaptic current
MH	malignant hyperthermia
mIPSC	mini inhibitory post-synaptic current

MmD	multiminicore disease
MRI	magnetic resonance imaging
mt	mitochondria
MTT	3-[4,5-dimethylthiazol-2-yl]-2,5-diphenyl tetrazolium bromide
NAD	nicotinamide adenine dinucleotide
NADPH	nicotinamide adenine dinucleotide phosphate
NeuN	neuron-specific nuclear protein
NFT	neurofibrillary tangles
NM	nemaline rod myopathy
NMDA	*N*-methyl-D-aspartate
NMDAR	*N*-methyl-D-aspartate receptor
NMS	neuroleptic malignant syndrome
nNOS	neuronal nitric oxide synthase
NP	neuritic plaques
Nrf2	NF-E2 p45-related factor 2
N-VGCC	neuronal-type voltage-gated calcium channel
PCR	polymerase chain reaction
PDAPP	platelet-derived growth factor β promoter driven APP expressing mice
PDGF	platelet-derived growth factor
PBS	phosphate buffered saline
PBST	phosphate buffered saline with 0.1% Tween 20
PET	positron-emission tomography
PHF	paired helical fragments
PI3K	phosphatidylinositol 3 kinase
PIP_2	phosphatidylinositol-4,5-bisphosphate
PKA	cyclic AMP-dependent protein kinase

PKC	protein kinase C
PLC	phospholipase C
PrP	prion promoter
PS1	presenilin, type 1
PS2	presenilin, type 2
PTZ	pentylenetertrazole
RFUs	relative fluorescence units
ROS	reactive oxygen species
Ry	ryanodine
RyR	ryanodine receptor
sAHP	slow afterhyperpolarizations
sAPPα	soluble APP, cleaved by α-secretase
sAPPβ	soluble APP, cleaved by β-secretase
SC	Schaffer collateral
siRNA	short-interfering ribonucleic acid
SK	small conductance potassium channels
SR	sarcoplasmic reticulum
STS	staurosporine
TBS	tris-buffered saline
TBST	tris-buffered saline with 0.1% Tween 20
Tg	transgenic
TGFβ1	transforming growth factor, β 1 isoform
TRPC	transient receptor potential channel
VDAC	voltage-dependent anion channel

1. GENERAL INTRODUCTION

1.1 ALZHEIMER DISEASE (AD)

Dementia is a syndrome resulting from a disorder that affects the brain and its function. Patients with dementia show significant impairment of intellectual functioning, memory failure, loss of emotional control and changes to personality or behaviour that interferes with performing the acts of daily living and negatively effects interpersonal relationships (The Merck manual of diagnosis and therapy. 2006). While increased age (greater than 65 years) is an important risk factor for developing dementia, it is different from age-related cognitive decline because symptoms are attributed to the loss of neuron or synapse function and significant neuron death (APA 1994). Dementia is chronic, progressive and in most cases irreversible. Researchers have identified four major types of dementia based on their clinical presentation, neuropathology and etiology: Alzheimer dementia; Parkinson type including Lewy Body disease; frontotemporal dementia; and vascular dementia. While each presentation is distinct, co-morbidities or mixed dementia is a frequent occurrence (APA 1994). In Canada, there are over 60,000 new cases of dementia every year and approximately 500,000 people are currently living with some form of dementia (The Alzheimer Society of Canada 1997-2009; The incidence of dementia in Canada. The Canadian Study of Health and Aging Working Group. 2000). Effective treatments for dementia are fervently pursued by researchers and clinicians but in spite of the considerable knowledge accumulated over the last 30 years, 95% of all dementias remain incurable (Khachaturian 2006). The prevalence of dementia is expected to rise exponentially as life expectancy increases and as the demographic shifts because of the aging baby-boomer population (Santacruz et al. 2001). For these reasons, it is predicted that treatment and management of dementia in North America and the developed world will require the majority of health care dollars and completely overwhelm resources that are currently available.

Alzheimer disease (AD) is the most common cause of dementia in people aged 65 years and older, accounting for 60-70% of all dementia in older adults (The Alzheimer Society of Canada 1997-2009). Patients with AD can live with the disease up to 20 years from the time of diagnosis (Patterson et al. 2001). Compounded by the fact that there is no available cure, a diagnosis of AD is devastating to both the patient and the affected families (Patterson & Gauthier 2001). Currently, there are approximately 5 million people in the United States (2008 Alzheimer's disease facts and figures 2008) and 320,000 people in Canada (The Alzheimer Society of Canada 1997-2009) diagnosed with AD. The costs associated with caring for those living with AD are great, especially in the later stages of the disease. The annual economic impact of caring for a patient living in a long-term care facility with mild or severe AD is approximately $10,000 and $37,000 respectively in Canada (Hux et al. 1998), with similar figures in the United States (2008 Alzheimer's disease facts and figures 2008). When health care expenses and lost wages of both patients and their caregivers are taken into account, AD costs approximately $80 to $100 billion per year in the United States alone (2008 Alzheimer's disease facts and figures 2008). The cost of the additional stress for spouses or family members that take on the burden of care giving is incalculable. Consequently, the discovery and development of effective AD therapeutics is imperative.

1.1.1 Clinical description

The course of AD is gradual in onset with a progressive cognitive decline. The initial clinical hallmark of AD is episodic memory impairment that is detected by the patient, spouse or close relative. Patients experience difficulty recalling newly acquired information while the memory of remote events remain unimpaired (Greene et al. 1996; Pillon et al. 1993). Other cognitive functions such as language, praxis and recognition skills can also be affected in the early stages of AD. These slight deficits are known as

mild cognitive impairment (MCI) which is considered an indicator of possible AD (Petersen et al. 1999). Motor and sensory disturbances, gait abnormalities and seizures are not apparent until later in the disease (APA 1994). Functional and behavioural changes are characteristic of AD. Patients progress from the loss of complex activities of daily living, for example they stop using public transportation, to the loss of basic activities of daily living, such as eating and grooming. It is common for mood change, especially depression and apathy, to develop early on and continue along the course of the disease. Psychosis, behaviour disorders and agitation are common in the middle and later phases (Reisberg et al. 1982).

For practical and research purposes, AD cases are grouped into categories depending on the age of onset and the heritability of the disease. The most common is known as sporadic (non-inherited), late-onset AD, where the age of onset is 65 years or greater. Early-onset AD, where dementia is evident before the age of 65, is very rare, accounting for 5-10% of all AD cases. Genetically inherited or familial forms of AD (FAD) account for approximately 50% of all early-onset AD cases (Cruts et al. 1998; Rademakers et al. 2003). Mutations in genes coding for 3 different proteins unequivocally cause FAD in an autosomal-dominant fashion. Missense mutations in the amyloid precursor protein gene (APP) on chromosome 21q21.3 (Goate et al. 1991) and the presenilin-1 gene (PS1) on chromosome 14q24.3 (Sherrington et al. 1995) and the presenilin-2 gene (PS2) on chromosome 1q31–42 (Levy-Lahad et al. 1995; Rogaev et al. 1995) all result in a shift in the kind of amyloid-beta (Aβ) protein fragments produced in the brain such that the Aβ42/40 ratio is increased (Scheuner et al. 1996). This leads to the aggregation and formation of toxic Aβ42 oligomers that induce the loss of synapses and neuronal death in AD (Hardy et al. 2002). Because genetically-linked early-onset AD is pathologically identical to sporadic AD, it is thought that Aβ42 over-production is the

causative factor, called the "amyloid cascade hypothesis" of AD. The cascade of events that ultimately results in the formation of the characteristic neuritic plaques (NPs) and neurofibrillary tangles (NFTs) is still unclear.

There are no identified genotypes associated with the other forms of AD in the same autosomal-dominant manner as in early-onset familial AD. The only other genetic factor that consistently influences risk or onset age is the apolipoprotein E ε4 allele (ApoE4) located on chromosome 19 (Mahley 1988). ApoE4 increases the likelihood of an individual to develop late-onset AD, with the risk increasing as the number of copies an individual carries increases (Saunders et al. 1993). The ApoE4 allele also reduces the age of late-onset AD, but not early-onset, by about a decade (Corder et al. 1993; Van Broeckhoven et al. 1994). In families with APP or PS2 mutations, those carrying the ApoE4 allele develop the disease at a much younger age (van Duijn et al. 1994).

AD is considered one of the leading causes of death in the industrialized world. As of 2004, AD was the 7th leading cause of death in Canada (Statistics Canada) and the United States (Lopez et al. 2006). The primary cause of death of AD patients is intercurrent illness, such as pneumonia. In the later stages of AD, patients become severely disabled, bed-ridden and malnourished because of increased difficulty in swallowing. Difficulty swallowing, in particular, is a risk factor for aspiration pneumonia, a lower respiratory tract infection that results from inhalation of stomach contents or secretions of the oropharynx (2008 Alzheimer's disease facts and figures 2008).

1.1.2 Diagnosis

To distinguish dementia as a condition that was unlike normal aging, Alois Alzheimer, a German psychiatrist and neuropathologist, recognized the need to combine

meticulous clinical observations with the systematic neuropathological analysis of brain lesions and first characterized AD in 1906. Quantitative and objective clinical measures were first outlined in 1968 by Blessed, Tomlin and Roth in the Dementia Scale (Information-Memory-Concentration Test) (Blessed et al. 1968), a scale of memory function, orientation, information, concentration and activities of daily living. Today, dementia is commonly recognized with the use of the criteria of the Diagnostic and Statistical Manual of Mental Disorders, fourth edition (DSM-IV) (APA 1994) which is defined as a combination of cognitive deficits manifested by memory impairment and at least one of aphasia (inability to produce and/or comprehend language), apraxia (inability to execute or carry out purposeful movements), agnosia (inability to recognize objects, people, sounds shapes or smell despite having functioning senses and in the absence of significant memory impairment) or disturbance of executive functioning.

The initial diagnosis of AD remains a clinical one and is often based on the criteria developed by the National Institute of Neurologic and Communicative Disorders and Stroke-Alzheimer's Disease and Related Disorders Association (NINCDS-ADRDA) (McKhann et al. 1984). The diagnosis is classified as definite, probable or possible AD, after history assessment, a battery of cognitive tests (starting with Mini-Mental Status Examination as a baseline) and physical work-up to rule out other causes of dementia, such as infection or brain tissue damage (Knopman et al. 2001). A definitive diagnosis of AD requires histological confirmation at autopsy. There are no laboratory tests or diagnostic markers to confirm AD.

Cerebrocortical atrophy is characteristic of AD and involves the cortical association region, particularly the medial aspect of the temporal lobe. Neuroimaging is used to predict the probability of AD and is particularly useful in excluding other causes of dementia. It is recommended that patients undergo structural imaging of the brain with computed tomography (CT) or magnetic resonance imaging (MRI) at least once

throughout the course of their dementia (de Leon et al. 2007). For example, patients can undergo structural MRI to detect the extensive neurodegeneration that occurs in AD as it allows for an accurate measurement of the 3-dimensional volumes of the brain. Of particular interest are the hippocampi, which undergo significant atrophy, and the ventricles, which become enlarged (de Leon et al. 2007). Functional imaging with positron-emission tomography (PET) or single-photon-emission CT can be helpful in the differential diagnosis of dementia-associated disorders (Silverman et al. 2001). Recently, imaging of amyloid deposits in brains of live patients using radioactive ligands (the Pittsburg compound B (Klunk et al. 2004)) visualized on PET scan has been demonstrated (Ikonomovic et al. 2008) and is in the experimental stages for use as a preclinical diagnostic marker of AD.

Laboratory tests are routine but do not serve to directly diagnose AD per se, but rather to rule out other causes of dementia and coexisting conditions that are common in elderly patients. In addition to routine blood work, patients undergo thyroid function tests and measurement of serum vitamin B_{12} levels to identify specific alternative causes of dementia (Knopman et al. 2001). If patient history requires, specialized tests like screening for heavy metals are ordered.

It is interesting to note that the rate of recognition of dementia by family members or physicians is very low. The "failure to recognize" rates are reportedly 97% for mild dementia and 50% for moderate dementia (Santacruz & Swagerty 2001), which constitutes a significant barrier to appropriate care for many patients with AD. Consequently, researchers and physicians are constantly looking to improve the clinical diagnosis of early dementia and AD by revising current methods of evaluation and determining clinical biomarkers.

1.1.3 Histopathological confirmation

In addition to the characteristic brain atrophy, the universally accepted pathological hallmarks of AD are NPs or senile plaques and NFTs that are microscopically identified at autopsy. Neuritic plaques are abnormal collections of degenerate nerve processes and reactive glia (astrocytes and microglia) surrounding a central core of extracellular aggregates of amyloid protein. Neurofibrillary tangles are abnormal bundles of filaments made up of hyperphosphorylated tau protein that form insoluble aggregates, or paired helical filaments (PHF), within neurons (Braak et al. 1991). The presence of NPs and NFTs is not diagnostic of AD, as NPs appear in normal aging and NFTs are found in other neurodegenerative disorders, such as progressive supranuclear palsy (Williams et al. 2009). Rather, the number and topographical distribution of NPs and NFTs in the neocortex is characteristic of AD, as determined by the Consortium to Establish a Registry for Alzheimer's Disease (CERAD), the most commonly used diagnostic criteria for AD (Mirra et al. 1991).

Other lesions have been recognized since Alzheimer's original papers were published. These include: granulovacuolar degeneration in the hippocampus (degeneration of cells characterized by basophilic granules surrounded by a clear zone in hippocampal neurons) (Ball 1978); threads of dystrophic neurites diffusely distributed around the cortical neuropil, the unmyelinated neuronal processes of the gray matter (Braak & Braak 1991); and neuronal loss and synaptic degeneration, which are thought to ultimately mediate the cognitive and behavioural manifestations of the disorder.

1.1.4 Current treatments

Because the cause of AD is still unknown, there is no cure. The therapies currently available treat the symptoms of the disease and do nothing to reverse or prevent disease progression. All United States Food and Drug Administration (FDA) and

Health Canada approved drugs for the treatment of AD modulate neurotransmitters - either acetylcholine (ACh) or glutamate (Glu). While Phase III trials for several potential disease-modifying therapies have been completed, none have been shown to be consistently efficacious. Given the multi-factorial nature of AD, in the future, such disease-modifying treatments may be combined with symptomatic therapies to effectively manage the disease.

The standard treatment for AD includes cholinesterase inhibitors (ChEIs) and partial *N*-methyl-D-aspartate (NMDA) receptor antagonists for moderate to severe AD. Psychotropic medications are often used to treat secondary symptoms of AD such as depression, agitation, and sleep disorders. These include antidepressants, anti-epileptic drugs (such as valproic acid) and neuroleptics to modify behaviour (2008 Alzheimer's disease facts and figures 2008). Several studies have examined the efficacy of psychotropic drugs; most have demonstrated no or limited efficacy (Ballard et al. 2008).

1.1.4.1 Acetycholine esterase inhibitors

Normally, presynaptic terminals release ACh into the synaptic cleft to bind to receptors on postsynaptic neurons and affect their function. ACh is degraded by cholinesterases in the synaptic cleft to terminate neurotransmission and avoid overstimulation of postsynaptic cells. The cholinergic systems that modulate the processing of information in the hippocampus and the neocortex are impaired in the early stages of AD, possibly by the decrease in ACh production. The basis for use of centrally acting ChEIs is to compensate for the depletion of ACh in the cerebral cortex and hippocampus. Donepezil (Aricept), rivastigmine (Exelon) and galantamine

(Razadyne, formerly Reminyl) are the three ChEIs approved by Health Canada for treatment of mild to moderate AD (The Alzheimer Society of Canada 1997-2009). Tacrine (Cognex) is approved for use in the United States but is no longer in use due to the potential for liver toxicity (Watkins et al. 1994). All these drugs inhibit acetylcholinesterase. Tacrine and rivastigmine also inhibit butyrylcholinesterase (Poirier 2002). Galantamine does not inhibit butyrylcholinesterase but does modulate presynpatic nicotinic receptors (Lilienfeld et al. 2000). There is no evidence that either of these secondary actions have an effect on efficacy.

All ChEIs have shown modest benefit compared with placebo on measures of cognitive function and activities of daily living (Lanctot et al. 2003), delaying clinical decline for up to 2 years (Courtney et al. 2004). Following 6 to 12 month treatment with donepezil, subjects showed a slower rate of hippocampal atrophy observed on MRI, suggesting that ChEIs have neuroprotective properties (Hashimoto et al. 2005; Krishnan et al. 2003). Although the ChEIs were originally expected to be efficacious in only the early and intermediate stages of AD because the cholinergic deficit becomes more severe later in disease due to the greater loss of cholinergic neurons, they are also helpful in advanced disease. Furthermore, ChEIs are helpful in patients with AD with co-morbidities and in patients with dementia with Lewy bodies (Giacobini 2004). However, the benefits of ChEIs are ultimately temporary as there are no data to suggest that they can prevent the progressive neurodegeneration in AD.

1.1.4.2 NMDA receptor antagonists

Glutamate is the predominant excitatory neurotransmitter in the central nervous system. The newest drugs indicated for the treatment of AD target cells that utilize a

particular class of Glu receptors, the NMDA receptors (NMDARs). The NMDARs are thought to be over-activated in a tonic manner in AD, leading to neuronal damage and/or death (Lipton 2007). As of July 2008, the only FDA approved drug in this class was memantine (Namenda, Axura); *a non-competitive, low-affinity, open-channel* NMDA receptor antagonist. Memantine (Ebixa) is conditionally approved by Health Canada for the treatment of patients with moderate to severe AD (The Alzheimer Society of Canada 1997-2009). This drug may be used alone or combined with ChEIs. Combination therapy over 6 months with memantine and donepezil significantly improved cognition, activities of daily living, and behaviour compared with placebo in patients with moderate to severe AD (Feldman et al. 2006; Schmitt et al. 2006; Tariot et al. 2004), but not patients with mild to moderate AD (Porsteinsson et al. 2008). Like ChEIs, the efficacy of memantine wanes over time (Walker et al. 2005).

1.1.4.3 Drugs in development

Disease-modifying therapies are the focus of modern drug development for AD. Different classes of potentially disease-modifying treatments that are designed to interrupt the early pathological events, namely Aβ42 generation and aggregation, and prevent downstream events, such as NP and NFT formation, are in Phase II or III clinical studies. These include immunotherapies that target Aβ, secretase inhibitors to block Aβ production, selective Aβ42-lowering agents, statins to enhance α-secretase activity and anti-Aβ aggregation agents (a full list of current trials at http://clinicaltrials.gov) (Clinical trials). In spite of strong experimental data from mouse models to suggest the efficacy of these therapies, most trials in the past have failed in the clinic. The first clinical trials employing active immunity against aggregated Aβ42, AN1792, was halted because 6% of patients developed aseptic meningoencephalitis, or inflammation of the brain and

meninges (Gelinas et al. 2004). Active and passive immunotherapy continues to be researched because the patients that mounted an antibody response to AN1792 showed small measures of improvement in cognitive function. However, a recently completed trial that used amyloid-binding monoclonal antibodies (Bapineuzumab) again showed limited benefit compared to placebo (Kokjohn et al. 2009). Other drugs such as the amyloid-binding compound tramiprosate (Alzhemed) (Aisen et al. 2007) and the γ-secretase inhibitor tarenflurbil (Flurizan) also failed to impact the clinical outcome of AD patients (Williams 2009). These results, along with other failed clinical trials of different classes of Aβ-targeting drugs, suggest that reduction of Aβ alone might be insufficient to modify AD outcomes and further highlights the complex, multi-factored disease aetiology.

1.1.5 Studying AD

A better understanding of disease mechanisms is required for the development of more effective AD therapies. To study AD progression and pathology, transgenic mice were generated expressing the APP and PS mutations responsible for early-onset FAD. Over the last decade, mouse models of AD have contributed greatly to the current knowledge because they have allowed investigators to test specific questions about the development of pathology and to evaluate potential therapeutics.

All mutations responsible for FAD affect the proteolysis of APP, a type 1 transmembrane glycoprotein with unknown function, as APP-deficient mice do not have any obvious phenotype (Zheng et al. 1996). Several APP isoforms exist as a result of differential splicing, APP_{695} is the main species present in neurons (Golde et al. 1990) and APP_{751} or APP_{770} are expressed predominantly in glia and peripheral tissue (Arai et al. 1991). Studies have revealed that APP could function as a scaffolding protein in

vesicle transport (Kamal et al. 2001) and signal transduction (Cao et al. 2001; Mbebi et al. 2002; Okamoto et al. 1996). APP is subject to endoproteolytic cleavages, initially by α-secretase, a membrane-associated metalloproteinase, or by β-secretase. Because α-secretase cleaves APP within the Aβ domain, it prevents the formation of Aβ and instead results in the release of the soluble amino (N)-terminal portion of APP (sAPPα) and a carboxy (C)-terminal fragment consisting of 83 residues (C83) (**Figure 1.1**). The proteolysis of C83 by γ-secretase generates the P3 peptide, which can be found deposited in diffuse plaques (Tekirian et al. 1998). β-secretase, also known as β-site APP cleaving enzyme (BACE), cleaves APP at the amino-terminal of the Aβ domain (Vassar et al. 1999) to generate soluble APP (sAPPβ) and the amyloidogenic carboxy-terminal fragment C99. The proteolysis of C99 by γ-secretase at the ε-site within the transmembrane domain generates the APP intracellular domain (AICD) and the Aβ-containing fragment, which is subject to cleavage by γ-secretase after residue 40 or 42 (Borchelt et al. 1996).

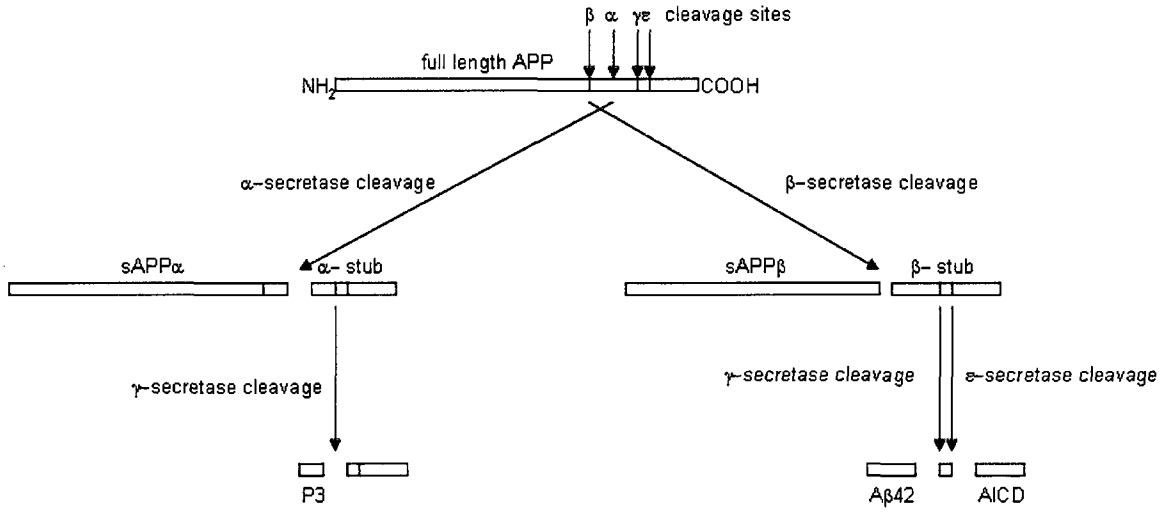

Figure 1.1 The proteolysis of the amyloid precursor protein. Illustration of APP metabolism by secretases. β-, α-, γ- and ε-secretase cleavage sites are indicated on the APP. The non-amyloidogenic pathway is initiated by α-secretase cleavage and the generation of sAPPα and α-stub fragments. Further processing of the α-stub generates the P3 peptide. The amyloidogenic pathway is initiated by β-secretase cleavage and the

generation of sAPPβ and β-stub fragments. Processing of β-stub by γ- and/or ε-secretase generates the APP intracellular domain (AICD) and Aβ42. Adapted from LaFerla 2002.

While Aβ40 and Aβ42 are generated under normal circumstances, APP and PS mutations result in the overproduction of the Aβ42 fragment, which is considerably more hydrophobic and prone to aggregation than Aβ40 (Seilheimer et al. 1997). For example, the APP-KM670/671NL, or Swedish mutation, is located close to the β-secretase cleavage site on APP, favouring BACE cleavage and the Aβ generating pathway (Haass et al. 1995). PS are the catalytic component of γ-secretase (Steiner 2008), which is a complex of four different proteins; PS1 and PS2, nicastrin, Aph-1 and Pen-2 (De Strooper 2003). PS1 and PS2 are integral membrane proteins that reside in the ER and undergo endoproteolytic cleavage prior to association into the γ-secretase complex, which eventually translocates to the plasma membrane (Hardy 2006). All four protein components of the complex are essential for full aspartyl proteolytic activity of γ-secretase (De Strooper 2003), whose substrates include APP, amyloid precursor-like proteins (APLP)1/2, Notch, ErbB4 and e-cadherin (De Strooper et al. 1999; De Strooper et al. 1998; Marambaud et al. 2002; Ni et al. 2001).

Mutations in PS, such as PS1-M146V and PS2-N141I, enhance γ-secretase activity at the Aβ42 site, thereby increasing the amount of Aβ42 generated (Citron et al. 1997; Scheuner et al. 1996). The accumulation of Aβ42 or its reduced clearance from the brain results in the formation of amyloid plaques and soluble amyloid, initiating neuronal dysfunction, inflammatory responses, tau hyperphosphorylation, neurofibrillary tangle formation, neuronal death, neurotransmitter deficits, loss of gray matter, dementia, and ultimately death (Cummings 2004; Hardy & Selkoe 2002).

1.1.5.1 Mouse models of AD

An animal model of disease attempts to recapitulate the pathological and behavioural characteristics of the human condition. Human APP, PS1 and PS2 mutations have been used to generate transgenic mouse models of AD. Ideally, the mouse model of AD should develop NPs, NFTs, show neuronal loss and behavioural deficits relating to memory and cognitive function. The first models developed were based on APP mutations. Games and colleagues developed the mouse model PDAPP that over-expressed a mini-gene construct encoding APP V717F, the Indiana mutation, under the control of platelet-derived growth factor (PDGF) β promoter (Games et al. 1995a). PDAPP mice display Aβ plaques, dystrophic neurites, gliosis, loss of synapses (Masliah et al. 1996) and hippocampal atrophy by 8 months of age (Dodart et al. 2000). PDAPP mice also have impaired reference and working memory and object recognition (Chen et al. 2000). The transgenic (Tg)2576 mouse model (Hsiao et al. 1996) is one of the most widely used models to study amyloid deposition and expresses the Swedish APP double mutation (K670N/M671L) under the hamster prion (PrP) promoter, maintained on a hybrid C57BL/6 X SJL background. Tg2576 mice display similar characteristics to PDAPP mice at 9 to 11 months of age with a more pronounced inflammatory and oxidative stress component (Lim et al. 2000; Smith et al. 1998), demonstrate synaptic impairment (Spires et al. 2005) and they have significant impairment of spatial reference and working memory (Hsiao et al. 1996; Westerman et al. 2002). There is little evidence that mutant APP mice develop extensive neuronal loss or show NFT formation, so these models do not give the complete AD phenotype.

PS1 mutant mice allowed for the first demonstration that mutant PS1 increases Aβ production *in vivo* (Duff et al. 1996). Despite increased Aβ production, PS1 mutant mice did not show amyloid pathology (Citron et al. 1997), nor did they display detectable

deficits in spatial reference memory tests (Holcomb et al. 1999; Janus et al. 2000a). When PS1-M146L and Tg2567 mice were crossed, the resulting bigenic TgAPP/PS1 mice showed accelerated amyloid deposition compared to their Tg2567 littermates, with deposits evident in the hippocampus and cerebral cortex at 6 to 16 weeks of age (Holcomb et al. 1998). TgAPP/PS1 mice showed significant impairment in the Y-maze alternation test for hippocampal memory function but they did not display significant differences in spatial reference memory compared to littermates (Holcomb et al. 1998). When TgAPP/PS1 were generated on a different background strain (C57BL/6 X SJL X DBA/2), they showed significant spatial reference and working memory deficits (Arendash et al. 2001; Sadowski et al. 2004). Again, these mice lack the NFT formation and neurodegeneration characteristics of AD, but provide information about the complexity of PS and APP interaction in the earlier stages of the disease.

The recently generated triple Tg mouse model of AD, 3XTg-AD, contains the APP-K670N/M671L, PS1-M146V and a mutation of the microtubule-associated tau protein, tau-P301L, that causes frontotemporal degeneration in humans (Clark et al. 1998; Oddo et al. 2003b). These mice develop amyloid plaques by 3 months and NFTs by 12 months, with a regional and temporal pattern that is comparable to human AD pathology (Oddo et al. 2003b). They do not display an age-related increase in reactive astrocytes but do show increased microglial infiltration of the hippocampal formation (Mastrangelo et al. 2008). 3XTg-AD mice also display deficits in long-term retention, working memory and contextual learning (Oddo et al. 2006) but there is no report of neuron loss in this model.

Models of AD are invaluable tools that have provided much insight to the interactions of AD-related genes, their role in the fundamental biochemical processes leading to disease and how they affect disease pathology. What is clear is that Aβ accumulation, and its relation to other pathological markers of AD, is very complex. As

such, no current AD mouse model completely duplicates all of the pathological and behavioral characteristics of the disease. This is very important to consider, especially when using models and their behavior as output to evaluate therapeutics that would be efficacious in humans.

1.1.5.2 Hypotheses of AD aetiology

Since the first documented case of AD over 100 years ago researchers have sought to determine the cause. Clinical and animal studies have revealed a multi-factorial disorder, so the origin of AD, particularly late-onset, is expected to be equally multifaceted. Nonetheless, there are many hypotheses regarding the pathogenic sequence of events leading to AD. Some are centered on Aβ plaques and NFTs, cytoskeletal defects, increased oxidative stress levels, disturbances in Ca^{2+} homeostasis and pathogens. The most prominent is the amyloid cascade hypothesis of AD, where Aβ accumulation is essential for the development of the disease.

1.1.5.2.1 The amyloid hypothesis

The most prevalent theory regarding the manifestation of AD is the "amyloid cascade hypothesis", penned by Higgins in 1992 (Hardy et al. 1992), which states that accumulation of Aβ, resulting from overproduction, altered processing or lack of clearance, is the initiating molecular event that ultimately leads to neurodegeneration in both sporadic and familial AD (Hardy & Selkoe 2002). Several lines of evidence have lead to the genesis of this hypothesis. The first was the identification and sequencing of the Aβ peptide (Glenner et al. 1984) found in the neuritic plaques of brain tissue from AD patients (Masters et al. 1985). APP mutations linked to AD lead to preferential cleavage by β– and γ-secretases and the generation of Aβ (Citron et al. 1992) (**Figure 1.1**).

Mutations in APP located within the Aβ-containing domain lead to the production of the more fibrillar, self-aggregating Aβ42 fragment (Wisniewski et al. 1991). Finally, AD mutations in PS1 and PS2 proteins enhanced the Aβ42/40 ratio by altering γ-secretase activity (De Strooper et al. 1998; Scheuner et al. 1996; Wolfe et al. 1999). The "amyloid cascade hypothesis" (**Figure 1.2**) has been a fundamental principle for much AD research over the last 25 years and is the basis for the design of many new potential therapeutics.

Since its conception, much work has supported the hypothesis. Accumulating data supports an initiating role for Aβ, not NFTs, in AD pathology. Missense mutations in the 5' splice site of the human tau protein lead to frontotemporal dementia and parkinsonism (Clark et al. 1998; Hutton et al. 1998). There are no mutations in human

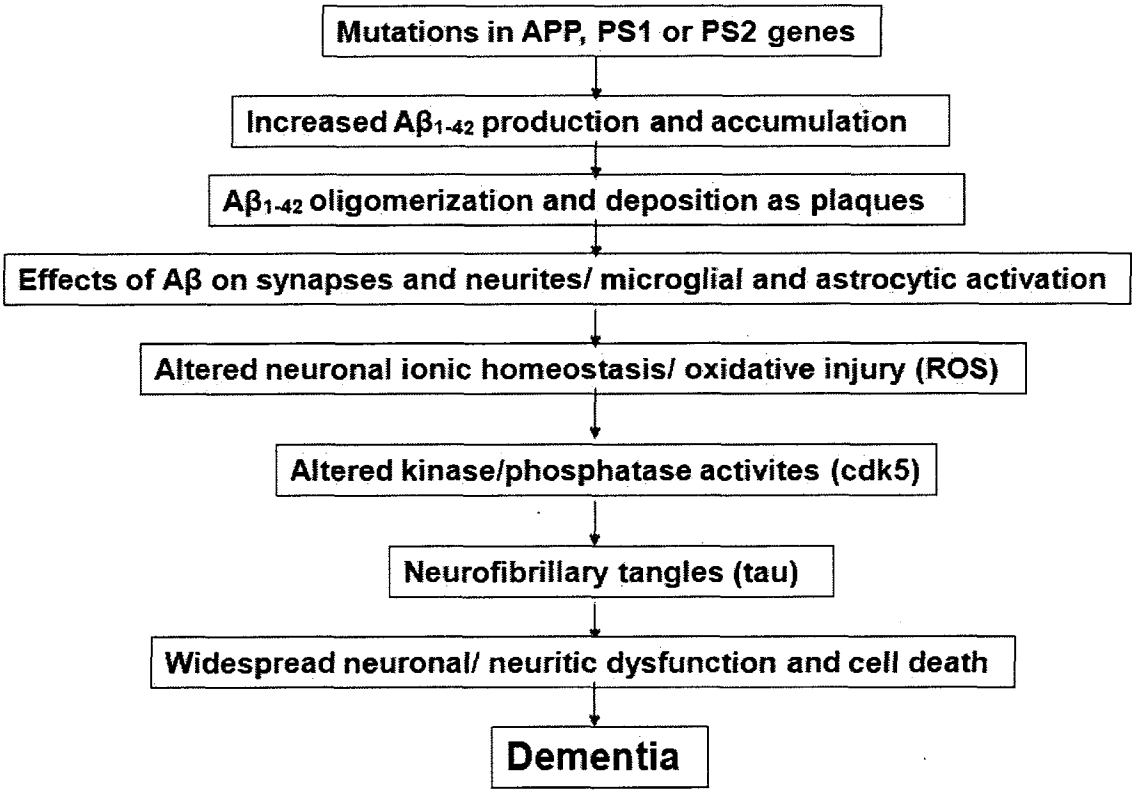

Figure 1.2 The amyloid cascade hypothesis. The proposed sequence of events leading to AD pathology. Reactive oxygen species (ROS) and cyclin-dependent kinase 5 (cdk5) (Haass et al. 2007).

stau that lead to classical AD. Lewis and colleagues, crossed Tg2576 mice with mutant tau-P301L mice and demonstrated that these bigenic mice had increased NFT pathology compared to mice with mutant tau alone (Lewis et al. 2001). Injection of synthetic Aβ42 into cortex and hippocampus of tau-P301L mice, but not wild-type tau, resulted in fivefold increase in NFT numbers in the amygdala, which receives projections from both injected sites (Gotz et al. 2001). Oddo and colleagues demonstrated that Aβ deposition preceded NFT formation in the 3XTg-AD model, in spite of similar levels of over-expression of the mutant APP and mutant tau genes (Oddo et al. 2003a). Blocking Aβ42 accumulation delayed tau pathology (Oddo et al. 2008) and increasing tau levels and hyperphosphorylation of tau by genetic modifications did not affect the onset or progression of Aβ pathology (Oddo et al. 2007).

There are concerns with the hypothesis and how Aβ ultimately leads to dementia and neurodegeneration in AD. For example, the number of Aβ-containing senile plaques in the brains of patients does not correlate well with the extent of impairment (Nagy et al. 1995). While neurons proximal to plaques have dystrophic neurites (Irizarry et al. 1997), decreased number of dendrites (Spires et al. 2005) and synaptic degeneration (Buttini et al. 2005), there is limited evidence to support that Aβ plaques are associated with cognitive impairment and widespread neuronal death in transgenic mouse lines. Tg2567 mice show no correlation between the extent of memory impairment and the levels of insoluble fibrillar Aβ, with memory deficits evident even before extensive plaque formation (Westerman et al. 2002). Finally, the accumulation of Aβ is not strongly associated with neuronal loss in AD models. Numerous studies show that the brains of mutant APP and TgAPP/PS1 mice consistently have minimal neuronal loss, even with a significant amyloid burden (Holcomb et al. 1998; Hsiao et al. 1996).

Studies have shown that Aβ exists in different assemblies; monomers, oligomers and mature fibrils that deposit in the extracellular space in senile plaques (Lambert et al. 1998; Walsh et al. 1999). Because Aβ immunization studies in transgenic mice showed that reductions in soluble oligomers of Aβ, with no reduction in amyloid pathology, could improve cognitive performance (Dodart et al. 2002; Janus et al. 2000b), it was hypothesized that the oligomer species, and not the fibrillar deposits, contributed to cognitive impairment. It was demonstrated that Aβ oligomers decreased long-term potentiation (LTP) (Walsh et al. 2002) and induced memory deficits in rats after injection into the brain (Cleary et al. 2005). Recently, it was identified that a 56-kDa species of Aβ (Aβ*56) which forms soluble oligomers in brains of 6-month-old Tg2567 mice strongly correlated with impairments in spatial memory (Lesne et al. 2006). Interestingly, the active and passive immunization of 3XTg-AD mice to reduce soluble Aβ42, and subsequently soluble tau levels, restored working memory and improved retention in 23-month-old mice with unaltered plaque and tangle pathology (Oddo et al. 2006). It has been shown that soluble Aβ dimers isolated from the cerebral cortex of AD patients caused long-term potentiation (LTP), enhanced long-term depression (LTD) and reduced dendritic spine density in normal rodent hippocampus (Shankar et al. 2008). The soluble species of Aβ may be responsible for the cognitive impairment observed in AD patients and would be a plausible mechanism to address the lack of correlation between severity of dementia and plaque load.

1.1.5.2.2 The calcium hypothesis

Calcium (Ca^{2+}) signalling is utilized by neurons to control a plethora of cellular functions, including membrane excitability, neurotransmitter release, gene expression, cellular growth, differentiation, free radical species formation and death (Berridge 1998;

Berridge et al. 1998). Because of the ubiquitous nature of Ca^{2+} in second-messenger signalling, neurons have strict mechanisms to maintain low concentrations of cytosolic Ca^{2+} ($[Ca^{2+}]_{cyto}$) when neurons are at rest or have minimal activity. Calcium-ATPases on the plasma membrane and on the endoplasmic reticulum (ER) are responsible for Ca^{2+} extrusion into the extracellular space and into ER stores, respectively. At rest, $[Ca^{2+}]_{cyto}$ range between 50-300 nM. Upon electrical or chemical activation, Ca^{2+} flux into the cytosol can occur through channels on the plasma membrane that are voltage-gated, ligand-gated (eg. NMDARs) or store-operated (eg. transient receptor potential channels, TRPC). Calcium can also be released from intracellular stores into the cytosol through ligand-gated channels on the ER, the inositol-1,4,5-trisphosphate receptors (IP_3Rs) or the ryanodine receptors (RyRs) (Mattson et al. 2000). When neurons are activated, $[Ca^{2+}]_{cyto}$ can be elevated to 100-500 μM (Verkhratsky et al. 1998) and can trigger buffering of Ca^{2+} by the mitochondria (mt) (Duchen 2000; Hajnoczky et al. 2002) (see **Figure 1.3**).

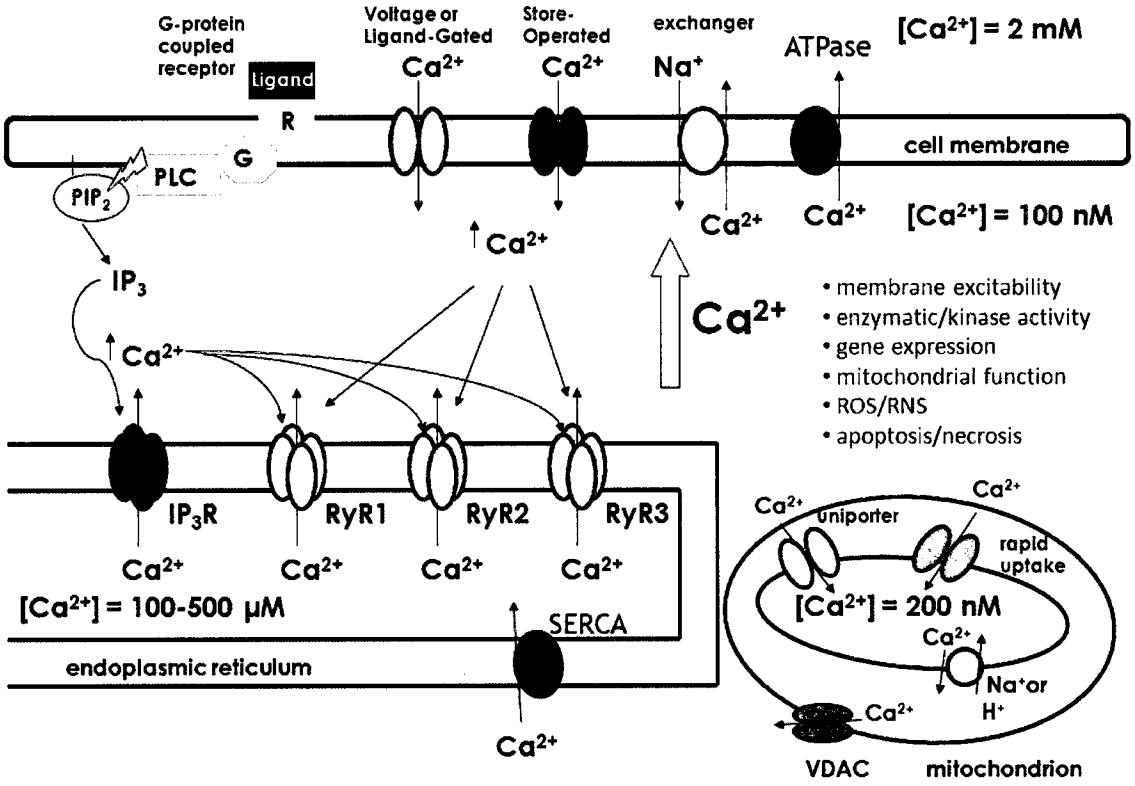

Figure 1.3. Ca^{2+} signalling in neurons. At rest, large Ca^{2+} gradients across the plasma membrane and the ER membrane are maintained by ATPase pumps. Upon neuronal activation, Ca^{2+} moves along its electrochemical gradient into the cytosol to increase $[Ca^{2+}]_{cyto}$ through channels on the plasma membrane or on the ER membrane. Local Ca^{2+} flux signals mitochontria (mt) to take up and release (or buffer) Ca^{2+}, through Ca^{2+} uptake channels on the inner mt membrane and Ca^{2+} release through the voltage-dependent anion channel (VDAC) on the outer mt membrane. Release of Ca^{2+} from ER IP_3R stores requires the activation of G-protein (G)-coupled receptor kinases (R) on the cell membrane that induce phospholipase C (PLC) to cleave phosphatidylinositol-4,5-bisphosphate (PIP_2) to diacylglycerol and inositol-1,4,5-triphosphate (IP_3). Ca^{2+} is also released from the ER through RyRs by C Ca^{2+} -induced Ca^{2+}-release (CICR). Increases in $[Ca^{2+}]_{cyto}$ can activate many cell signalling cascades that affect cellular health, some aspects are listed above. Refilling of ER Ca^{2+} stores is mediated by the sarco/endoplasmic reticulum Ca^{2+} ATPase (SERCA). Adapted from LaFerla 2002.

As neurons age, their ability to maintain tight regulation of Ca^{2+} gradients across membranes becomes compromised, likely due to inefficient energy metabolism and accumulating oxidative stress. Old neurons display Ca^{2+} dysregulation compared to young neurons, or changes in Ca^{2+} regulation that lead to sustained increases in $[Ca^{2+}]_{cyto}$, an observation that inspired the hypothesis that such changes in Ca^{2+}

signalling could contribute to brain aging, neuronal dysfunction and degeneration (Khachaturian 1987; Landfield 1987; Landfield 1983). Ca^{2+} influx associated with action potentials induces larger Ca^{2+}-dependent afterhyperpolarizations (AHPs) (Landfield et al. 1984; Moyer et al. 1992; Stutzmann et al. 2006) and impaired short-term synaptic plasticity (Thibault et al. 2001) in aged neurons from rats and rabbits compared to young neurons. Pharmacologically isolated Ca^{2+} action potentials (Disterhoft et al. 1996), whole-cell Ca^{2+} currents (Campbell et al. 1996) and Ca^{2+} transients during repetitive spike trains are larger in hippocampal neurons from aged animals (Hemond et al. 2005; Thibault et al. 2001). Aging enhanced large (L-type) voltage-gated Ca^{2+} channel (L-VGCC) activity in partially dissociated hippocampal slices (Thibault et al. 1996). Functionally, antagonists of L-VGCC appear to improve learning and memory in aged animals (Disterhoft et al. 2006) and in some patients with dementia (Forette et al. 2002). Clearly, there are changes to different components of Ca^{2+} handling with aging.

In 1989, Khachaturian proposed that sustained changes in Ca^{2+} homeostasis could provide the common pathway for the neuropathological changes associated with AD, termed the "calcium hypothesis of brain aging and Alzheimer's disease" (Khachaturian 1989). The proposition was not based on empirical data but was intended to direct the research at the time towards studies of the cellular mechanisms underlying aging and AD. Evidence to support the hypothesis came soon after. Fibroblasts from asymptomatic patients at risk for AD displayed enhanced IP_3R-mediated Ca^{2+} signalling (Ito et al. 1994). Expression of Ca^{2+}-handling genes are significantly altered in brain tissue from AD patients (Emilsson et al. 2006). Recently, memantine has been approved by the FDA for use in the treatment of patients with moderate to severe AD. Because memantine antagonizes the Ca^{2+}-permeable NMDA receptor by blocking open, over-activated channels (Lipton 2007), its efficacy illustrates the potential involvement of altered Ca^{2+} signalling in the clinical manifestation of AD. Nimodipine, a dihydropyridine

derivative and L-VGCC antagonist, has beneficial effects in AD patients and slows the progression of the disease (Lopez-Arrieta et al. 2002; Tollefson 1990). A nimodipine derivative, MEM-1003, has completed Phase II clinical trials (Memory Pharmaceuticals). Finally, a single nucleotide polymorphism in a newly identified cell membrane Ca^{2+} channel, CALHM1, interferes with Ca^{2+} permeability and slightly increases susceptibility to sporadic, late-onset AD (Dreses-Werringloer et al. 2008). Functionally, Ca^{2+} dysregulation appears to be a genuine consequence of AD pathology.

Do changes in Ca^{2+} homeostasis affect Aβ production? If so, changes in Ca^{2+} handling could be the trigger of AD pathology. Past studies have addressed this question but there are conflicting conclusions. The earliest study reported that cultured human embryonic kidney cells expressing APP had increased Aβ production after treatment with the Ca^{2+} ionophore, A23187 (Querfurth et al. 1994). The same result was obtained after treating the cells with caffeine, a RyR agonist, suggesting that both Ca^{2+} influx and release of Ca^{2+} from intracellular stores promoted Aβ production (Querfurth et al. 1997; Querfurth & Selkoe 1994). However, after treatment with thapsigargin, which irreversibly blocks SERCA activity and increases cytosolic Ca^{2+} levels, cultured cells showed dose-dependent decreases in their production of Aβ (Buxbaum et al. 1994). More recently it was demonstrated that influx of Ca^{2+} from L-VGCC and elevated $[Ca^{2+}]_{cyto}$ increased intraneuronal Aβ42 production, while release of ER Ca^{2+} was inadequate for Aβ production (Pierrot et al. 2004). Conversely, it has been shown that loss of Ca^{2+} influx through plasma membrane channels due to polymorphisms increases Aβ42 formation and Aβ42/40 ratio (Dreses-Werringloer et al. 2008). The processing of APP is complex and is clearly affected by altered cyotsolic Ca^{2+} signalling but further study, particularly in neuronal systems, is required to determine which Ca^{2+} sources are important for Aβ production.

However, the effects of APP and its metabolites on cytosolic Ca^{2+} signalling are well established. Aβ40 and 42 can form Ca^{2+}-permeable pores on the plasma membrane (Arispe et al. 1993), generally leading to an increase in $[Ca^{2+}]_{cyto}$ (Goodman et al. 1994; Mattson et al. 1992). Pore formation is enhanced by exposure of phophatidylserine on the cell surface; an indication that a cell will undergo apoptosis (Lee et al. 2002). Because destabilization of cytosolic Ca^{2+} levels can trigger free radical formation (Mattson 1995), lipid peroxidation (Huang et al. 1999) and apoptosis (Mark et al. 1995), such mechanisms could be involved in Aβ neurotoxicity. Aβ oligomers can cause increased NMDA receptor activity (Ye et al. 2004) and sensitivity to NMDA-mediated excitotoxicity (Mattson et al. 1992). In contrast, Aβ oligomers can suppress activity of presynaptic P/Q-type (neuronal) VGCC (Nimmrich et al. 2008). Secreted APPs have neuroprotective qualities because they attenutate the elevated $[Ca^{2+}]_{cyto}$ evoked by Aβ (Goodman & Mattson 1994) and moderate Glu-induced cytosolic Ca^{2+} levels in hippocampal neurons by increasing cyclic GMP (Barger et al. 1995). Changes in Ca^{2+} dynamics are thought to contribute to the altered synaptic transmission observed in PDAPP mice (Larson et al. 1999). More recently, *in vivo* Ca^{2+} imaging experiments with Tg2567 mice displayed elevated $[Ca^{2+}]_{cyto}$, or Ca^{2+} overload, in neurites and spines that were in close proximity to Aβ plaques (Kuchibhotla et al. 2008).

The role of the ER in the dysregulation of cytosolic Ca^{2+} in AD has been a major focus of research because mutations that cause AD also affect ER Ca^{2+} signalling. Skin fibroblasts from human patients that harbour mutant PS1-A246E showed exaggerated Ca^{2+} release from IP_3-gated stores compared to controls after treatment with bombesin and bradykinin (Ito et al. 1994). These alterations in Ca^{2+} signalling were detected before the development of overt clinical symptoms (Ito et al. 1994) and such changes were not present in cells from subjects that failed to develop AD (Etcheberrigaray et al. 1998b).

Cells expressing mutant PS1 (Leissring et al. 1999b) and primary cortical neurons from mice expressing mutant PS1 displayed similar alterations in signalling (Leissring et al. 2000; Stutzmann et al. 2004). Clinical mutations of the PS2 gene also enhanced Ca^{2+} release from IP_3R-gated ER stores (Leissring et al. 1999a). PS1 mutations affect the activity and/or expression of many proteins involved in ER Ca^{2+} signalling and consistently results in enhanced release of Ca^{2+} from ER stores. The exaggerated IP_3- and caffeine-evoked Ca^{2+} responses in PS1-M146V hippocampal and cortical neurons are attributed to increased Ry receptor (RyR) expression (Smith et al. 2005; Stutzmann et al. 2006). *Xenopus laevis* oocytes expressing PS1-M146V have increased SERCA activity compared to those with wild-type PS1 (Green et al. 2008), a mechanism that could contribute to the overfilling of ER Ca^{2+} stores. It was recently discovered that PS also function as ER Ca^{2+} leak channels and that familial AD mutations in PS1 disrupts this function (Nelson et al. 2007; Tu et al. 2006), resulting in overloaded ER Ca^{2+} stores and exaggerated ER Ca^{2+} release in PS1-A246E human fibroblasts and mouse hippocampal neurons (Nelson et al. 2007). PS1 mutants also display attenuated capacitative Ca^{2+} entry, a refilling mechanism for depleted Ca^{2+} stores (Yoo et al. 2000). It is clear that familial AD PS1 mutations are involved in ER Ca^{2+} dysregulation. In comparison, there are very few studies that concentrate on the effects of mutated APP on ER Ca^{2+} signalling. It has been documented that fibroblasts from AD patients harbouring the Swedish double mutation, APP-K670N/M671L, showed reduced bombesin-induced Ca^{2+} elevations compared to controls and all other pools of Ca^{2+} were unaffected (Gibson et al. 1997).

1.2 THE RYANODINE RECEPTORS (RyRs)

1.2.1 Structure and function

Ryanodine receptors are Ca^{2+} release channels located on the ER that mediate Ca^{2+}-induced Ca^{2+} release (CICR) by direct interaction with dihydropyridine receptors (DHPRs) in skeletal muscle or by Ca^{2+} binding the receptors in cardiac muscle and other tissues, including neurons (Augustine et al. 1992; Berridge 1998). The channels bind the ligand ryanodine (Ry), a neutral, insecticidal plant alkaloid isolated from the roots and stems of the South American shrub *Ryania speciosa* (Pessah et al. 1985). Ryanodine receptors are large, 2.35 kDa homotetrameric complexes of 565 kDa monomers that associate to form an ion conducting pore (Lai et al. 1989). Based on sequence analysis, RyRs contain two functional domains; a large (4000 amino acids) N-terminal cytoplasmic domain that modulates channel gating and ligand binding sites and a C-terminal (1000 amino acids) containing several hydrophobic domains that form the pore. Both the N- and C-terminals protrude into the cytosol. Definitive structural evidence is still lacking but 4-12 transmembrane domains (M4-M12) have been predicted (Du et al. 2002; Takeshima et al. 1989; Zorzato et al. 1990).

Three subtypes (isoforms) of RyR exist in mammalian vertebrates with 66-70% amino acid sequence homology (Sorrentino et al. 1993a; Takeshima et al. 1989; Zorzato et al. 1990). The homology among all RyR isoforms is higher in certain functionally important, conserved domains, such as the leucine/isoleucine zipper domains (for binding of adaptor proteins), the pore region, and the transmembrane domains. The highest homology between the isoforms is in the transmembrane pore-forming regions between M8 and M10. Based on phylogenetic analysis, all RyR isoforms evolved from a single ancestor and it is possible that RyRs and IP_3Rs evolved from a common channel (Vazquez-Martinez et al. 2003). A comparison of the sequences of RyRs and IP_3Rs show a high degree of homology between the pore region and transmembrane domains lining the pore region (Vazquez-Martinez et al. 2003). The pore-forming region of RyRs has structural homology to the superfamily of ion channels, including most of the

voltage-gated ion channels and TRPCs (Harteneck et al. 2000). The highest degree of variability between the RyR isoforms is contained in three divergent regions (D1-3), potentially the source of the isoform-specific functional differences (Liu et al. 2002; Liu et al. 2004; Zhang et al. 2003). D1 is located near the C-terminal in the pore forming domain and D2/3 are located in the cytoplasmic domain (Sorrentino et al. 1993b).

Ryanodine receptors control Ca^{2+} release from the sarcoplasmic reticulum (SR) in skeletal and cardiac muscle and activate muscle contraction during excitation-contraction coupling (ECC), the link between depolarization of the plasma membrane and muscle-fibre contraction. The L-VGCC types $Ca_v1.1/1.2$ or DHPR of the plasma membrane are activated by action potentials that are transmitted along transverse-tubule membranes. In skeletal muscles, $Ca_v1.1$ co-localizes with RyR1 and gating of the channel is controlled by physical interactions between the two proteins (Ferguson et al. 1984; Franzini-Armstrong et al. 1999). In cardiac muscle, the primary activator of RyR2 is Ca^{2+} entry through the $Ca_v1.2$. In the brain and spinal cord, co-immunoprecipitation studies indicate RyR1 interaction with $Ca_v1.2$ and RyR2 interaction with $Ca_v1.3$ (Ouardouz et al. 2003). Ryanodine receptors are essential for ECC and failure to express either RyR1 or 2 results in death in neonates or *in utero* (Takeshima et al. 1994a; Takeshima et al. 1998). RyR2 and RyR3 in non-muscle cells are activated by elevated cytosolic Ca^{2+} levels and/or by cyclic ADP ribose (cADPR) by an unknown mechanism (Kunerth et al. 2004; Takasawa et al. 1998). Calcium release by ligand-gated mechanisms is slower compared to protein-mediated CICR (Nabauer et al. 1989). RyRs mediate CICR from the ER in neurons to modulate action potentials, neurotransmitter release, gene expression and other Ca^{2+}-dependent cellular mechanisms. In rat hippocampal neurons RyR2 interacts physically and functionally with the neuronal $Ca_v1.3$ (Kim et al. 2007). RyRs are expressed in other cell types, such as

pancreatic β cells and T cells, but the role of intracellular Ca^{2+} release in cellular function is not well understood.

1.2.2 Expression of RyR isoforms

RyR1 and RyR2 were first cloned from mammalian skeletal and cardiac muscle, respectively (Marks et al. 1989; Otsu et al. 1990; Takeshima et al. 1989). RyR3 was cloned from rabbit brain (Hakamata et al. 1992) and a mink lung epithelial cell line (Giannini et al. 1992). In humans, RyR1, RyR2 and RyR3 genes are located on chromosomes 19q13.2 (MacLennan et al. 1990; McCarthy et al. 1990), 1q43 (Otsu et al. 1993) and 15q13.3-14 (Sorrentino et al. 1993a), respectively. In mice, RyR1, RyR2 and RyR3 are located on chromosomes 7A2-B3, 13A1-2 and 2E5-F3 (Mattei et al. 1994), respectively. RyR isoforms have also been identified in non-mammalian vertebrates, such as chicken, bullfrog and blue marlin, and in invertebrates, including *Caenorhabditis elegans* and *Drosophila melanogaster* (Maryon et al. 1996; Ottini et al. 1996; Oyamada et al. 1994; Takeshima et al. 1994b). RyR2 is likely a result of a duplication of RyR1 and RyR3 a duplication of RyR2, as non-mammalian vertebrates only express genes that are similar to RyR1 and RyR2 (Oyamada et al. 1994). Additional diversity in the RyRs has resulted from alternative splicing. In mammals, little is known about functional properties of alternatively spliced RyR1 and RyR2 (Nakai et al. 1990; Sutko et al. 1996). RyR1 has tissue-specific splice variants in the cytoplasmic domain, generating developmentally regulated spliced RyRs (Futatsugi et al. 1995). A dominant-negative splice variant of RyR3 with reduced caffeine sensitivity was found to negatively regulate Ca^{2+} release in smooth muscle (Jiang et al. 2003) by modulation of the RyR2 receptor (Dabertrand et al. 2006).

RyR isoforms are expressed differentially in many tissue types. RyR1 is abundant and predominantly expressed in skeletal muscle and present in lower levels in

cardiac and smooth muscle, Purkinje cells of the cerebellum (Kuwajima et al. 1992), testis, adrenal gland and ovaries (Giannini et al. 1995; Marks et al. 1989; Ottini et al. 1996; Takeshima et al. 1989). RyR2 is highly expressed in the heart and brain, and at lower levels in the stomach, lung, thymus, adrenal gland and ovaries (Giannini et al. 1995; Nakai et al. 1990). RyR2 is localized mainly in the soma of most neurons (Kuwajima et al. 1992). The RyR3 isoform is expressed in the brain, diaphragm, slow twitch skeletal muscle and several abdominal organs (Giannini et al. 1992; Hakamata et al. 1992; Ottini et al. 1996). The levels of expression of the RyR isoforms vary during development. For example, RyR3 is highly expressed in skeletal muscle in the early stages of but expressed in very low levels in the adult (Ogawa et al. 2000). Splice variants of RyRs are also expressed differentially during development (Futatsugi et al. 1995; Marziali et al. 1996; Miyatake et al. 1996; Mori et al. 2000).

1.2.3 Regulation of RyRs

The activation and release of Ca^{2+} from RyRs is modulated by many different endogenous effectors. RyRs are selective for cations but have low selectivity among cations and have physiologically relevant interactions with a number of intracellular proteins and signalling molecules, such as calmodulin (CaM), cADPR and ATP. Channel activity can also be modified by many exogenous effectors (Zucchi et al. 1997) which will be discussed herein.

1.2.3.1 Modulation of RyRs by physiological ligands

Ca^{2+} is the most important ligand that modulates the gating of RyR. Ca^{2+} has both activating and inactivating effects on Ca^{2+} release from single channels in isolated SR vesicles and single channel activity (Meissner 1994). As a regulator of RyRs, Ca^{2+} shows a biphasic bell-shaped relationship: activation at low [Ca^{2+}] and inhibition at high

[Ca^{2+}]. Ca^{2+} affects the open probability of the channel, decreasing the life-time of closed states when activating RyR and shifting from short-lived closures to long-lived closures when inhibiting the channel (Zucchi & Ronca-Testoni 1997). Isolated RyR1 showed activation by 1 μM Ca^{2+} and inhibition by 1 mM Ca^{2+} (Meissner 1994). The presence of high affinity Ca^{2+} binding sites that stimulate Ca^{2+} release and low affinity Ca^{2+} binding sites that inhibit Ca^{2+} release on the cytoplasmic side of the channel is an accepted model for the biphasic response of RyR to Ca^{2+}. Occupation of the low affinity Ca^{2+} binding site(s) resulted in the inhibition of Ca^{2+} release from SR vesicles and inhibition of the activity of channels reconstituted into planar bilayers (Ma et al. 1988; Meissner 1994). It has been demonstrated with RyR2 that inactivation of the channel requires significantly higher [Ca^{2+}] and a decrease of SR [Ca^{2+}] on the luminal side contributes to the termination of CICR (Terentyev et al. 2002). Sensitivity to CICR is about ten times lower for RyR3 than for the other isoforms (Takeshima et al. 1995). The exact molecular mechanism of RyR regulation by Ca^{2+} is still unknown.

Cytosolic magnesium (Mg^{2+}) is a RyR inhibitor at millimolar concentrations. Regulation of RyR channels by Mg^{2+} decreases sensitivity to Ca^{2+} at two different binding sites (Laver et al. 1997). Mg^{2+} also exerts a negative modulatory effect in single channel [^{3}H]Ry binding experiments in SR vesicles and isolated RyR proteins reconstituted into planar bilayers (Meissner et al. 1992). Sensitivities of the different isoforms to Mg^{2+} are RyR1>RyR2>RyR3 (Zimanyi et al. 1991a). RyRs are sensitive to H^+, where optimal pH is 7.2-7.6 (Ma et al. 1988) and low pH can lead to decreased channel conductance (Rohra et al. 2003). Adenine nucleotides such as ATP, AMP, ADP, cyclic AMP (cAMP), adenosine and adenine potentiate the release of Ca^{2+} from RyRs by enhancing the open probability of the channel (Pessah et al. 1987; Zarka et al. 1993). Binding of adenine nucleotides appears to occur at a site that is different from, but interacts with, the Ca^{2+} and Mg^{2+} binding site. cADPR is an endogenous metabolite of

nicotinamide-adenine dinucleotide (NAD) and is thought to indirectly mediate the Ca^{2+} signalling by RyR in muscle (Morrissette et al. 1993; Wang et al. 2004) and non-muscle cells (Clementi et al. 1996; Empson et al. 1997; Kunerth et al. 2004). Recently it has been shown that hypoxic conditions trigger cADPR-mediated RyR activation (Aley et al. 2006; Zhang et al. 2006), suggesting that activation of RyRs is dependent on the redox state of the channel. Each RyR monomer contains 80-100 cysteine residues with approximately 25-50 in the reduced state, making them sensitive to modulation by oxidation (Kawakami et al. 1998) and nitrosylation (Xu et al. 1998) which can alter channel activity. For example, reactive oxygen increases Ca^{2+} release from RyR (Kawakami & Okabe 1998). Serine and threonine residues of RyR have been identified as possible phosphorylation sites by protein kinases, but the functional consequences of phosphorylation are still controversial. It has been shown that RyR2 is phosphorylated by cyclic AMP-dependent protein kinase (PKA), cyclic GMP-dependent protein kinase or protein kinase C (PKC) to modulate channel activation (Patel et al. 1995) either directly or through the phosphorylation of RyR binding proteins such as FK-506 binding protein 12.6 (Marx et al. 2000) or sorcin (Lokuta et al. 1997). The effect of phosphorylation of RyR1 and RyR2 is still unclear as sensitization to Ca^{2+}, inhibition of the channel or no effects have all been reported (Chu et al. 1990b; Suko et al. 1993; Wang et al. 1992). The significance and/or mechanism of RyR3 phosphorylation is not known. A potential PKA phosphorylation site conserved in mink, rabbit, chicken and frog RyR3 and one potential phosphorylation site for cAMP protein kinase conserved in all RyR3 was identified by Marziali and collegues using sequence analysis (Marziali et al. 1996). Dephosphorylation of RyR occurs via the protein phosphatases PP1 and PP2A (Marx et al. 2001) but their role in modulating RyR activity is confusing as reports are conflicting.

1.2.3.2 Modulation of RyR by protein-protein interactions

Structure-function studies of RyR suggest that inter-domain interaction within the RyR serves as a key mechanism in the process of channel gating. Because of mutations that lead to problems in channel regulation, it is hypothesized that the N-terminal domain, central domain and a transmembrane channel domain are important in RyR gating. The N-terminal and central domain in particular constitute a 'domain-switch' that form the 'off' or 'on' conformation of the channel depending on the absence or presence of agonists, respectively (Ikemoto et al. 2002). In skeletal muscle, RyRs are activated by direct interaction with DHPRs on the plasma membrane after voltage-dependent activation (see **Figure 1.4**). Based on sequences, there are several DHPR binding regions along the RyR polypeptide chain in the divergent region 2 (D2) (Perez et al. 2003). Junctiphilins (JPs) are proteins that stabilize the association between the plasma membrane and the ER to facilitate the DHPR-RyR interaction (Kakizawa et al. 2007). JPs have a motif that interacts with the plasma membrane and a transmembrane segment that spans the ER or SR membrane (Takeshima et al. 2000) to anchor the ER or SR to the plasma membrane and stabilize DHPR-RyR interaction.

Calmodulin is a Ca^{2+} binding protein that has been shown to associate with RyR (Seiler et al. 1984) and inhibit activation of the channel by Ca^{2+}, caffeine and AMP in cardiac and skeletal muscle (Meissner 1986; Meissner et al. 1987; Plank et al. 1988). CaM also inhibits Ry binding in microsomes from brain and skeletal muscle (Fuentes et al. 1994; McPherson et al. 1993). CaM binding sites have been described (2-6 sites per monomer) (Chen et al. 1994; Takeshima et al. 1989; Yamaguchi et al. 2005; Zorzato et al. 1990) and binding is dependent on free Ca^{2+}, pH and Mg^{2+} (Yang et al. 1994). It has been reported that CaM reduces the frequency of open channel events and stabilizes the closed channel (Fuentes et al. 1994).

Cytosolic proteins that bind the immunosuppressant drug, FK-506, have been shown to associate with RyRs. A 12-kDa FK-506 binding protein (FKBP12 or calstabin1) associates 1:1 with RyR monomers in skeletal (Collins 1991) and cardiac

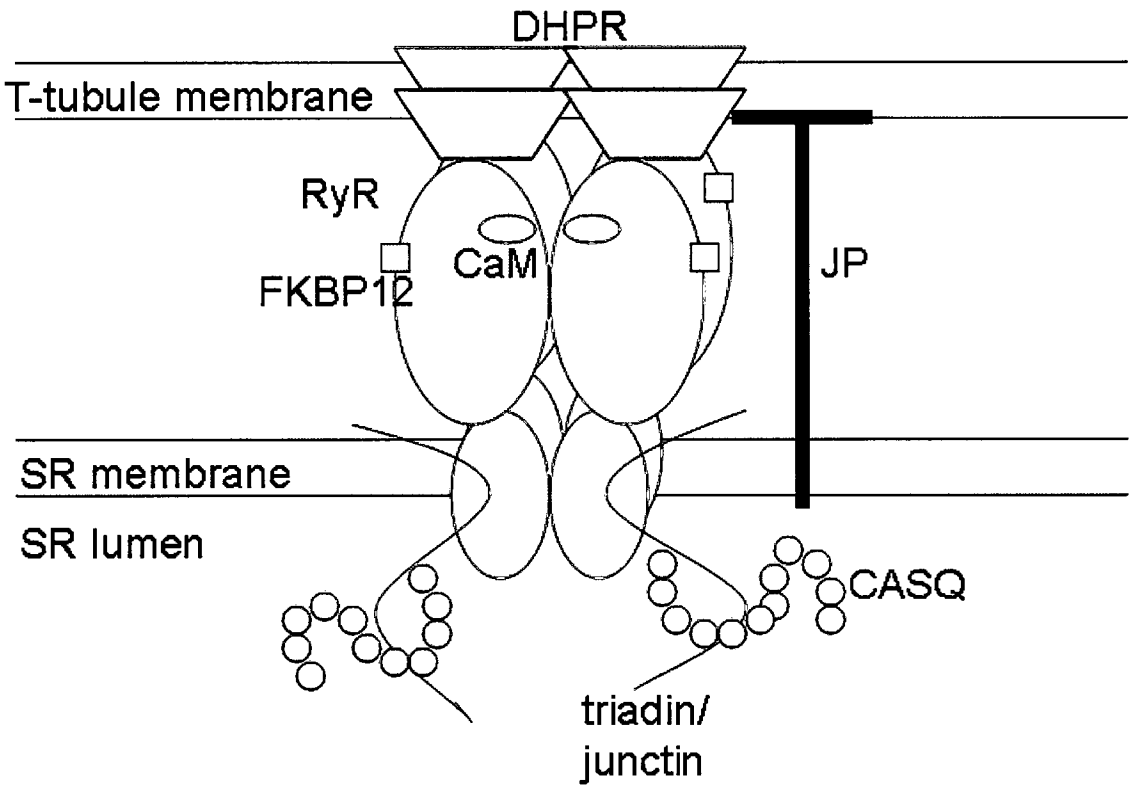

Figure 1.4. Modulation of RyR by protein-protein interactions. Illustration of some of the many protein-protein interactions that contribute to the modulation and regulation of skeletal muscle ryanodine receptor (RyR) activity. Dihydropyridine receptor triad (DHPR), calsequestrin (CASQ), calmodulin (CaM) juctiphillin (JP), FKBP12 (12 kDa FK-506 binding protein), sarcoplasmic reticulum (SR). Adapted from Dulhunty 2006 and Kakizawa et al. 2007.

muscle (FKBP12.6 or calstabin2) (Lam et al. 1995). FKBP12 stabilizes the open, fully conducting states instead of subconductance states (Brillantes et al. 1994; Ma et al. 1988). When FKBP12 dissociates from RyR by addition of FK-506 or rapamycin, the subconductance state becomes prominent and the channel is termed "leaky". FKBP12.6 is a crucial component for ventricular Ca^{2+} homeostasis. FKBP12.6 knock-out mice

demonstrated exercise-induced cardiac ventricular arrhythmias that caused sudden cardiac death and mutations in RyR2 that reduced FKBP12.6 affinity caused exercise-induced cardiac arrhythmias in patients with catecholaminergic polymorphic ventricular tachycardia (CPVT) (Wehrens et al. 2003).

Luminal [Ca^{2+}] can also modulate RyR activity. During Ca^{2+} release from the ER, luminal [Ca^{2+}] decreases, which is a signal for the channel to close. A protein complex associated with the RyR on the luminal side of the ER membrane affects RyR activity in response to low luminal [Ca^{2+}]. Calsequestrin (CASQ), a Ca^{2+} binding protein and the anchoring proteins triadin and junctin appear to be important in modulating the activity of the RyR (Dulhunty 2006). At rest, triadin/junctin is situated in the ER and associates with the luminal side of RyR while CASQ is bound up by Ca^{2+} in the ER lumen. When luminal [Ca^{2+}] decreases, CASQ dissociates from Ca^{2+} and is free to associate with triadin/junctin. The association of CASQ and triadin/junctin serves to inhibit RyR by decreasing the open probability of the channel (Gyorke et al. 2004).

1.2.3.3 Pharmacology of RyR

Numerous exogenous substances have been reported to modulate RyR function. The actions of these substances on RyR are often complex or not fully described. Even the distinction between agonist and antagonist is difficult because it depends on the amount of time the receptor is exposed to substance and the concentration of the substance. Chemicals routinely used in RyR studies are discussed below.

Ryanodine and its derivatives (ryanoids) have been shown for many years to modulate cardiac and skeletal muscle function (Jenden et al. 1969). Mechanistic studies using single channel recordings and radio-labelled Ry ([^{3}H]Ry) for binding studies have provided much insight to the mechanism of action of Ry on RyRs. Ryanodine had a dual concentration-effect, where ~10 nM [Ry] opened the channel as does intermediate [Ry]

of 1μM and higher [Ry] of ~100 μM closed the channel (Buck et al. 1992; Smith et al. 1988; Zimanyi et al. 1992). The open probability of the Ry-bound channel was voltage-dependent, insensitive to activation by Ca^{2+} and ATP, and less sensitive to normal Mg^{2+} and H^{+} inhibition (Zucchi & Ronca-Testoni 1997). When [Ry] was raised to higher micromolar, the channel was irreversibly locked in the closed state, or "shut" (Bidasee et al. 1998). To explain such observations, the two-site binding model was adopted; Ry interacts with the high-affinity site to stabilize the open channel and at higher concentrations Ry binds to low-affinity sites to further reduce channel conductance until complete blockade. The RyR has multiple Ry binding sites, both high and low affinity (Chu et al. 1990a; Pessah et al. 1991; Wang et al. 1993). However, studies using other ryanoids have shown that the gating of RyRs is not as simple as the proposed model, having a wide range of subconductance states, effective concentrations, dissociation half times and degree of reversibility (Callaway et al. 1994; Hui et al. 2004). Ryanodine stabilized the channel in the open state to a greater extent in skeletal tissue versus heart tissue (Meissner 1986; Northover 1991). Extrusion of Ca^{2+} is slower in skeletal muscle compared to heart muscle, which could explain the difference in the ability of Ry to stabilize the different RyR subtypes. Studies are ongoing to further characterize the binding mechanisms of ryanoids as their selectivity, low subconductance and reversibility are desirable for therapeutic purposes.

Caffeine is a methylxanthine known to stimulate release of Ca^{2+} from RyRs by increasing the sensitivity of the channel to Ca^{2+} (Meissner & Henderson 1987). The stimulatory effect of caffeine is higher in cardiac versus skeletal muscle microsomes, additive with adenine nucleotides, and inhibited by Mg^{2+}. Single channel recordings have shown that caffeine increased the open channel probability of RyR without any conductance change. At 0.5-2 mM, caffeine sensitized the channel to < millimolar [Ca^{2+}] and reduces the lifetime of the closed channel state. At higher concentrations of caffeine

(0.5-10 mM), RyR was activated by picomolar [Ca^{2+}] and the lifetime of the open channel was increased (Hernandez-Cruz et al. 1995; Zimanyi & Pessah 1991a). Caffeine and other methylxanthines are useful experimental tools but are not good candidates for in-patient use as the effective concentration required for activation of RyR is much higher than the caffeine concentration that can ever be achieved in plasma.

Dantrolene sodium is a lipohilic hydantoin derivative (hydrated 1-(((5-(4-nitrophenyl)-2-furanyl)-methylene)-amino)-2,4-imidazolidineione sodium) first synthesized by Snyder and colleagues in 1967 and reported to have intracellular muscle relaxant activity (Ellis et al. 1973). Physiological and pharmacological studies have shown that dantrolene suppresses the release of Ca^{2+} from RyR1 in skeletal muscle. Dantrolene is the only therapeutic agent in use for the treatment of malignant hyperthermia (MH), a pharmacologic sensitivity to volatile anesthetics where as mutations in RyR1 result in exaggerated intracellular Ca^{2+} release, hypercontracture of the skeletal muscle and hypermetabolism. In skeletal muscle microsome preparations, 10-90 mM dantrolene inhibited Ca^{2+} release (Flewellen et al. 1983). Dantrolene reduced the rate of Ca^{2+} release, was more effective in the presence of caffeine and ATP, and the response was temperature dependent (Yang et al. 2006). The mechanism of action of dantrolene is still unclear as there are contradictory reports regarding the involvement of particular regions of the RyR (El-Hayek et al. 1999), RyR subtypes (Fruen et al. 1997) and whether or not RyR is even involved in the action of dantrolene at all (Nelson et al. 1999). Nonetheless, dantrolene blocks Ca^{2+} release from the ER and likely involves blockade of the RyRs, particularly RyR1 and possibly RyR2 and RyR3 (Zhao et al. 2001). Because of its clinical history, the use of dantrolene treatment for ailments other than MH is being explored, such as spasticity after stroke (Barnes 2001; Ketel et al. 1984), 3,4-methylenedioxy-n-methylamphetamine intoxication (Schmidt et al. 1990; Webb et al. 1993) and heat stroke (Grogan et al. 2002) .

Ruthenium red is a polycationic dye that has been shown to inhibit Ca^{2+} release from the SR in cardiac and skeletal muscle, mitochondrial Ca^{2+} uptake and at higher concentrations can inhibit ATPase activity (Blaustein et al. 1978; Ma 1993; Shamoo et al. 1975; Zhu et al. 1992). Effective concentrations for ruthenium red are 19-90 nM in skeletal muscle and cardiac muscle but require Mg^{2+} for complete blockade. In single channel bilayer experiments, micromolar concentrations of ruthenium red decreased the open probability of RyR without affecting conductance, producing long-term closure of the channel (Buck et al. 1992). The action of ruthenium red was voltage-dependent and was inhibited by Ry binding (Ma 1993; Zimanyi et al. 1991b). Based on binding studies, the ruthenium red binding site on RyR1 overlaps with the Ca^{2+}, Ry and CaM sites (Chen & MacLennan 1994).

1.2.3.4 Clinical relevance of RyRs

Mutations in the RyR1 and RyR2 are linked to several human pathologies. Mutations in RyR1, which for the most part are autosomal-dominantly inherited, are known to cause MH (Gillian et al. 1991), central core disease (CCD) (Zhang et al. 1993), multiminicore disease (MmD) and nemaline rod myopathy (NM) (Jurkat-Rott et al. 2002). MH is a very rare disorder that is the most common cause of death related to general anaesthesics used during surgery (such as halothane) and muscle relaxants, such as succinylcholine (Jurkat-Rott et al. 2000). The anaesthetics trigger uncontrolled intracellular Ca^{2+} release in skeletal muscle characterised by tonic muscle contraction, resulting in excessive ATP hydrolysis, acidosis and hyperthermia, followed by multisystem failure (MacLennan et al. 1992). Dantrolene, a muscle relaxant, is a specific treatment for the condition, but the drug must be administered immediately to be efficacious. Mutations responsible for over 50% of all MH cases in humans occur in three RyR1 gene clusters: C35-R614 in the N-terminal region, D2129-R2458 in the

central region and I3916-A4942 in the C-terminal region. These mutations are thought to destabilize the closed state of the channel, making them more sensitive to activation by drugs such as halothane (Parness et al. 1995).

Central core disease and MmD are early-onset congenital myopathies, a heterogenous group of neuromuscular disorders with shared characteristics, including fetal hypotonia and proximal muscle weakness during infancy (Shuaib et al. 1987). Symptoms can sometimes result in fatalities in the first few months of life and histology typically shows significant atrophy of type 1 skeletal muscle fibres (Taratuto 2002). Central core disease is the most common congenital myopathy and is associated with mutations in RyR1 in the same regions affected in MH (Rueffert et al. 2004). Few mutations linked to CCD and MmD are inherited in an autosomal-recessive manner and CCD patients are often found to be MH susceptible (Shuaib et al. 1987). Multiminicore disease also results in muscle weakness and a lack of oxidative enzyme activity is apparent (Guis et al. 2004). Central core disease-related mutations alter RyR1 Ca^{2+} release, cause Ca^{2+} leak from SR and result in excitation-contraction uncoupling (Avila et al. 2001).

Ryanodine receptor type 2 dysfunction has also been linked to genetic forms of arrhythmias and heart failure. Autosomal-dominant mutations in RyR2 have been associated with CPVT, a stress- or exercise-induced juvenile sudden death disorder with no available treatment (Lehnart et al. 2004). Missense mutations responsible for CPVT cluster in the N-terminal region (176-420), central region (2246-2504) and C-terminal region (3778-4950) (Marks et al. 2002). Single channel studies of RyR2 containing CPVT mutations demonstrated a gain-of-function defect following PKA phosphorylation at serine 2808, consistent with "leaky" RyR2 channels, or SR Ca^{2+} leak, during stress or exercise (Lehnart et al. 2004; Wehrens et al. 2003). Catecholaminergic polymorphic ventricular tachycardia mutations in RyR2 coincide with decreased calstabin2- or

FKBP12.6-binding affinity, enhanced dissociation from the RyR2 during PKA phosphorylation and enhanced SR Ca^{2+} leak (Laitinen et al. 2001). In heart failure (HF), activation of a neurohumoral compensatory mechanism to counteract reduced cardiac output results in increased catecholamine concentration in plasma. Chronic enhanced stimulation of the β-adrenergic signalling cascade results in hyperactivity of PKA, hyperphosphorylation of RyR2 causing dissociation of calstabin2 and chronic SR Ca^{2+} depletion, worsening the initial HF (Antos et al. 2001; Marx et al. 2000). Pharmacological interventions that increase calstabin2 binding to PKA phosphorylated RyR2 have been shown to increase contractility in dog and mouse models of HF, arrhythmias and sudden cardiac death, highlighting the critical role of RyR2 in HF. Interestingly, approximately 50% of patients with the CPVT mutation RyR2-R22474S present with seizures (Postma et al. 2005). Given the relative abundance of RyR2 in the hippocampus, an area susceptible for seizure generation, the symptom was logical. The observation was duplicated mice carrying the mutation, indicating that RyR2-mediated ER Ca^{2+} leak can contribute to defective neuronal excitability (Lehnart et al. 2008).

There are no known human diseases clearly linked to mutations in RyR3. Mutation analysis identified a possible connection between RyR3 and some cases of recurrent neuroleptic malignant syndrome (NMS), a life-threatening neurological disorder most often caused by an adverse reaction to neuroleptic or antipsychotic drugs (Dettling et al. 2004). Neuroleptic malignant syndrome presents with muscle rigidity, fever, autonomic instability and cognitive changes such as delirium, and is associated with elevated creatine phosphokinase (CPK).

1.2.4 RyR function in neurons

In brain, RyRs are primarily located on the ER and have been demonstrated in presynaptic terminals, postsynaptic cell bodies, astrocytes and oligodendrocytes. RyRs

regulate CICR, membrane potential and excitability, and the activity of second messenger systems in neurons. The role of RyRs in CICR was first demonstrated by Friel and Tsien when proving the existence of CICR in bullfrog sympathetic neurons (Friel et al. 1992). They determined that after depleting RyR-gated ER Ca^{2+} stores with 10-20 mM caffeine, the amplitude and rate of rise of depolarization-induced (30-50 mM KCl) $[Ca^{2+}]_{cyto}$ transients was decreased compared to control. A similar effect was observed after treatment with 1 μM Ry to empty ER Ca^{2+} stores. Finally, blockade of RyR using high concentrations of Ry eliminated CICR.

ER Ca^{2+} is important for the regulation of neuronal excitability and in particular, CICR has been shown to activate Ca^{2+}-dependent K^+ channels. These changes control the AHPs that follow short bursts of action potentials and restrain repetitive firing in many types of neurons. There are three components of the AHP, the fast AHP mediated by large-conductance Ca^{2+}-activated K^+ (BK) channels, the medium AHP (mAHP) mediated by small-conductance Ca^{2+}-activated K^+ (SK) channels and the slow AHP (sAHP) that could be mediated by RyRs (Sah et al. 2002; van de Vrede et al. 2007). Both mAHP and sAHP are mediated by CICR, where up to 50% of the AHP current (I_{AHP}) is reliant on ER Ca^{2+} release. In bullfrog sympathetic neurons, RyRs co-localize with N-type (neuronal) VGCC and Ca^{2+} influx through N-VGCC triggers regenerative CICR near the plasma membrane, which activates I_{AHP} (Akita et al. 2000). Depending on the species and preparation of hippocampal neurons, L-type and/or N-type VGCC have been shown to be involved in I_{AHP} (Rascol et al. 1991; Shah et al. 2000; Tanabe et al. 1998). RyRs also appear to be functionally coupled to large-conductance Ca^{2+}-activated K^+ (BK) channels, which could provide feedback between ER Ca^{2+}, membrane excitability and AP frequency. Recently, it has been shown that RyR3 plays a substantial role in mediating sAHP current (I_{sAHP}) in hippocampal cornu ammonis (CA)1 pyramidal neurons (van de Vrede et al. 2007). Functional blockade of RyR3 with a RyR3-specific antibody reduced

the I_{sAHP} by approximately 70% and blockade by 100 μM Ry did not further reduce the I_{sAHP}, implying a minimal contribution of RyR1 or RyR2 (van de Vrede et al. 2007).

The involvement of Ca^{2+} in neurotransmission has long been established. Ca^{2+} influx through plasma membrane Ca^{2+} channels causes large increases in local $[Ca^{2+}]_{cyto}$ which trigger the fusion of vesicles with the plasma membrane and release of neurotransmitters into the extracellular space (Bennett 1999). There is also a role for ER Ca^{2+} in neurotransmission. Pharmacological experimentation has shown that ER Ca^{2+} was involved in cytosolic Ca^{2+} elevations required for neurotransmission, and release of Ca^{2+} from the ER significantly modulated exocytosis of neurotransmitter in synaptic terminals. In hippocampal (pyramidal) and cortical neurons (Savic et al. 1998; Simkus et al. 2002), the frequency and amplitude of miniature inhibitory and excitatory postsynaptic currents (mIPSCs and mEPSCs, respectively) were sensitive to Ry, demonstrating that spontaneous RyR-mediated presynaptic cyotsolic Ca^{2+} transients that triggered neurotransmitter release at rest. Ca^{2+} imaging of presynaptic terminals performed in parallel confirmed the spontaneous cytosolic Ca^{2+} transients (Savic & Sciancalepore 1998). However, the involvement of RyRs in the regulation of neurotransmission is not present at all synapses. In the mossy fiber synapses in CA1 and CA3 of the hippocampus and the parallel fiber Purkinje neuron synapse of the cerebellum, CICR or caffeine-induced Ca^{2+} release was not involved in the regulation of neurotransmitter release (Carter et al. 2002). In a study of giant mEPSCs (similar to large ACh-mediated mEPSCs) in the mossy fiber-CA3 synapse, inhibition of RyR only slightly affected normal mEPSC (Henze et al. 2002). These data suggest that the role of RyR and CICR in neurotransmission varies depending on the type of synapse.

Neuronal networks are constantly strengthening, weakening, creating or destroying synapses in response to continually changing physiological activity and cues. These processes whereby synaptic transmission efficacy is modified in response to

changes in neuronal activity are termed "synaptic plasticity" (Gaiarsa et al. 2002). Short-term and long-term synaptic plasticity are proported mechanisms through which learning and memory manifest. Long-term potentiation (LTP) and long-term depression (LTD) of synaptic transmission are two electrophysiological correlates of long-term synaptic plasticity which result from high-frequency stimulation of single synaptic inputs or simultaneous activation of several distinct inputs. Rises in cytoplasmic Ca^{2+} signal have been shown to be important in the generation of LTP in hippocampal neurons (Bliss et al. 1973) and LTD in cerebellar neurons (Ekerot et al. 1985), particularly by Ca^{2+} influx through NMDAR that induce the changes in gene expression and modification in postsynaptic neurons. Recent experiments demonstrate that CICR contributes to the rises in $[Ca^{2+}]_{cyto}$ required for LTP and LTD but the role of RyRs in synaptic plasticity is not well characterized (Emptage et al. 1999; Emptage et al. 2001).

Because RyRs are present in the dendritic spines of CA1 hippocampal neurons, RyRs are appropriately situated to contribute to the CICR required to induce synaptic changes (van de Vrede et al. 2007). In hippocampal slices, it was demonstrated that blockade of CICR using 10μM Ry inhibited the induction of LTD in Schaffer collateral (SC)-CA1 synapses (Reyes et al. 1996). Studies with mice containing RyR deletions were used to further explore the role of RyR in synaptic plasticity. Knock-outs of RyR1and RyR2 were neonatal and embryonic lethal, respectively, and therefore not useful for these studies. RyR3 knock-out ($RyR3^{-/-}$) mice showed normal growth and reproduction. Interestingly, while the EC coupling in adult $RyR3^{-/-}$ skeletal muscle was similar compared to wild-type RyR3 mice (Bertocchini et al. 1997), they displayed increased locomotor activity, indicating potential differences in their nervous system (Takeshima et al. 1996). $RyR3^{-/-}$ were generated by three different groups (Balschun et al. 1999; Futatsugi et al. 1999; Takeshima et al. 1996) and were used to perform electrophysiological studies. While all groups reported changes in synaptic plasticity and

performance in behavior tests indicative of spatial learning and memory, their conclusions were far from unanimous. Futatsugi and collegues observed that RyR3 deletion lead to facilitated LTP and eliminated LTD in CA1 neurons in hippocampal slices. $RyR3^{-/-}$ mice also showed enhanced spatial learning in the Morris water maze test for hippocampal-dependent learning (Futatsugi et al. 1999). The LTP characterized in $RyR3^{-/-}$ was NMDA-independent, was partially dependent on VGCC and metabotrophic Glu receptors (Futatsugi et al. 1999). The mouse generated by Takeshima, et al., displayed a smaller LTP and diminished synaptic α-amino-3-hydroxy-5-methyl-4-isoxozolepropionic acid receptor (AMPAR), a Glu receptor, without impacting AMPAR expression, suggesting postsynaptic regulation of LTP by RyR3 (Takeshima et al. 1996). Balschun and colleagues observed that slices obtained from $RyR3^{-/-}$ mice had no changes to robust LTP but showed that depotentiation of LTP was impaired compared to control (Balschun et al. 1999). These mice also displayed increased speed of locomotion, but in the Morris water maze test the mice displayed an impaired ability to re-learn a new target (Balschun et al. 1999).

RyR2 is the most abundant isoform in the brain, therefore it is predicted that RyR2 function would be involved in modulating cytosolic Ca^{2+} important for synaptic plasticity and learning and memory. Rats that were trained in the Morris water maze showed increased RyR2 mRNA and protein levels in the hippocampus (Zhao et al. 2000). These changes were evident at 12 h and 24 h after completing the spatial learning task, indicating a role for RyR2 in long-term memory storage, but this was not confirmed by electrophysiological studies (Zhao et al. 2000). Recently, a study employing anti-sense oligonucleotides delivered by intracerebroventricular injection to specifically target and decrease expression of RyR isoforms in mouse brain demonstrated that RyR2 and RyR3 expression are involved in the modulation of memory

formation (Galeotti et al. 2008). Mice that were administered RyR1 anti-sense did not perform any different than controls in a passive avoidance test. (Galeotti et al. 2008). It is clear that RyRs are important for neuronal function and for processes involved in memory formation and further studies are required to specify their role in synaptic plasticity mechanisms.

1.3 THE ROLE OF RyRs in AD

Sustained disruption of intraneuronal Ca^{2+} homeostasis appears to be an early event preceding the neurodegeneration that occurs in Alzheimer's disease (AD) (Arundine et al. 2003; Berridge 2001; Brzyska et al. 2003; Ghosh et al. 1995; LaFerla 2002; Paschen 2000). Given the involvement of RyRs in CICR, neuronal function and hippocampal learning and memory, it is rational to hypothesize that RyRs could be affected in AD. In human post-mortem tissue, Ry binding is elevated in hippocampal regions (subiculum, CA2 and CA1) of AD brain in the early stages of the disease prior to extensive neurodegeneration and overt Aβ plaque deposition (Kelliher et al. 1999). Furthermore, it has been reported that RyR levels are increased in 3 different mouse models of AD; PS1-M146V, PS2-N141I and 3XTg-AD (Chan et al. 2000; Lee et al. 2006; Smith et al. 2005). The expression of RyRs in transgenic (Tg) CRND8 mice has not yet been characterized. TgCRND8 mice express the Swedish and Indiana mutations of the APP_{695} (KM670/671NL+V717F) under the hamster prion promoter. They were designed to produce high levels of Aβ42 at an early age, by 8 weeks, and display plaques in the hippocampus (Chishti et al. 2001). In addition, TgCRND8 mice display altered neurophysiology, both facilitated LTP (Jolas et al. 2002) and depressed basal synaptic transmission in the hippocampal CA1 by BK channels (Ye et al. 2008), and impaired spatial learning and working memory (Chishti et al. 2001; Hyde et al. 2005;

Lovasic et al. 2005). It is conceivable that changes in RyR expression in TgCRND8 mice could mediate the changes observed.

Increased RyR levels enhanced Ca^{2+} release from the ER and sensitized cortical neurons from PS1-M146V and PS2-N141I mice to neurotoxic insults, such as treatment with high Glu concentration (Chan et al. 2000; Lee et al. 2006). High levels of RyRs are expressed throughout the lifetime of 3XTg-AD mice and electrophysiological studies showed that RyR Ca^{2+} stores were responsible for the exaggerated hyperpolarization responses of 3XTg-AD neurons to IP_3 (Stutzmann et al. 2006). Up-regulation of RyRs has also been demonstrated in the hippocampus of mice after administration of kainic acid to induce seizures (Mori et al. 2005), further implicating a role for RyRs in the modulation of neuronal excitability. Excitotoxicity is thought to be a contributing factor to AD pathology (Lipton 2007) and it appears that up-regulated RyRs could mediate the susceptibility to Glu observed in AD neurons (Arundine & Tymianski 2003). Furthermore, it was demonstrated that Ca^{2+} release from RyR stores enhanced Aβ production in cells transfected with APP (Querfurth et al. 1997). These observations coupled with the potential role of RyRs in learning and memory processes make RyRs a candidate for both symptomatic and disease-modifying therapeutic intervention in AD. However, as seen with other candidate drug targets, a lack of understanding of the role of RyRs in normal and pathological neurophysiology can lead to ambiguous or even dangerous outcomes in animal testing and clinical trials.

1.4 EXPERIMENTAL GOALS

Given the importance of intracellular Ca^{2+} signalling in AD and the significant contribution of RyRs to intracellular Ca^{2+} signalling in neurons, **it is hypothesiszed that up-regulation of RyRs in AD is responsible for the dysregulated Ca^{2+} signalling in**

AD neurons, which could lead to neuronal dysfunction and contribute to AD pathophysiology. The TgCRND8 mouse model of AD will be used to test the hypothesis because it is a well characterized AD model which displays both behavioural and histopathological hallmarks of the disease. The hypothesis will be tested by addressing the following specific aims:

1. **Determine if and where RyRs are increased in the TgCRND8 model of AD.**

   It has been demonstrated that RyRs are increased in expression and contribute to Ca^{2+} dysregulation in several mouse models of AD. The specific RyR subtype(s) up-regulated and their distribution in the brain of AD mice have not been determined. An objective of this thesis is to determine if and where RyRs are increased in TgCRND8 mice and identify which RyR subtype(s) are increased (see Chapter 4, page 98).

2. **Determine the contribution of RyRs to cytosolic Ca^{2+} in TgCRND8 neurons.**

   RyRs have contributed to dysregulated intracellular Ca^{2+} signalling in neurons from several mouse models of AD. Neuronal Ca^{2+} regulation in TgCRND8 neurons has not been characterized (see Chapter 2, page 46).

3. **Determine how RyRs are up-regulated in TgCRND8 neurons.**

   Studies have linked increased RyRs in AD models to neurotoxicity in culture, yet the whole animal lacks extensive neurodegeneration. Investigations in this thesis aim to determine how RyRs are increased in TgCRND8 brain (see Chapter 2, page 46).

4. **Determine a physiological role for up-regulated RyRs in AD neurons.**

   The role of RyRs in AD neurons is not well understood. It is an objective of this study to identify a role for RyRs in neuronal physiology (see Chapter 3, page 74 and Chapter 4, page 98).

2. AMYLOID β 1-42 INCREASES RYANODINE RECEPTOR TYPE 3 EXPRESSION AND FUNCTION IN NEURONS OF TgCRND8 MICE

Published: Charlene Supnet, Jeff Grant, Hong Kong, David Westaway and Michael Mayne, *$A\beta_{1-42}$ increases ryanodine receptor-3 expression and function in neurons of TgCRND8 mice*. J Biol Chem, 2006. **281**(50): p. 38440-7.

2.1 ABSTRACT

Disruption of intracellular Ca^{2+} homeostasis precedes neurodegeneration that occurs in AD. Of the many neuronal Ca^{2+}-regulating proteins, we focus on ER-resident RyRs because they are increased in the hippocampus of mice expressing mutant PS1 and are associated with neurotoxicity after treatment with Glu. Others have observed that Ry binding is elevated in human hippocampal regions post-mortem suggesting that RyR(s) may be involved in AD pathogenesis. Here, we report that synthetic Aβ42 specifically increased RyR3, but not RyR1 or RyR2, gene expression in cortical neurons from C57Bl6 mice. Further, endogenously produced extracelluar Aβ42 increased RyR3 mRNA and protein in cortical neurons from transgenic (Tg)CRND8 mice, a mouse model of AD. In experiments performed in nominal extracellular Ca^{2+}, neurons from Tg mice had significant increases in intracellular Ca^{2+} following Ry or Glu treatment compared to littermate controls. Treatment of cortical neurons with small interfering RNA directed to RyR3, abolished the enhanced intracellular Ca^{2+} responses in Tg neurons, indicating that the higher levels of Ca^{2+} originated from RyR3-regulated stores. Taken together, these observations suggest that Aβ42-mediated changes in intracellular Ca^{2+} homeostasis are regulated in part, through a direct increase of RyR3 expression and function.

2.2 INTRODUCTION

AD is characterized by neuritic plaques composed of aggregated extracellular Aβ, intracellular neurofibrillary tangles, hippocampal and cortical neuron dysfunction and synapse loss leading to irreversible cognitive decline and memory impairment (Kelliher et al. 1999). Although the cause of AD is still unknown, it is believed that the accumulation of Aβ in the brain is an initial pathogenic event (Hardy & Selkoe 2002). Aβ is a protein resulting from the endoproteolytic cleavage of the APP by α or β- and γ-secretase into various peptide fragments (LaFerla 2002). Neuritic plaques are composed primarily of two Aβ species that are either 40 or 42 amino acid residues long (termed Aβ40 and Aβ42). Overproduction of Aβ42 leading to the aggregation and deposition of Aβ is associated with both FAD and sporadic AD (Selkoe 2001). Consequently, there is an extensive effort to determine the molecular and cellular actions of Aβ on neurons and glial cells. Aβ has been shown to produce deleterious effects on brain cells, including impairment of synapse and dendrite function in neurons, activation of microglia and astrocytes and ultimately neurotoxicity (Canevari et al. 2004).

Alterations in intracellular Ca^{2+} homeostasis are thought to be an early signalling event involved in the manifestation of AD (LaFerla 2002). Cytosolic Ca^{2+} levels are maintained by voltage-gated, ligand-gated or store-operated Ca^{2+} channels on the plasmalemma and ligand-gated Ca^{2+} channels on the ER (Ghosh & Greenberg 1995). Several studies have indicated that disruption of ER-regulated intracellular Ca^{2+} homeostasis is associated with neurotoxicity in AD (O'Neill et al. 2001). The ER is an important dynamic Ca^{2+} source and sink, and regulates neurotransmitter release, synaptic plasticity, gene expression and signal transduction to the nucleus (Verkhratsky 2002). RyRs and IP_3Rs are the two major Ca^{2+} release channels found on the ER

(Sorrentino et al. 2001) and are activated through Ca^{2+}-induced Ca^{2+} release and IP_3-induced Ca^{2+} release, respectively (Mattson et al. 2000).

This study focuses on the role of RyRs in the regulation of cytosolic Ca^{2+} homeostasis because others have observed that hippocampal brain specimens from AD patients with early cognitive decline have increased Ry binding, suggestive of increased RyR levels (Kelliher et al. 1999). Further, up-regulated RyRs mediated dysregulation of intracellular Ca^{2+} in cortical neurons from other mouse models of FAD (Chan et al. 2000; Lee et al. 2006; Smith et al. 2005). In brain, RyRs are concentrated in dendritic spines, astrocytes and oligodendrocytes, where they regulate cytosolic Ca^{2+} levels, membrane potential and second messenger systems. Three isoforms of RyR exist in brain; RyR1 is prominent in Purkinje cells of the cerebellum (Kuwajima et al. 1992), RyR2 is expressed in the soma of most neurons (Kuwajima et al. 1992) and RyR3 is concentrated in the hippocampus (Giannini et al. 1995), cerebral cortex and corpus striatum (Ogawa 1994). RyR2 is the most abundant RyR in neurons, but previous studies give no indication as to which isoform is important in the dysregulation of cytosolic Ca^{2+} homeostasis in AD neurons.

The mechanism by which Aβ regulates the expression and function of the machinery that mediates the disruption of intracellular Ca^{2+} homeostasis in AD remains unclear. The following studies found that Aβ42 selectively elevated RyR3 mRNA and protein levels in cortical neurons from TgCRND8 mice, a model of AD designed by Chishti and colleagues (Chishti et al. 2001). TgCRND8 mice contain both the Indiana (APP-V717F) and Swedish (APP-KM670/671NL) mutations of the APP, resulting in robust Aβ40 and Aβ42 production (Chishti et al. 2001). Increased RyR3 facilitated significant increases in cytosolic Ca^{2+} levels following Ry or Glu treatment. These observations highlight a possible role for RyR3 in AD pathology.

2.3 MATERIALS AND METHODS

2.3.1 Animals

Experiments using animals were conducted according to the guidelines of the Canadian Council of Animal Care. Protocols were approved by the institutional Animal Care Committees of the University of Manitoba, the University of Prince Edward Island and the National Research Council of Canada. Transgenic (Tg) CRND8 mice were a gift from Dr. D. Westaway (University of Alberta) and described previously (Chishti et al. 2001). TgCRND8 mice were heterozygous for (or contained one copy of) the human APP_{695} double mutant (KM670/671NL+V717F) transgene, while nonTg littermates did not harbour the transgene. TgCRND8 mice were generated on a C57BL/6 X C3H/C57BL/6 background (Chishti et al. 2001).

2.3.2 Breeding and Genotyping of CRND8 mice

NonTg females were used for breeding because Tg females were unable to care for their litters and/or were infertile. Tg males were used for breeding and maintaining the transgene in the colony. The litters that resulted were 1:1 for nonTg and Tg genotypes. Four-week-old non-Tg and TgCRND8 pups were weaned and genotyped for the human APP_{695} double mutation or transgene by polymerase chain reaction (PCR) using the REDExtract-N-Amp Tissue PCR kit (Sigma, Oakville, ON) as per manufacturer's instructions. The sequences of the primers used for the detection of the transgene were (forward, 5' to 3') TGT CCA AGA TGC AGC AGA ACG GCT ACG AAAA and (reverse, 5' to 3') AGA AAT GAA GAA ACG CCA AGC GCC GTG ACT (from Dr. D. Westaway's lab). The 1000 base pair PCR fragment was generated by 25 cycles of 94/68/72°C using the Bio-Rad iCycler (Mississauga, ON) and visualized on a 1.2%

agarose gel (Bio-Rad) stained with 0.4 μg/mL ethidium bromide (Invitrogen, Burlington, ON) under UV illumination.

2.3.3 Primary cortical neuron cultures

Timed-pregnant C57BL/6 or non-TgCRND8 mice were euthanized at gestation or embryonic day 16 (e16) by 50 mg/kg intraperitoneal (i.p.) injection of pentobartital (Euthanyl®, Bimeda-MTC Animal Health Inc.) diluted to 60 mg/mL in phosphate buffered saline (PBS, Sigma), followed by decapitation. Each timed-pregnant dam was considered one n. The fetuses were quickly harvested and immediately placed in ice cold Hank's balanced salt solution (HBSS) from Hyclone (Logan, UT) supplemented with 5 mM HEPES (Sigma) and 25 μg/mL gentamicin reagent solution (Invitrogen). Cerebral cortices were dissected in HBSS and used for primary culture of neurons as described previously (Chan et al. 2000), (see full procedure in **Appendix B**). Briefly, cortices from 3-4 fetuses were pooled and triturated using glass pipettes for cell dissociation. Prior to pooling, CRND8 cortices were maintained on ice in HBSS while being genotyped for the human APP_{695} *double mutation* by PCR. Tissue was then pooled according to genotype prior to dissociation. Dissociated cells were suspended in Neurobasal medium (Invitrogen) containing 10% fetal bovine serum (see **Appendix A**) and seeded at $8X10^5$ cells per well onto poly-D-lysine (Sigma) coated 6-well polystyrene tissue culture plates from BD Biosciences (Mississauga, ON) for mRNA analysis or 25 mm glass coverslips from VWR (Mississauga, ON) for immunocytochemistry (ICC). For detailed poly-D-lysine coating procedure see **Appendix B**. After 18 h at 37°C and 5%CO_2, media was changed to Neurobasal medium supplemented as above but without serum. Experiments were performed on C57BL/6 cultures following 7 days *in vitro* (DIV). Experiments conducted on nonTg or TgCRND8 cultures were completed following 5 DIV to ensure high viability

of Tg neurons. Cultures at 5 DIV were approximately 80% positive for microtubule-associated protein-2 (MAP-2) from Chemicon (Sunnyville, CA), a marker for mature neurons, and 20% positive for glial fibrillary acidic protein (GFAP) from Abcam (Cambridge, MA), a marker for astrocytes by immunocytochemistry (ICC) (see procedure below) (**Figure 2.1.**).

2.3.4 Treatments

Aβ peptide fragments 25-35, 35-25, 1-40, 1-42 and 42-1 from Bachem (Torrance, CA) were prepared as 200 μM stocks in Locke's buffer (**Appendix A**) and incubated at 37°C/5%CO_2 for 24 h prior to use to allow fibril formation. On 6 DIV, C57BL/6 cultures were incubated with 1nM to 10000 nM of each Aβ peptide for 6, 12, 18 and 24 h to induce up-regulation of RyRs. A concentration of 1000nM Aβ42 peptide at 18 h gave consistent up-regulation of RyR3 (see **Appendix C**). Cells were also treated with 20 μM Glu for 18 h or 100 and 1000 nM of ionomycin (Sigma) for 30 min in conditioned media as a control. On 4 DIV, CRND8 cultures were incubated with 1000 nM of Aβ 1-40, 1-42 and 42-1 peptide, 1.3 μg/mL $Aβ_{1-42}$ antibody (rabbit polyclonal IgG) from Biosource International (Camarillo, CA) or as a negative control 1.3 μg/mL glycoprotein-116 (HHV-6) antibody (mouse monoclonal IgG) from Advanced Biotechnologies, Inc. (Columbia, MD) for 18 h in conditioned media.

2.3.5 Reverse-transcriptase (RT)-PCR for mRNA analysis

Total RNA was purified from $8x10^5$ neurons using the GenElute Total Mammalian RNA Isolation Kit (Sigma). Genomic DNA was removed from total RNA samples using DNase I (Sigma). Complete DNA digestion was confirmed by β-actin PCR (**Table I**) of DNase treated RNA samples. β-actin amplification from these samples was indicative of

DNA contamination. One μg of total RNA was reverse-transcribed to cDNA using the First-strand Synthesis Kit from Fermentas Life Sciences

A MAP-2 and GFAP

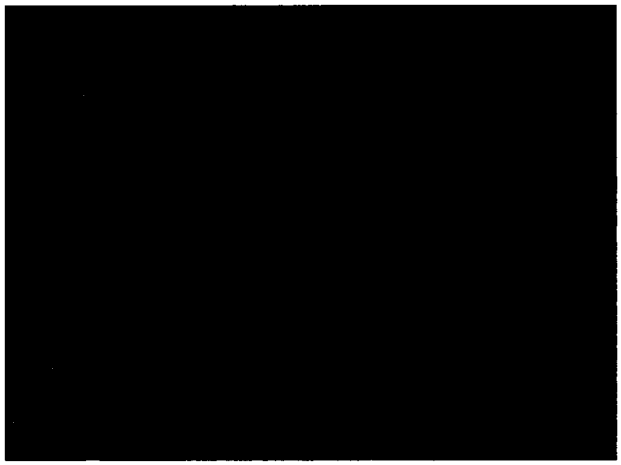

B secondary antibodies only

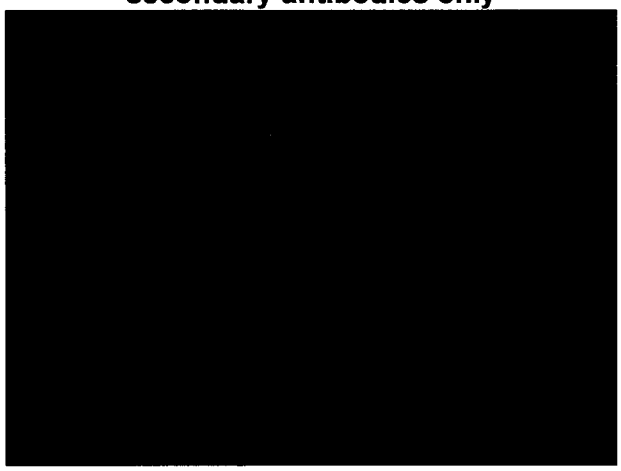

Figure 2.1. Characterization of 5 DIV TgCRND8 primary cortical cultures. A. ICC for MAP-2 positive neurons in red (1:400 dilution) and GFAP positive glia in green (1:10000 dilution) of 5 DIV TgCRND8 primary cortical neurons. Nuclei were stained with 10 μg/mL Hoechst 33342. Images were exposed for 180 ms. **B.** Controls stained with secondary antibodies only (1 in 10000 dilution). Image was taken using the fluorescein isothiocyanate (FITC) channel. Under the rhodamine channel, image was similar.

Table I. Primer sequences for RT-PCR of ER-resident Ca^{2+} channels and pumps

Gene	Forward Primer (5' to 3')	Reverse Primer (5' to 3')	Ta* (^{O}C)/# of Cycles/ Product Size (bp**)
β-actin	ATGGATGACGATATCGCTGC	CGTACATGGCTGGGGTGTTG	53/25/399
RyR1	CTCTTCTGGGGCATTTTGACTCT	ACCCTCCCTGGCCTTCTCTATCGT	53/35/456
RyR2	GAATCAGTGAGTTACTGGCATGG	CTGGTCTCTGACTTCTCCAAAAGC	53/30/650
RyR3	GGCGCTGCGGAAGACCTACAC	GCCGGGCCGAAGCAC TC	53/35/699
IP_3R1	TCATGGAAAGCAGACACGAT	CCGCTCTGTGGTGTAATATA	54/30/404
SERCA2b	GGGAGTGGGGCAGTGGCAGC	CGTCTCTCTGGGCTGAGGGG	62/30/350

Ta* = annealing temperature

bp** = base pairs

(Burlington, ON). PCR amplification of RyR1 and RyR3 was conducted as outlined previously (Chan et al. 2000) using T*aq* Master Mix from QIAGEN (Mississauga, ON). RyR2, IP_3R1, SERCA2b and β-actin primers were designed using Vector NTI (Invitrogen) and cycle parameters are described in **Table I**. Alignment analysis of each primer was conducted to ensure that they were gene- and/or isoform-specific. PCR products were visualized on a 1.2% agarose gel (Bio-Rad) stained with 0.4 μg/mL ethidium bromide (Invitrogen) under UV illumination. Densitometric analysis of PCR products was performed using NIH Scion Image software (version 1.60). RyR pixel density levels subtracted from background were normalized to β-actin levels and are depicted as fold changes, where the untreated condition was considered 1 fold.

2.3.6 Immunocytochemistry

After experimental treatments, CRND8 cultures on 25 mm glass coverslips were fixed with 4% paraformaldehyde (Fisher Scientific) in phosphate buffered saline (PBS, Sigma) on 5 DIV for 12 min at 37°C and 5%CO_2 and permeabilized with HEPES-Triton buffer (**Appendix A**) for 10 min at room temperature. Coverslips were blocked with 5% goat serum (Sigma) in PBS for 1 h at room temperature and incubated with 1:1000 dilution of RyR isoform-specific antibodies (Rossi et al. 2002) in blocking buffer overnight at 4°C. Coverslips were washed twice with PBS + 0.1% Tween 20 (PBST) then incubated for 1 h at room temperature with 1:1000 dilution of AlexaFluor 488 secondary antibody from Molecular Probes (Burlington, ON) in blocking buffer. Nuclei were stained using Hoechst 33342 (Sigma) at 10 μg/mL for 30 s and coverslips were washed twice with PBST. Coverslips were mounted on glass slides (VWR) using FluorSave Reagent from Calbiochem (San Diego, CA). Cells were imaged using an Axioskop 2 *plus* with

Axiovision Release 4.2 software from Carl Zeiss Canada, Ltd. (Toronto, ON). For detection of RyRs, all images were exposed for 260 ms under the FITC channel.

2.3.6 Small Interfering RNA (siRNA) Design and Delivery

siRNAs were generated as per manufacterer's instructions using the Dicer siRNA Generation Kit (Genelantis, San Diego, CA) and were based on the rabbit RyR3 mRNA sequence (accession number: X68650). The region of the RyR3 mRNA chosen showed 88% alignment with mouse RyR3, 9.6% with mouse RyR2 and 0% with mouse RyR1 after BLAST analysis. Primers used to amplify the region of RyR3 from plasmid for diced siRNA generation were specific to mouse and rabbit RyR3 as determined by alignment analysis: (forward, 5' to 3') TCA TCT CTC GAT ATC GAA TGG and (reverse, 5' to 3') GGA AGG TCA TAC TCC AT. Tg neurons seeded at $8X10^5$ per well in 6 well plates were transfected with 200 ng of siRyR3 or nonspecific control siRNA (Qiagen, Mississauga, ON) using 3 μL of GeneSilencer® siRNA Transfection Reagent (GSR, Genelantis) per mL of conditioned media for 24 h. Gene silencing was detected 72 h post-transfection by RT-PCR and ICC as described previously. Transfection efficiency was determined using 1 μg of AlexaFluor 546® labeled nonspecific siRNA (Qiagen) and calculated as the number of nuclei localized with siRNA ÷ total number of nuclei X 100%.

2.3.8 Western Blot Analysis

After siRNA treatments, neurons were washed with PBS and 100 μL of non-denaturing lysis buffer (**Appendix A**) was added to each well. Samples were incubated on ice for 1 h, collected and centrifuged at 950X*g* to pellet insoluble proteins. Supernatant containing soluble protein was collected and total protein was determined using the *DC* Protein Assay (BioRad) as per manufacturer's instructions. Soluble protein

(125 μg) was resolved on a 3-8% tris-acetate NuPAGE® gradient gel (Invitrogen) and separated after running at 150 volts (V) for 1.25 h at room temperature. Proteins were transferred under reducing conditions onto 0.4 μm polyvinylidene fluoride membranes (Fisher Scientific, Ottawa, ON) on ice at 20 V for 24 h at 4°C. NuPAGE® tris-acetate sodium dodecyl sulphate running buffer (20X) and NuPAGE® transfer buffer were purchased from Invitrogen and used as per manufacturer's instructions. Membranes were blocked with 5% non-fat milk in tris-buffered saline (TBS, **Appendix A**) for 1 h at room temperature and incubated with 1:1000 dilution of RyR1, RyR2, or RyR3 antibodies in blocking buffer overnight at 4°C. Isoform-specific RyR rabbit polyclonal antibodies were a gift from Dr. V. Sorrentino, University of Siena, Italy. The same membranes were probed for actin (Santa Cruz Biotechnology, Santa Cruz, CA) and incubated with 1:1000 dilution in blocking buffer overnight at 4°C. Membranes were washed twice with TBS + 0.1% Tween 20 (TBST) (Fisher Scientific) and incubated with 1:1000 dilution of the appropriate secondary antibodies (Jackson ImmunoResearch Laboratories, Inc., West Grove, PA) in blocking buffer for 1 h at room temperature. Membranes were washed twice with TBST, incubated with BM Chemiluminescence Blotting Substrate (Roche Diagnostics) for 1 min at room temperature and imaged using the ChemiDoc™ XRS System (Bio-Rad). NIH Image software, version 1.60 was used to obtain pixel density levels of proteins. RyR levels were normalized to actin levels and are depicted as fold changes, where the untreated condition is considered 1 fold.

2.3.9 Measurement of Free Intracellular Ca^{2+}

Free intracellular Ca^{2+} levels were detected using fluorescence ratio microscopy as described elsewhere (Chan et al. 2000), using the Ca^{2+} indicator dye Fura-2 (Molecular Probes). Fura-2-acetoxymethylester (AM) is internalized then de-esterified by

live cells and subsequently is maintained in the cytosol. Upon Ca^{2+} binding, the fluorescent excitation maximum of Fura-2 undergoes a shift from 380 nm (Ca^{2+}-free) to 340 nm (Ca^{2+}-bound), while the fluorescence emission maximum is relatively unchanged at ~510 nm. Intracellular Ca^{2+} levels are depicted as a ratio of 340/380 nm signal emitted at 510 nm. Briefly, 8 X 10^5 cells were loaded with 1 μg/mL of Fura-2-AM in Locke's buffer (**Appendix A**) with 0.1% bovine serum albumin (Fisher Scientific) for 30 min. Experiments were performed in nominal extracellular Ca^{2+} (Locke's buffer without $CaCl_2$). Glu (**Appendix A**) and Ry treatments were delivered to cells by perfusion using a peristaltic pump with a flow rate of 0.5 mL/min (Instech, Plymouth Meeting, PA) and switching between perfusion solutions was achieved using solenoid valves (Valvelink 8 controller, Automate Scientific, Berkeley, CA). Ry (Ry, Sigma) was prepared as a stock solution of 50 mM in 100% dimethylsulfoxide (DMSO, Sigma). Cells were imaged at 40X with a heated oil objective lens using a closed-chamber system (Bioptechs) on an inverted-Zeiss microscope with a CoolSnapHQ camera (Roper Scientific Inc., Trenton, NJ). Changes in intracellular Ca^{2+} levels were determined using Stallion Imaging software (Downingtown, PA). Each experiment was repeated at least 3 separate times, 15-30 cells imaged at each time. Of the cells imaged, data were pooled from cells that responded to both Glu and Ry. Area under the curve (AUC) calculations are the ratio of 340/380 nm multiplied by time and depicted in arbitrary units (A.U.)

2.3.10 Trypan Blue exclusion assay

Trypan Blue is a stain for use in estimating the proportion of viable cells in a population (Phillips et al. 1957). The chromophore is negatively charged and does not react with the cell membrane unless it has been compromised; therefore live (viable) cells do not take up the dye and dead (non-viable) cells do. After treatment, cultures

were washed once with PBS, then stained with trypan blue (Invitrogen) diluted 1:1 with PBS for 5 min. Cultures were washed with PBS and for cell counts images were taken using a Nikon 4500 digital camera under a light microscope with a magnification of 100X.

2.3.11 Statistical Analysis

Densitometric analysis was performed using NIH Scion Image software, version 1.60. Data were analysed using GraphPad Prism, version 3.02 (San Diego, CA). One-way ANOVA with Tukey's post-test was performed to determine the difference between means after treatment. Differences were considered significant at $p<0.05$. All data are presented as mean ± standard error (S.E.).

2.4 RESULTS

2.4.1 Aβ induced RyR3 mRNA expression in primary cortical neurons

To test the hypothesis that Aβ directly increased RyR mRNA levels, C57Bl6 cortical neurons were treated with Aβ42 peptide (1000 nM) for 18 h (see **Appendix C** for dose-response and time-response of Aβ42 peptide) and analyzed for RyR mRNA levels (**Figure 2.2. A**). As determined by RT-PCR, C57Bl6 primary cortical cells incubated with 1000 nM Aβ42 increased RyR3 mRNA levels 3.5 ± 1.38 fold (n=4, ***p<0.001, one-way ANOVA, Tukey's post-test). Though not statistically significant, RyR1 mRNA increased approximately 2.4 ± 0.84 fold. Treatment with Aβ25-35, Aβ35-25, Aβ1-40 and Aβ42-1 peptides did not alter RyR gene expression in primary cortical neurons from C57Bl6 (**Figure 2.2. A**). Further, identical treatments did not alter RyR2, IP_3R1 or SERCA2b mRNA levels (**Figure 2.2. B**). To determine if rapid increases in intracellular Ca^{2+} are involved in the up-regulation of RyR gene expression, C57Bl6 primary cortical neurons were treated with an ionophore, ionomycin, at various concentrations for 30 min. The treatment was removed and replaced with conditioned media for 18 h at 37°C. Consistent with the observations made in a previous study (Genazzani et al. 1999), we did not see an induction of RyR gene expression after treatment with ionomycin (n=2). Cell viability was unaltered by a 30 min treatment with ionomycin as assessed 18 h after treatment using the trypan blue exclusion assay (**Figure 2.3.**).

2.4.2 Aβ increased RyR3 mRNA and protein levels in CRND8 cortical neurons

Based on the observations that Aβ increased steady state levels of RyR3 mRNA in naïve cortical neurons (**Figure 2.2. A**), it was hypothesized that the cortical neurons of TgCRND8 mice had increased RyR gene expression. Primary neuronal cultures from Tg mice had an increase of approximately 3.6 ± 0.71 fold (n=3,

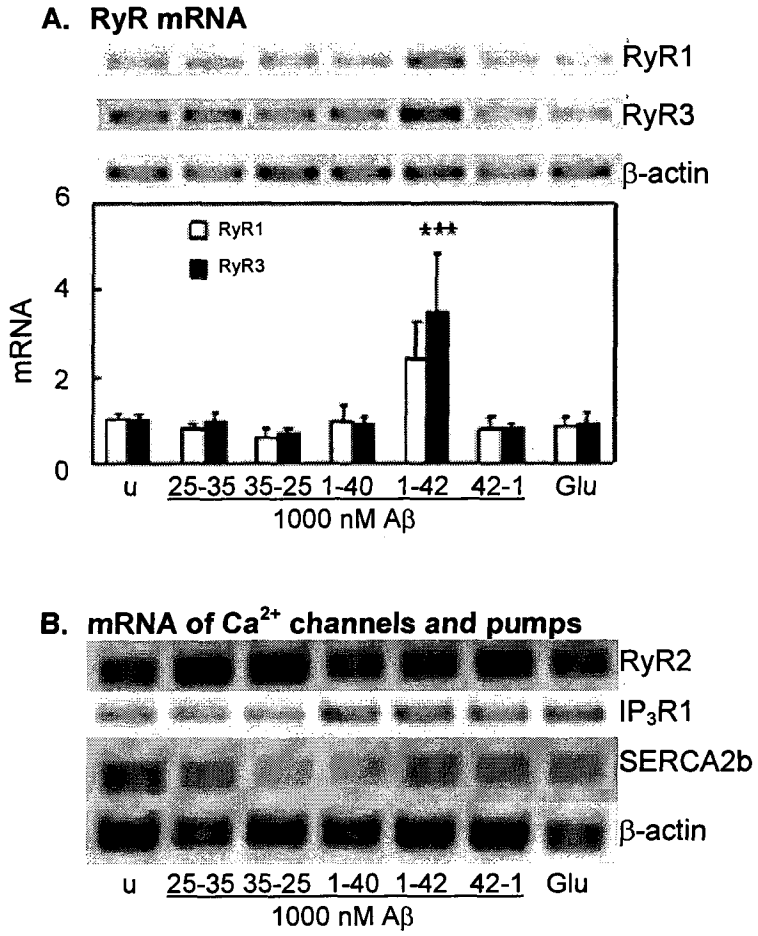

Figure 2.2. Aβ42 increases RyR expression in C57Bi6 corticai neurons. A. A representative agarose gel showing relative levels of RyR RT-PCR products from C57Bl6 cells. Neurons (*in vitro* culture day 8) were treated with 1000nM of various Aβ peptide fragments for 18 h. Relative RyR1 and RyR3 RT-PCR products were normalized to β-actin levels. Neurons were treated with 20 μM of Glu as a stress response control. Values are the mean and S.E. of fold change determinations made in samples from 4 cultures, ***$p<0.001$ compared with values for untreated (u) cells (one-way ANOVA with Tukey's post-test). **B.** A representative agarose gel of 2 separate experiments showing RT-PCR products of RyR2, IP_3R1 and SERCA2b after treatment with various Aβ peptide fragments as in **A.**

A. RyR mRNA

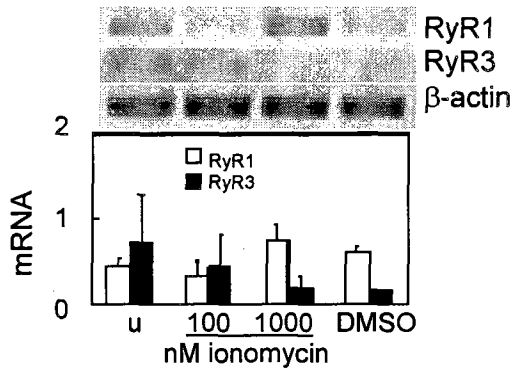

B. trypan blue assay

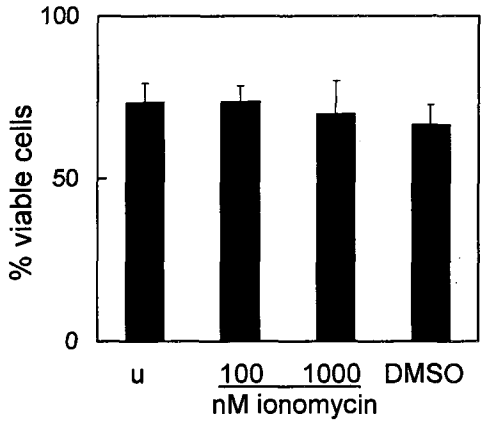

Figure 2.3. RyR expression is not up-regulated by increases in intracellular Ca^{2+}. **A.** A representative agarose gel showing relative levels of RyR1 and RyR3 RT-PCR products normalized to β-actin from C57Bl6 primary cortical neurons treated acutely with ionomycin for 30 min and DMSO vehicle. Untreated (u) and treated neurons were collected 18 h after treatment. **B.** Percentage of the cell population that was viable 18 h after ionomycin treatment by trypan blue assay. Values are the mean and S.E. of samples from 2 separate experiments.

***p<0.001, one-way ANOVA, Tukey's post-test) in RyR3 mRNA levels as determined by RT-PCR compared to nonTg littermate controls on in vitro day 5 (**Figure 2.4. A**). Aβ42 treatment of nonTg neurons increased gene expression of RyR3 3.1 ± 0.17 fold compared to untreated (n=3, ###p<0.001, one-way ANOVA, Tukey's post-test) to levels comparable to those expressed in Tg neurons (**Figure 2.4. A**). It was also determined that Aβ1-42 did not increase RyR3 further in Tg neurons. Treatments with other fragments including Aβ1-40 and Aβ42-1 did not influence RyR3 gene expression. IP_3R1 and SERCA2b mRNA levels did not vary between nonTg and TgCRND8 neurons (not shown). To further understand the relationship between Aβ and RyR3 gene expression, TgCRND8 neurons were treated with Aβ42 antibody (1.3 μg/mL) for 18 h. Quenching of extracellular Aβ42 decreased neuronal RyR3 mRNA levels in Tg neurons by 2.2 ± 0.30 fold (n=3, ###p<0.001, one-way ANOVA, Tukey's post-test) to levels similar to that observed in nonTg littermates (**Figure 2.4. B**). Statistical tests reveal that these differences in RyR3 expression are attributed to the genotype (p<0.0001) and specific to the type of treatment (p= 0.0056). To determine relative RyR protein levels in non-Tg and TgCRND8 neurons, an ICC was performed using isoform specific RyR antibodies. RyR3 levels were markedly increased in TgCRND8 primary cortical neurons compared to their nonTg littermate control cultures (**Figure 2.4. C**) while RyR1 and RyR2 levels had not changed (p>0.05). Similarly, nonTg neurons treated with Aβ42 (1000 nM) for 18 h had increased RyR3 levels comparable to Tg neurons. RyR1 and RyR2 levels did not change (p>0.05).

2.4.3 Targeting RyR3 by gene silencing

It was reported recently that RyR levels are increased in other models of AD and

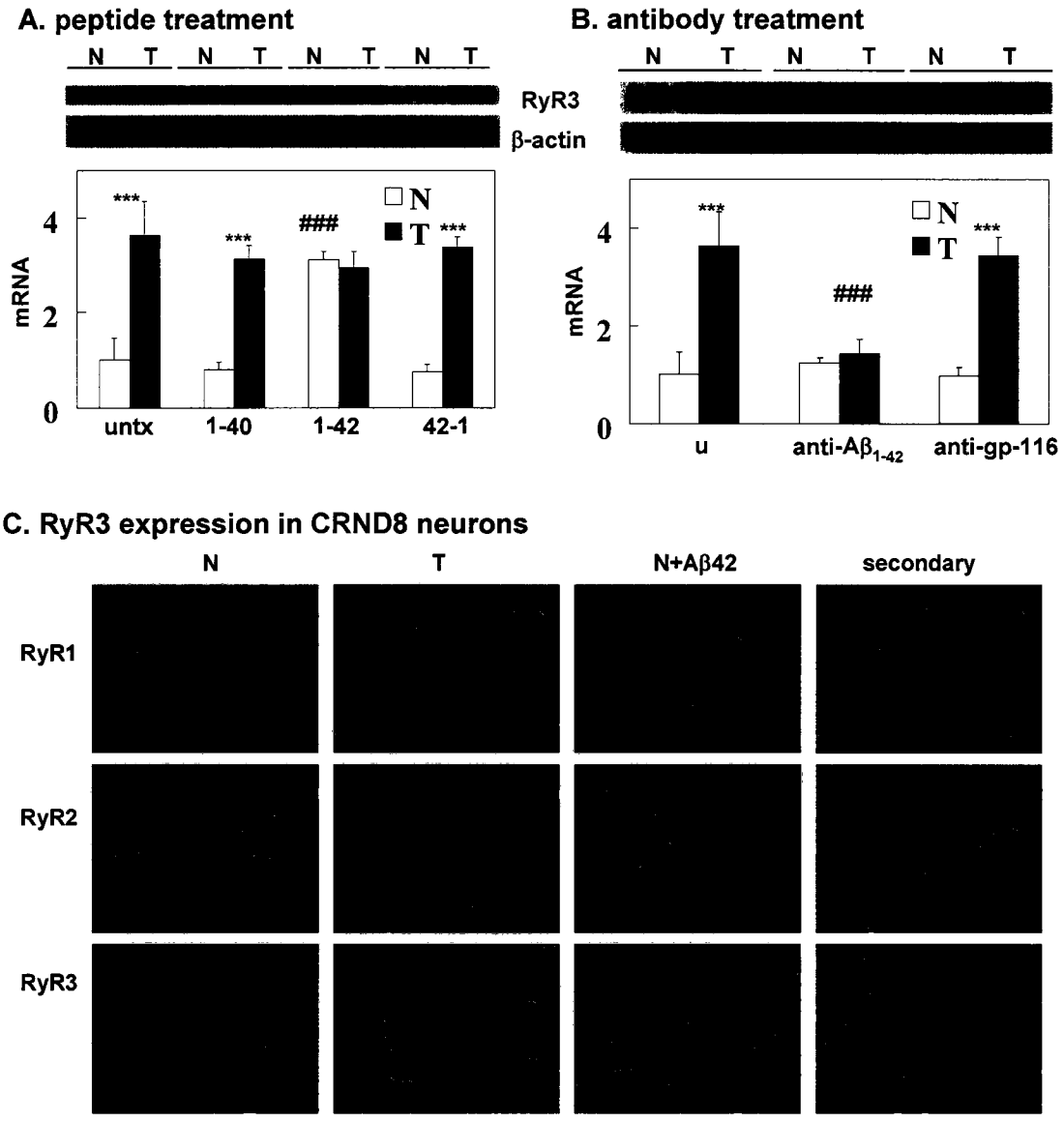

Figure 2.4. Aβ42 increases RyR3 expression in TgCRND8 cultures A. A representative agarose gel showing fold changes of RyR3 RT-PCR products from e16 CRND8 primary cortical neurons. 4 DIV cultures were treated with 1000nM Aβ peptides as before (**Figure 2.2. A**). Cells were collected after 5 DIV. NonTg (N) are littermate controls and Tg (T) neurons are heterozygous for the APP_{695} double mutation. Values are the mean and S.E. from 3 separate cultures. T values were compared to controls (N) at all treatments (***$p<0.001$) and Aβ treated N values were compared to untreated (u) N (###$p<0.001$, one-way ANOVA with Tukey's post-test). **B.** A representative agarose gel showing fold changes of RyR3 RT-PCR products from 4 DIV cultures treated with 1.3 μg/mL $Aβ_{1-42}$ antibody or 1.3 μg/mL gp-116 antibody (antibody control) for 18 h at 37°C before analysis. Values are the mean and S.E. from 3 separate cultures. T values were compared to controls (N) at all treatments (***$p<0.001$) and anti-Aβ treated T values were compared to untreated T (###$p<0.001$, one-way ANOVA with Tukey's post-test). **C.** ICC for RyR1, RyR2 and RyR3 protein in N and T cultures and is representative of 3

separate cultures. N was treated with Aβ42 as in **A.** Cells were imaged at 400X magnification.

as a result neurons from transgenic mice have elevated responses to 20-25 mM caffeine (Smith et al. 2005; Stutzmann et al. 2006). Given the observations showing increased RyR3 levels in TgCRND8 neurons, the involvement of RyR3 in the elevated response was determined. Due to a lack of pharmacological tools to selectively block RyR3, a molecular approach was used to target RyR3 and depress its expression in Tg neurons prior to Ca^{2+}imaging studies. At 72 h post-transfection, RyR3 levels were significantly decreased by 2.9 ± 0.47 fold compared to untreated (n=4, $^{###}p<0.001$, one-way ANOVA, Tukey's post-test) and were comparable to nonTg neurons (**Figure 2.5. A**) while RyR1 and RyR2 levels did not change (fold changes not shown). Tg neurons treated with GSR, siRyR3 alone, non-specific siRNA alone (200 ng) and siRNA with GSR did not show significant changes in RyR1, 2 or 3 (**Figure 2.5. A**) mRNA levels. To determine the transfection efficiency of the siRNA experiments, Tg neurons were transfected with AlexaFluor 546 labelled non-specific siRNA (1 µg) under the same conditions as the siRyR3 experiments. A transfection efficiency of 74.2 ± 8.3 SE % (n=4 (12 separate fields total), $^{***}p<0.001$, one-way ANOVA, Tukey's post-test) was obtained at 72 h post-transfection (**Figure 2.5. B**). Knock-down of RyR3 protein levels in Tg neurons was confirmed by Western blot using isoform specific antibodies (n=3, **Figure 2.5. C**). At 72 h post-transfection, RyR3 levels were reduced to 1.79 fold ± 5.4 SE ($^{*}p<0.05$, one-way ANOVA, Tukey's post-test) that of untreated Tg neurons. This is a reduction of 44.4 ± 4.5 SE %. RyR1 and RyR2 levels were unchanged after any treatment (fold changes not shown).

2.4.4. Calcium released from ER stores is increased in TgCRND8 neurons expressing elevated levels of RyR3

To determine a functional consequence of increased levels of RyR3 in TgCRND8 mice, intracellular Ca^{2+} levels of neurons were measured after treatments of Glu and Ry.

A. siRyR3 treatment of CRND8 neurons

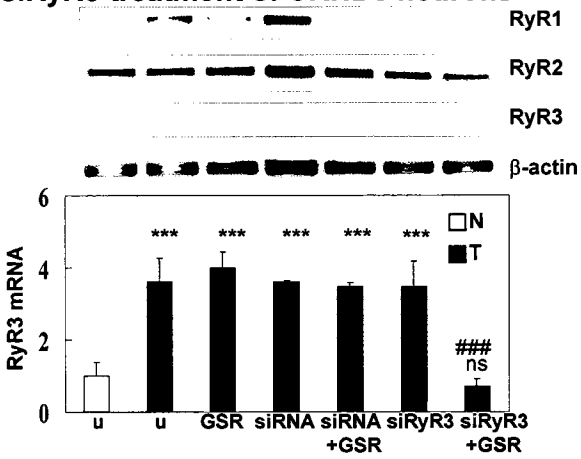

B. siRNA transfection efficiency

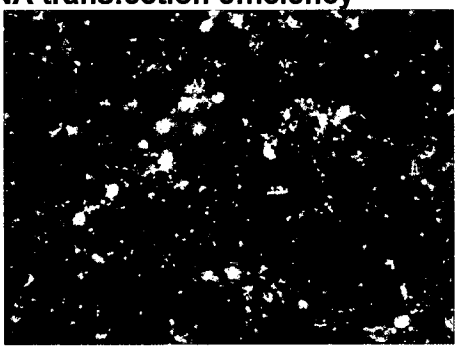

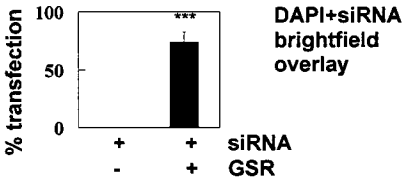

C. RyR3 protein levels after siRyR3

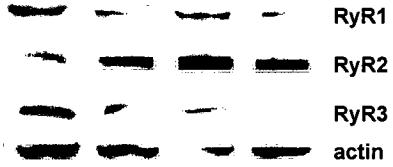

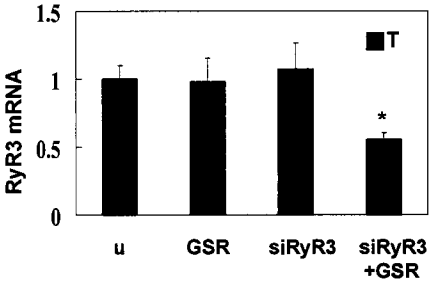

Figure 2.5. Levels of RyR3 mRNA and protein are decreased in TgCRND8 neurons after treatment with siRNA. A. is a representative agarose gel showing fold changes of RyR1, RyR2 and RyR3 RT-PCR products from nonTg (N) and TgCRND8 (T) $8.0X10^5$ primary cortical neurons treated with siRNA. RT-PCR analysis was conducted 72 h post-transfection. The treatments include untreated (u), 3 μL Gene Silencer Reagent (GSR), 200 ng control siRNA (siRNA) or 200 ng siRyR3. The graph shows the relative expression of RyR3. Values are the mean and S.E. of the fold change of RyR3 RT-PCR levels from 4 cultures each of N and T. T values were compared to untreated (u) littermate (N) at all treatments (no statistical difference (ns), $^{***}p<0.001$) and T+siRyR3+GSR was compared to untreated T ($^{\#\#\#}p<0.001$, one-way ANOVA with Tukey's post-test). **B.** is an image of T neurons transfected with 1 μg of AlexaFluor 546® labelled nonspecific siRNA at 72 h post-transfection. Nuclei were labelled with Hoechst 33342 and imaged under DAPI. The graph shows the transfection efficiency of GSR and is data pooled from 3 separate experiments. siRNA+GSR was $^{***}p<0.001$ (one-way ANOVA with Tukey's post-test) $p<0.001$ siRNA treatment alone. **C.** is a representative immunoblot for RyR1, RyR2 and RyR3 of T neurons treated with siRyR3 as in panel ***A*** and is representative of 3 separate cultures. The graph is representative of the RyR3 protein levels relative to actin and values are the mean and S.E. of the fold change of RyR3. $^{*}p<0.05$ (one-way ANOVA with Tukey's post-test) compared to untreated.

Experiments were conducted in the presence of nominal extracellular Ca^{2+} to minimize the contribution of Ca^{2+} influx because of the interest in the contribution of ER stores to the overall cytosolic Ca^{2+} response. Increased intracellular Ca^{2+} levels due to Glu are closely associated with neurotoxicity (Glazner et al. 2000; Guo et al. 1999; Jarvis et al. 1999; Kim et al. 2000; Mattson et al. 2001). Therefore, the effect of increased RyR3 on Ca^{2+} responses in Tg neurons was determined. TgCRND8 neurons at 5 days *in vitro* demonstrated an elevated intracellular Ca^{2+} response to 250 μM Glu treatment as compared to nonTg littermate controls (**Figure 2.6. A**), with a peak of 0.67 ± 0.01 SE Fura-2 fluorescence ratio 340/380 nm (n=15, ***p<0.001, one-way ANOVA, Tukey's post-test) for Tg neurons in contrast to 0.55 ± 0.03 SE 340/380 nm for nonTg (n=18) (**Figure 2.6. B**). To determine the contribution of RyR3 to the observed increases in intracellular Ca^{2+} levels, Tg neurons were treated with siRyR3 for 72 h prior to Ca^{2+} imaging experiments. Knock-down of RyR3 levels resulted in a decreased Ca^{2+} response of Tg neurons to Glu (**Figure 2.6. A**), with a peak response of 0.52 ± 0.02 SE ratio 340/380 nm (**Figure 2.6. B**) that was significantly lower than nonTg (0.55 ± 0.06 SE, n=15, *p<0.05, one-way ANOVA, Tukey's post-test).

To determine the direct contribution of RyR-gated Ca^{2+} stores to intracellular Ca^{2+} levels, we performed experiments using 100 nM of Ry in the presence of nominal extracellular Ca^{2+}. After treatment of Glu, ER stores become charged with Ca^{2+} which is then available for Ca^{2+} liberation (Shmigol et al. 1994). TgCRND8 neurons had increased intracellular Ca^{2+} levels after 100 nM Ry treatment (**Figure 2.6. A**), with a peak response of 0.50 ± 0.01 SE ratio 340/380 nM (n=15, ***p<0.001, one-way ANOVA, Tukey's post-test) as compared to littermate controls (**Figure 2.6. C**). siRyR3 treatment of Tg neurons prior to the experiment reduced the Ca^{2+} response to Ry (**Figure 2.6. A**) to peak levels that were not significantly different than nonTg (**Figure 2.6.C**).

A. CRND8 neurons in nominal extracellular Ca^{2+}

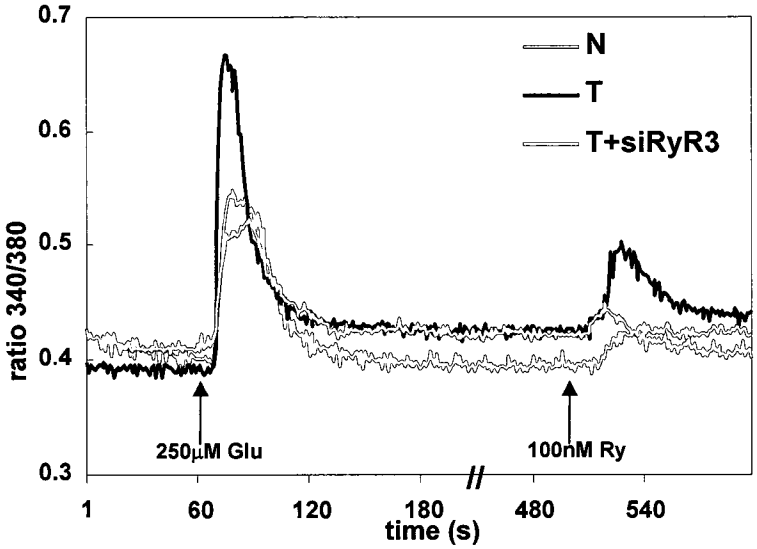

B. peak ratio and area under the curve

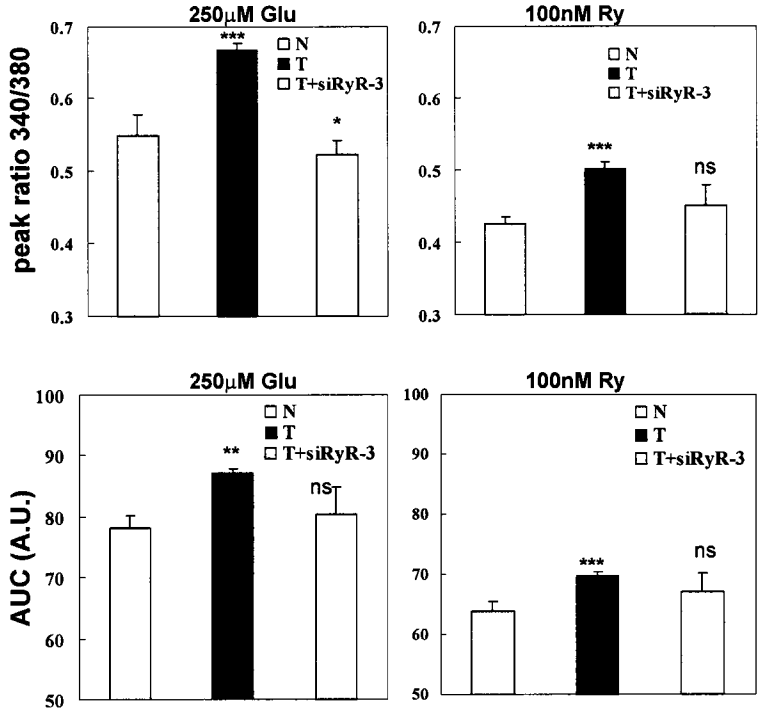

Figure 2.6. Ca^{2+} release from ER stores was significantly enhanced in TgCRND8 cortical neurons due to up-regulated RyR3 compared to littermate controls. A. A representative recording of the average changes in Fura-2 340/380 nm ratios of nonTg (N), Tg (T) and T+siRyR3 neurons in the presence of nominal extracellular Ca^{2+}. The arrows represent the application of Glu or Ry and were applied for 2 min. The traces are representative of at least 3 separate experiments, n= 15 (N), n=18 (T) and n=12 (T+siRyR3). **B.** Graphs showing the average peak response and area under the curve

(AUC) of the corresponding traces in **A.** Values are mean and S.E. of at least 3 experiments. No statistical significance (ns), *p<0.05, **p<0.01 and ***p<0.001 compared to N (one-way ANOVA with Tukey's post-test).

To determine the role of ER Ca^{2+} load in the Ca^{2+} response of the neurons, the area under the curve (AUC) of the Fura-2 traces was calculated (**Figure 2.6. D** and **E**), which represents the total amount of Ca^{2+} being liberated from the ER after Glu or Ry treatment. In both instances, Tg neurons had higher levels of ER Ca^{2+} released after agonist treatment (n=15, $^{**}p<0.01$, $^{***}p<0.001$, one-way ANOVA, Tukey's post-test) compared to littermate controls. After knock-down of RyR3 levels by siRyR3 treatment, Tg neurons had similar AUC values to nonTg littermates.

2.5 DISCUSSION

Several studies now clearly implicate a role for RyRs in the development and progression of AD (Chan et al. 2000; Lee et al. 2006; Smith et al. 2005; Stutzmann et al. 2006). Findings here have implicated RyR3 as a key player in altering cytosolic Ca^{2+} homeostasis of neurons in response to Aβ. The *in vitro* studies show that Aβ42, regardless of the source of peptide (endogenously produced or synthetic), increased levels of RyR3. As a direct consequence, Tg neurons had exaggerated cytosolic Ca^{2+} responses to Ry and to Glu, which can trigger CICR from RyR stores (Arundine & Tymianski 2003; Clodfelter et al. 2002; Emptage et al. 1999; LaFerla 2002; Linn et al. 2001). Second, after knock-down of RyR3 levels by siRNA, Ca^{2+} imaging experiments confirmed that the RyR3 specifically was involved in the Glu-induced increase in Ca^{2+} in Tg neurons.

The impact of dysregulated Ca^{2+} homeostasis as a result of increased RyR3 in AD is still unclear. The function of RyR3 in brain is yet to be determined, although their relative abundance in neurons of the hippocampus suggests a role for RyR3 in hippocampal Ca^{2+} regulation (Giannini et al. 1995). The generation of RyR3 knock-out mice has given some insight into its function. Two independent groups have generated RyR3 knock-out mice and each performed electrophysiological and behavioral studies to determine the role of RyR3 in synaptic plasticity and hippocampus-dependent learning (Balschun et al. 1999; Futatsugi et al. 1999). Both groups demonstrated evidence of increased LTP, a physiological correlate for learning and memory, after particular types of stimulation, namely short or weak tetanus, suggesting a role for RyR3 in the depression of LTP and long-term depression (LTD). However, after subjecting the RyR3 deficient mice to the Morris water maze to assess spatial learning competencies, the two groups came to contradictory conclusions. While Futatsugi *et al.* showed that mutant mice had enhanced spatial learning, which would be expected if RyR3 mediated the

depression of LTP , Balschun *et al.* observed that RyR3 knock-outs had significant deficiencies in their ability to acquire new information compared to mice with wild-type RyR. Interestingly, it has been shown that RyR-mediated Ca^{2+} release from post-synaptic CA1 (Nishiyama et al. 2000; Reyes & Stanton 1996) or pre-synaptic CA3 (Reyes & Stanton 1996; Unni et al. 2004) neurons is required for the induction of LTD. Of the three different RyR isoforms, RyR3 would be the likely candidate for the fine-tuning of these synaptic changes. RyR3 is less sensitive to Ca^{2+} in comparison to RyR1 and RyR2 and therefore requires higher cytosolic Ca^{2+} levels to be activated and deactivated (Bouchard et al. 2003). Taken together, these observations suggest that RyR3 may contribute to synaptic plasticity by modulating the balance between LTP and LTD and the up-regulation of RyR3 could be a response to an increase in neuronal excitability.

Such a mechanism could be at play in AD and the up-regulation of RyR3 might be an effort mounted by neurons to protect against the increased excitability brought about by the pathology of AD, specifically Aβ accumulation, by suppressing LTP or enhacing LTD. Other aspects of intracellular Ca^{2+} signalling in AD neurons are also enhanced, in particular NMDA receptor (Rogawski et al. 2003) and IP_3R (Stutzmann 2005) -mediated signalling, leading to increased excitotoxicity. Stutzmann *et al.* showed that RyR Ca^{2+} stores were directly responsible for the exaggerated hyperpolarization responses of PS1 mutant neurons to IP_3 (Stutzmann et al. 2006) and therefore impacted membrane excitability. Furthermore, RyR3 mRNA was transiently increased in mouse brain after kainic acid-induced status elipticus (Mori et al. 2005), implicating a role in modulating excitability. Higher levels of RyRs could be considered advantageous in protecting against the putative excitotoxicity in AD but the implications of chronic up-regulation of RyR3, which could occur as long as Aβ is being produced, might lead to the opposite effect. As the balance of excitation and depression are skewed, the resulting effect could be an increase to overall Ca^{2+} levels, oxidative stress and activation of

pathways leading to toxicity and neurodegeneration (Chan et al. 2000; Lee et al. 2006; Mori et al. 2005). Further studies are required to resolve why RyR3 is being up-regulated so significantly and specifically in TgCRND8 mice.

The results of our study describe a mechanism by which Aβ contributes to the dysregulation of intraneuronal Ca^{2+} homeostasis, namely by up-regulating the expression and function of a specific ER Ca^{2+} release channel, RyR3. There is much evidence to suggest that RyR Ca^{2+} pools play an important role in the neuronal dysfunction initiated by Aβ deposition in AD (Chan et al. 2000; Lee et al. 2006; Smith et al. 2005; Stutzmann et al. 2006). Our findings further focus on RyRs and implicate RyR3 as the primary ER channel that facilitates Ca^{2+} disruption in AD. This information could be significant in understanding the neurobiology of AD pathology. RyR(s) may play a role in normal aging as well as contributing to AD pathology. In a report by Lu *et al.*, RyR1 mRNA was increased significantly in aged human cortical tissue from individuals that were not demented, which suggests that increased RyRs may have a protective or positive role to play in neuronal function (Lu et al. 2004). Further, it has been recently shown that RyR3 mRNA and protein levels are increased in the superior cervical ganglia of aged rats and may serve to protect neurons from oxidative stress by modulating and increasing the protein expression of neuronal nitric oxide synthase (nNOS) (Vanterpool et al. 2006). A clearer picture of how RyRs are involved in balancing normal and pathological ageing is required before they can be considered a feasible therapeutic target.

3.INCREASED RYANODINE RECEPTOR TYPE 3 IS NEUROPROTECTIVE IN TgCRND8 PRIMARY CORTICAL CULTURES

Submitted: Charlene Supnet, Charmaine Noonan, Kelly Richard, John Bradley and Michael Mayne. Up-regulation of the type 3 ryanodine receptor is neuroprotective in the CRND8 mouse model of Alzheimer's disease. J Neurochem, July 2009.

3.1 ABSTRACT

The cellular pathology of AD is progressive and protracted leading to considerable neuronal death. The underlying mechanisms of AD pathology are complex, but subtle changes in the control of intracellular Ca^{2+} are believed to contribute to neurodegeneration. Because neurons from other AD mutants showed increased RyR expression leading to neurotoxicity, the objective of this study was to determine the effect of increased expression of RyR3 on TgCRND8 neuronal viability. Data showed that Tg neurons were no more sensitive to cell stressors (Glu, hydrogen peroxide (H_2O_2), staurosporine (STS) and time in culture) than compared to nonTg neurons, in spite of having up-regulated RyR3. Considering these observations combined with the knowledge that Tg mice lack overt neurodegeneration, it was hypothesized that increased RyR3 was involved in maintaining Tg neuron viability. Interestingly, after treatment with siRNA directed to RyR3 to suppress its up-regulation, Tg cultures at 18 DIV showed a 50% decrease in viability, as assessed by MTT assay, compared to Tg treated with control siRNA cultures. After staining with the neuron marker NeuN, the signal intensity in Tg treated with siRyR3 cultures was decreased 50% compared to Tg treated with control siRNA and nonTg cultures. One possible mechanism by which RyR3 up-regulation may prevent neuronal death is by suppression of Aβ42 synthesis. However, no difference in the ratio of Aβ42/Aβ40 was detected in the media of TgCRND8 neurons in which RyR3 was knocked down compared with untreated TgCRND8 neurons. These data suggest that increased expression of RyR3 is

neuroprotective in TgCRND8 cortical cultures and offers a novel role for RyRs in AD pathology.

3.2 INTRODUCTION

The cause of AD is unknown but it is widely accepted that the Aβ peptide found in the neuritic plaques in AD brain, particularly the highly fibrillogenic fragment 1-42, plays a central function in both FAD and sporadic AD neuropathology (Selkoe 2001). The study of Aβ-related mechanisms that occur prior to irreversible cognitive impairment and neurodegeneration in AD could reveal targets for therapeutic intervention and disease prevention. Marked and sustained changes to intracellular Ca^{2+} signalling occur prior to cognitive decline and extensive neuronal death in AD (LaFerla 2002). Fibroblasts from asymptomatic patients at risk for AD displayed enhanced cytosolic Ca^{2+} levels after treatment with drugs targeting Ca^{2+} channels on the ER (Etcheberrigaray et al. 1998a; Gibson et al. 1997). Furthermore, neurons from murine models of AD show similar changes in intracellular Ca^{2+} handling by ER Ca^{2+} channels and pumps (Chan et al. 2000; Green et al. 2008; Lee et al. 2006; Stutzmann 2005). These observations implicate the ER in the dysregulation of intracellular Ca^{2+} observed in AD (LaFerla 2002).

Ca^{2+} channels on the ER, the RyRs, could mediate the early changes to intracellular Ca^{2+} signalling in AD brain. Post-mortem brain specimens from AD patients with early cognitive decline had increased [^{3}H]ryanodine binding in the hippocampus, suggestive of increased RyR protein levels (Kelliher et al. 1999). Both RyR protein and Ca^{2+} release from RyR stores were increased in cortical neurons from mutant presenilin (PS)1-M146V (Chan et al. 2000) and PS2-N141I mice (Lee et al. 2006). Increased expression of RyRs contributed to exaggerated caffeine-induced Ca^{2+} responses in cortical neurons from the triple transgenic mouse model of AD (3XTg-AD) (Smith et al. 2005). Furthermore, 3XTg-AD hippocampal neurons displayed enhanced IP_3R Ca^{2+} signalling due to increased RyR expression and function in organotypic brain slices (Stutzmann et al. 2006). Our group recently reported that Aβ42 induced the up-

regulation of RyR type 3, and that it was the isoform responsible for increased Ca^{2+} release from the ER in cortical neurons from transgenic (Tg)CRND8 mice that harbour a double mutation of the amyloid precursor protein $(APP)_{695}$-KM670/671NL+V717F (Supnet et al. 2006). Such data offer a link between changes in neuronal intracellular Ca^{2+} and a particular aspect of AD pathology; namely Aβ42.

The objective of this study was to determine the impact of increased RyR3 expression on the neurobiology of TgCRND8 cortical cultures. Given that increased RyRs and cytosolic Ca^{2+} levels have been shown to be involved in neurotoxicity in PS1 and PS2 mutants (Chan et al. 2000; Lee et al. 2006), we wanted to investigate the effect of increased RyR3 on the viability of TgCRND8 neurons. The following chapter will provide evidence that up-regulated RyR3 is important for the viability of TgCRND8 neurons. After application of various stressors or long-term culture, Tg cultures did not show increased sensitivity to death compared to littermate controls. However, after knock-down of RyR3 with siRNA to inhibit up-regulation, Tg cultures showed decreased viability and significant neuronal loss after long-term culture compared to controls. Knock-down of RyR3 did not alter Aβ production in TgCRND8 neurons and therefore is not a mechanism of protection. These data suggest that increased expression of RyR3 is neuroprotective in TgCRND8 cortical cultures and reveals a novel function for increased RyRs in AD.

3.3 MATERIALS AND METHODS

3.3.1 Animals

See Chapter 2, page 45 for details.

3.3.2 Primary cortical neuron cultures

See Chapter 2, page 45 for details. Briefly, tissue was genotyped, pooled and digested with 1 mL 0.25% trypsin in HBSS/EDTA (Hyclone) for 15 min at 37 ^{o}C. After digestion, 1 mL of Neurobasal medium containing 10% FBS to inactivate trypsin and tissue was triturated using a 1000 μL pipette. Dissociated cells were suspended in Neurobasal medium containing 10% FBS and seeded at $2X10^6$ cells per well onto poly-D-Lysine coated 6-well polystyrene tissue culture plates for siRNA treatments, $2.5X10^5$ cells per 12 mm glass coverslip (VWR) in 24-well plates (BD Biosciences) for long-term viability studies, or $1X10^5$ cells per well onto 96-well polystyrene tissue culture plates, that were either black from E&K Scientific (Santa Clara, CA) for cell viability assays or clear (BD Biosciences) for MTT assays. After 18 h at 37 °C and 5%CO_2, media was changed to Neurobasal medium without FBS. To maintain cultures long-term, media changes occurred every 3 days, where half the conditioned medium in each well was replaced by fresh Neurobasal medium lacking serum.

3.3.3 Treatments

Glu was prepared as in Chapter 2, page 48. H_20_2 (Sigma) was prepared from a 30% stock and diluted in Neurobasal medium lacking serum. STS (Sigma) was prepared from a 1mM stock solution in DMSO. On 5 DIV, CRND8 cultures were incubated with various concentrations of stressors for 24 to 72 h.

3.3.4. Reverse-transcriptase (RT)-PCR for mRNA analysis

See Chapter 2, page 48 for details.

3.3.5 Quantitative reverse-transcriptase-PCR (qRT-PCR) for RyR mRNA

RNA extraction and cDNA generation as in Chapter 2, page 48. Sequences for β-actin, RyR2 and RyR3 primers were taken from the Primer Bank at http://pga.mgh.harvard.edu/cgi-bin/primerbank (Wang et al. 2003) and RyR1 primers were designed using Vector NTI (Invitrogen) (see sequences in **Table II**). Alignment analysis (BLAST) of each primer was conducted to ensure that they were gene- and/or isoform-specific. Optimal annealing temperature for all primers was 61°C. To quantify mRNA levels, amplification of cDNA was conducted using iQ SYBR Green Supermix kit and the iCycler iQ Real-time PCR Detection System (BioRad). The comparative C_T (cycle threshold) method ($\Delta\Delta C_T$) for relative quantification of gene expression was used, where nonTg brain samples were considered the control condition and $2^{-\Delta\Delta C}{}_T$ gives the relative expression level of the gene of interest.

3.3.6 Cell viability assay

The cell viability of cortical cultures was assessed using the acetoxymethyl (AM) ester derivative of calcein (Molecular Probes). Calcein-AM is a membrane permeant, non-fluorogenic dye taken up by cells during incubation. Calcein-AM is hydrolyzed by endogenous esterases into the highly negatively charged calcein, which is fluorogenic (excitation|emission of 485|530 nm) and retained in the cytoplasm of cells with intact membranes (Papadopoulos et al. 1994). The fluorescent signal generated is proportional to the number of living cells in a sample (Mayne et al. 2004). Briefly, calcein-AM was prepared in 100% DMSO at 1 mg/mL. After treatment with appropriate stressors, media

Table II. Primer sequences for qRT-PCR of ryanodine receptor mRNA.

Gene	Forward Primer (5' to 3')	Reverse Primer (5' to 3')	Product Size (base pairs)	Primerbank ID #
actin	GGCTGTATTCCCCTCCATCG	CCAGTTGGTAACAATGCCATGT	154	6671509a1
RyR1	CCCAGGGGAGGATGACATAGA	CATCTTCATCGCCCTCTACC	115	N/A
RyR2	CCTCCCGGTCTTCCACTGA	TGCTTAGAGGCAGGATGTATGG	100	29165716a3
RyR3	ATCGCTGAACTCCTGGGTTTG	TTCATGTCGATGGAACTTAGCC	110	639817a1

was removed from cortical cultures grown in 96-well black plates and replaced with 2 μg/mL of calcein-AM in PBS; total volume of 200 μL/well. Plates were incubated for 45 min at room temperature in the dark. After incubation, plates were read on a SpectraMax M2 plate reader from Molecular Devices (Sunnyvale, CA), giving a read-out of relative fluorescence units (RFUs). The average RFUs of treated wells were compared to the average RFUs of untreated wells to determine % cell viability, which was calculated as (average RFUs of treated wells ÷ average RFUs of untreated wells) X 100%.

3.3.7 MTT assay

The metabolic activity of cortical cultures was assessed using the 3-[4,5-dimethylthiazol-2-yl]-2,5-diphenyl tetrazolium bromide (MTT) assay (Denizot et al. 1986; Mosmann 1983). Because damaged or dying cells lose the ability to maintain the energy levels required for metabolic function, the metabolic activity of a cell is an indication of viability. MTT (Sigma) is a yellow salt that is reduced to insoluble purple formazan crystals by electron donors in mitochondria (succinate) and, to a greater extent, in the cytosol (nicotinamide adenine dinucleotide/ phosphate (NADH/NADPH)) (Berridge et al. 1993). Formazan crystals are dissolved and a spectrophotometer is used to quantify the signal at 570 nm, where the signal is proportional to the metabolic activity of living cells in the culture. MTT was prepared in PBS at 0.5 mg/mL. After treatment with appropriate stressors, siRyR3 or after growing in culture for a pre-determined time, half of the total volume of media per well was removed from cortical cultures grown in 96-well, 24-well or 6-well plates. The same volume of 0.5 mg/mL MTT in PBS was added to the wells. Plates were incubated for 3 hr at 37°C and 5%CO_2. After incubation, MTT and media was removed and replaced with 100% DMSO to dissolve the formazan crystals; 200 μL/well for 96-well plates, 300-600 μL/well in 24-well plates and 1-2 mL/well in 6-well

plates. Plates were read on a SpectraMax M2 plate reader (Molecular Devices), giving a read-out of absorbance at 570 nm. The average absorbance readings of treated wells were compared to the average absorbance readings of untreated wells to determine the percent absorbance of untreated, calculated as (average absorbance of treated wells ÷ average absorbance of untreated wells) X 100%.

3.3.8 NeuN assay

The expression of a DNA-binding, neuron-specific nuclear protein (NeuN), has been used to determine neuronal populations in hippocampal slice preparations, where a loss of NeuN signal by immunohistochemistry indicated a loss of neurons (Shinozaki et al. 2007). NeuN expression in CRND8 cortical cultures was used as an indicator of neuronal viability, where loss of the fluorescent signal as measured by ICC (see Chapter 2, page 49 for details) indicated a loss of neurons due to death (Arrasate et al. 2004). After treatment(s), cortical cells grown on glass coverslips were fixed with 4% paraformaldehyde from Alfa Aesar (Ward Hill, MA) in PBS for 10 min at 37°C and 5%CO_2, washed three times with PBS and permeabilized with HEPES-Triton buffer for 5 min at room temperature. Non-specific binding sites were blocked with 5% goat serum (Sigma) in PBS for 1 h at room temperature and incubated with 1.25 μg/mL anti-NeuN, Clone:A60 from Chemicon (Temecula, CA) in PBST overnight at 4°C. After washing, cells were incubated with 2 μg/mL AlexaFluor 488® (Invitrogen) in PBST for 1 h then with 1μM of TO-PRO®-3 (Invitrogen) in PBST for 15 min at room temperature in the dark. Coverslips were mounted on slides using FluorSave™ Reagent from Calbiochem (San Diego, CA) and imaged by a researcher blind to the genotype and treatment condition of the cells. Approximately 10 images were acquired for each coverslip using an Axioskop 2 *plus* from Carl Zeiss Canada, Ltd. (Toronto, ON) equipped with a digital camera

(Axiocam MRm) and Axiovision Release 4.2 software. All 12-bit images were acquired under identical conditions (2 s exposure) using a 10x objective and a FITC filter set from Chroma (Rockingham, VA). NeuN signal in each image was quantified by image analysis (ImageJ, NIH). A threshold was applied to each image using an empirically determined value and the total area of all objects in the image was calculated.

3.3.9 siRNA Design and Delivery

See Chapter 2, page 51 for details of siRNA generation. NonTg and TgCRND8 cortical cultures seeded at $2X10^6$ per well in 6 well plates were transfected for 2 h at 37°C/5%CO_2 with 200 ng of siRyR3 or control siRNA for green fluorescent protein (siGFP) (Genelantis) using 1 μL of Lipofectamine™2000 Transfection Reagent (Invitrogen) per mL of Opti-MEM® Reduced Serum Medium (Invitrogen). Gene silencing was tested 72 h and 17 days post-transfection by reverse-transcriptase PCR. Transfection efficiency was determined using 0.8 μg of AlexaFluor 546® labeled nonspecific siRNA (Qiagen) and calculated as the number of nuclei (stained with 2.5 μg/mL of Hoechst 33258 (Sigma) in PBS) localized with siRNA ÷ total number of nuclei X 100%.

3.3.10 Enzyme-linked immunosorbent assay (ELISA) for Aβ42/40

After treatment(s), supernatants from CRND8 cultures were collected for the quantification of human Aβ using the hAmyloid β40/42 ELISA (Highly Sensitive) kit from the Genetics Company (Schlieren, Switzerland) as per manufacturer's instructions. The ratio of Aβ42/40 was calculated as pg/mL of Aβ42 ÷ pg/mL of Aβ40.

3.3.11 Statistical Analysis

Densitometric analysis was performed using NIH Scion Image software, version 1.60. Data were analysed using GraphPad Prism, version 3.02 (San Diego, CA). One-way ANOVA with Tukey's post-test was performed to determine the difference between means after treatment. Data is presented as mean ± standard deviation (S.D.). Differences were considered significant at $p<0.05$.

3.4 RESULTS

3.4.1 TgCRND8 cortical cultures do not have increased sensitivity to cell death compared to nonTg controls

TgCRND8 cortical neurons show an up-regulation of RyR3 and an enhanced release of ER Ca^{2+} in response to Glu and Ry (Supnet et al. 2006). Therefore, the possibility that TgCRND8 neurons would be more sensitive to cell death or may die more prematurely as a result of dysregulated control of intracellular Ca^{2+} was considered. To test this hypothesis, both TgCRND8 and cortical cultures derived from the same cell preparation were treated with Glu or H_2O_2. These cell stressors were added at 6 DIV, a time in culture when there is a significant increase in the concentration of Aβ42 in the culture media and a significant increase in the expression of RyR3 in TgCRND8 cultures (**Figure 3.1.**). As reported by others, both Glu and H_2O_2 treatment induced a concentration-dependent loss of cells indicative of toxicity (Chan et al. 2000; Nakajima et al. 2001) (**Figure 3.2. A & B**). However, TgCRND8 cultures did not show a significant difference in cell viability compared to nonTg cultures indicating no difference in the susceptibility to cell death. Since apoptosis plays an important role in the pathophysiology of AD and since both RyRs and increased intracellular Ca^{2+} levels can trigger apoptotic signalling pathways (Borghi et al. 2002), the sensitivity of TgCRND8 neurons to cell death specifically by apoptosis was determined. After treatment with STS, an inhibitor of PKC, to induce apoptosis, neuronal loss was not significantly different between TgCRND8 and cultures (**Figure 3.2. C**). Finally, a more subtle neuronal stress is aging and neurons in culture show a progressive decline in number due to cell death (Arrasate et al. 2004). Therefore, the effect of aging on the viability of TgCRND8 and cultures was tested. Cortical cultures were grown for 18 DIV and cell viability was determined by MTT assay at the end of this culture period. Again, TgCRND8 cultures were no more susceptible to cell death over time compared with

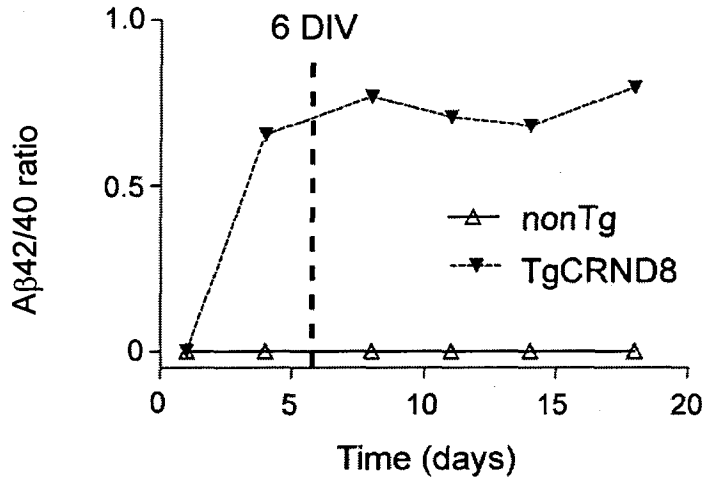

Figure 3.1. Aβ42/40 is increased in expression early in the culture of TgCRND8 neurons. ELISA analysis of the culture media from TgCRND8 and cultures reveals a significant and sustained increase in the ratio of Aβ42/40 as early as day 4 in TgCRND8 cultures and remains elevated throughout the culture period (to day 18). The dotted line indicates the time at which cell stressors were added to the culture for the following experiments.

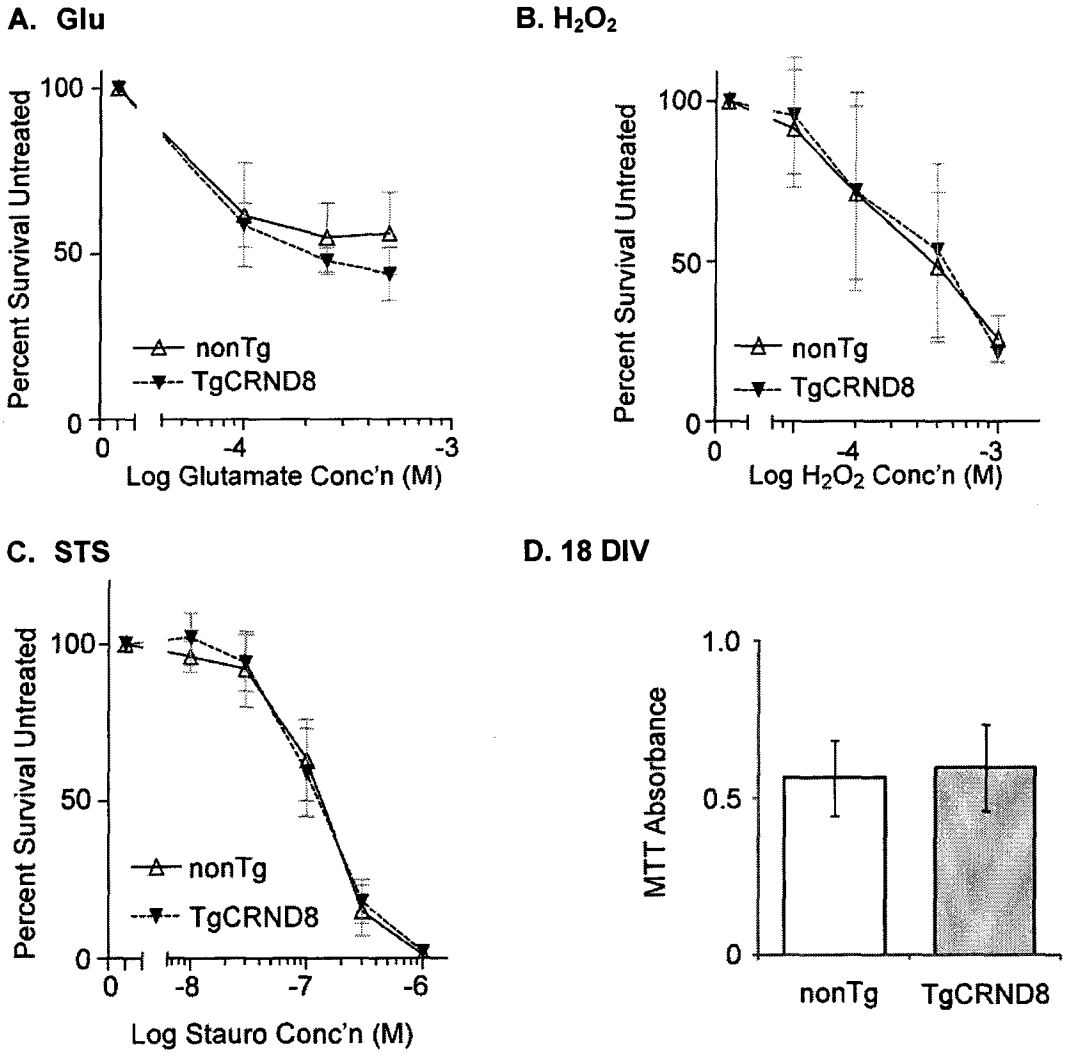

Figure 3.2. TgCRND8 cortical cultures are no more susceptible to cell death than nonTg cortical cultures. A. Concentration-response of cortical cultures (6 DIV) to Glu treatment (0 - 500 μM for 24 h). Cell viability was assessed with calcein-AM and fluorescence was read at 530 nm. **B.** Concentration-response to H_2O_2 treatment (0 - 1000 μM for 24 h). Cell viability was assessed with the MTT assay and absorbance was read at 570 nm. **C.** Concentration-response to STS treatment (0 - 1000 μM for 48 h). Neuronal viability was determined as the amount of NeuN signal by ICC. For each assay in A-C, cell viability is expressed as a percentage relative to the untreated condition. **D.** MTT absorbance of cortical cells grown to 18 DIV. For all graphs, values are the mean ± S.D. of at least 3 independent experiments and no statistically significant difference was found between genotypes at any drug concentration.

nonTg cultures (**Figure 3.2. D**). Despite an up-regulation of RyR3 and an increase in the release of ER Ca^{2+} in TgCRND8 cultures (Supnet et al. 2006), there does not appear to be an associated increase in the susceptibility for cells to die.

3.4.2 Knock-down of RyR3 induces cell death in TgCRND8 neurons

Because there was no detectable effect of RyR3 up-regulation on cell viability in TgCRND8 neurons, it was hypothesized that RyR3 up-regulation may have no functional consequence in neurons, or, conversely, that it may be a beneficial or compensatory function to protect neurons. To test this hypothesis, RyR3 up-regulation was prevented in TgCRND8 neurons using siRNA-mediated knockdown, cultures were then maintained long-term and the viability of cultures was determined. TgCRND8 and nonTg cultures were transfected with siRNA directed at RyR3 or a control siRNA directed at GFP 24 h after cell isolation. Knock-down of RyR3 mRNA was confirmed 72 h after transfection by RT-PCR (**Figure 3.3. A**). No change in the expression of RyR3 mRNA was detected with the control siRNA and the expression of mRNA of RyR1 and RyR2 was the same in all conditions (**Figure 3.3. A**). To determine the effect of preventing RyR3 up-regulation on the long-term survival of TgCRND8 cultures, knock-down of RyR3 was confirmed 13 days after transfection (**Figure 3.3. B**). To evaluate the transfection efficiency of the vehicle with siRNA, Tg cultures were treated with 800 ng of AlexaFluor 546® labelled nonspecific siRNA and cells were fixed and stained with Hoechst 33258 or NeuN 72 h later (**Figure 3.4. A**). A transfection efficiency of 25.4 ± 1.7 S.D. % (n=2, 20 images per experiment) and virtually all cells transfected with siRNA were positive for NeuN (**Figure 3.4 B**).

After 18 DIV, there was a significant reduction in the cell viability of TgCRND8 cultures in which RyR3 was knocked down, as assessed by MTT assay (**Figure 3.5.**

A. RyR3 knock-down 72 h post-transfection

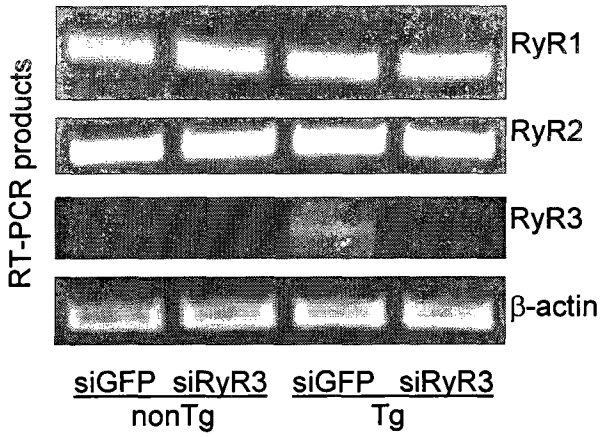

B. RyR3 knock-down at 13 days post-transfection

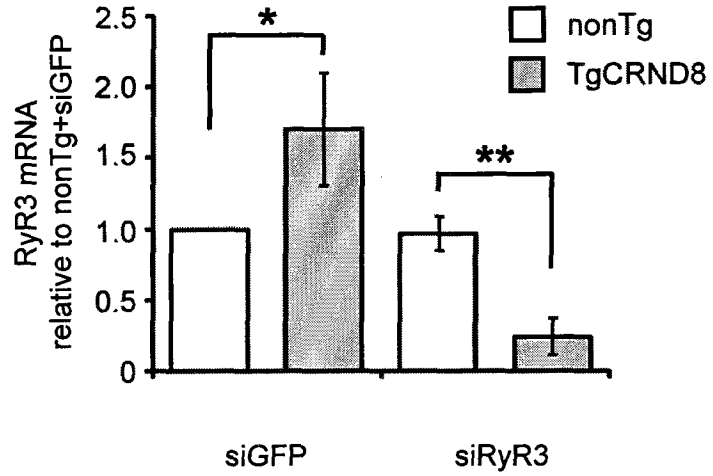

Figure 3.3. Specific and sustained knock-down of RyR3 in cortical cultures from TgCRND8 mice. A. An agarose gel showing RyR1, RyR2, RyR3 and β-actin RT-PCR products from cortical cultures treated with either siRNA to RyR3 (siRyR3) or siRNA to GFP (siGFP). Cultures were transfected for 2 h and total RNA was extracted 72 h later. The gel is representative of 3 independent experiments. **B.** Quantification of RyR3 mRNA expression in cortical cultures on DIV14, 13 days after siRNA transfection. mRNA expression was determined using quantitative RT-PCR and RyR3 expression was normalized to β-actin. All RyR3 mRNA expression was normalized to the culture treated with siGFP. Means ± S.D. are shown for 6 independent experiments. $*p<0.05$, $**p<0.01$; one-way ANOVA with Tukey's post-test.

A. NeuN + siRNA + brightfield

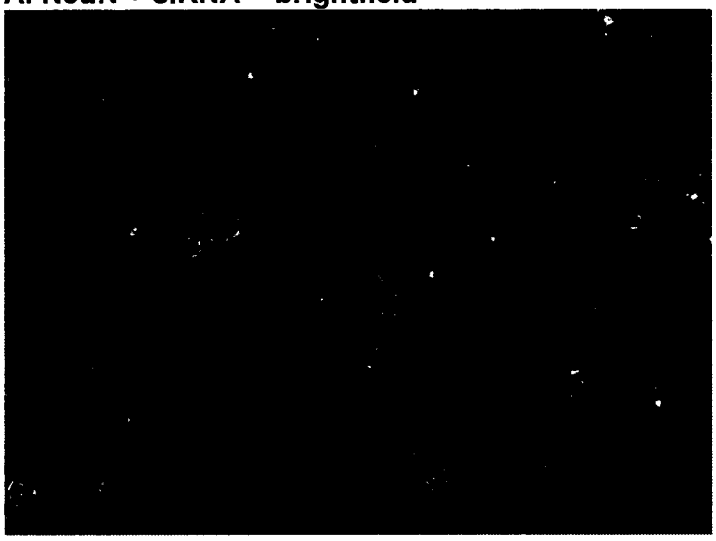

B. NeuN + siRNA

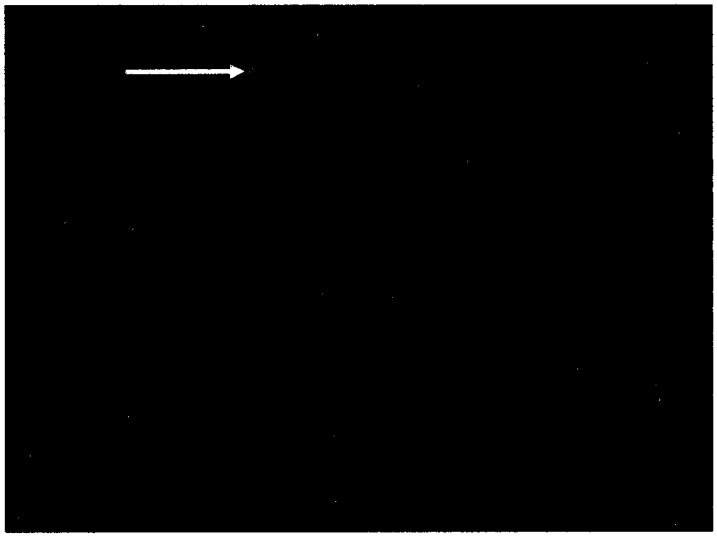

C. secondary antibody alone

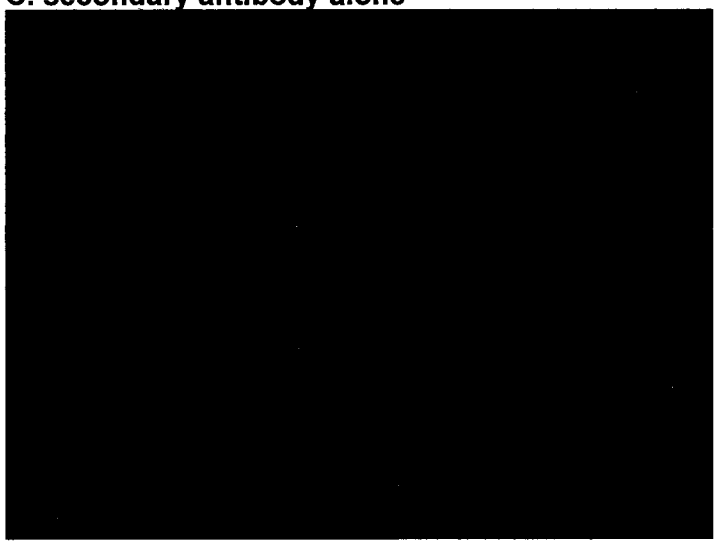

Figure 3.4. Transfection efficiency of siRNA. A. A representative image showing TgCRND8 neurons labelled with NeuN in green, nuclei labelled with Hoechst 33258 (blue) and nonspecific siRNA labelled with AlexaFluor 546® in red. Brightfield channel was used to determine if siRNA associated with cell bodies. Images were used to determine the transfection efficiency of Lipofectamine™ 2000 + siRNA to neurons. A transfection efficiency of 25.4 ±1.7 S.D. % (n=2, 20 images per experiment) of NeuN positive nuclei. **B.** Same as **A.** but with the brightfield channel removed. Arrow indicates a transfected NeuN positive cell. **C.** Secondary antibody alone.

A). However, knockdown of RyR3 in cultures did not affect survival, nor did control siRNA or transfection reagent alone (**Figure 3.5. A**). To specifically examine the effect of RyR3 knockdown on neuronal survival and to evaluate the time course over which cell death occurs, ICC for the neuron specific marker, NeuN, was performed at 10, 14 and 18 DIV (**Figure 3.5. B**). As anticipated, there was a gradual, time-dependent loss of NeuN staining, indicative of neuron loss (Arrasate et al. 2004), in all treatment conditions. However, there appeared to be decreased NeuN fluorescence signal in TgCRND8 cultures transfected with siRNA directed to RyR3 compared with control siRNA at 14 DIV. There was significantly less NeuN signal at 18 DIV and again, fewer neurons in Tg cultures treated with siRyR3 compared to control siRNA.

3.4.3 Knock-down of RyR3 in TgCRND8 cultures does not affect production of Aβ42

Although preventing the up-regulation of RyR3 in TgCRND8 neurons leads to a striking increase in cell death over time, the mechanism by which this occurs is not clear. Because Aβ42 induces a concentration-dependent neuronal death (Butterfield 2002), it was considered whether a reduction in RyR3 expression increased production of Aβ42 in TgCRND8 cultures. Media from TgCRND8 cultures treated with siRNA were assayed for Aβ40 and Aβ42 expression by ELISA. It was determined that the ratio of Aβ42/40 in the media of TgCRND8 cultures in which RyR3 was knocked down was not significantly different from TgCRND8 cultures treated with control siRNA (**Figure 3.6**).

A. MTT assay at 18 DIV

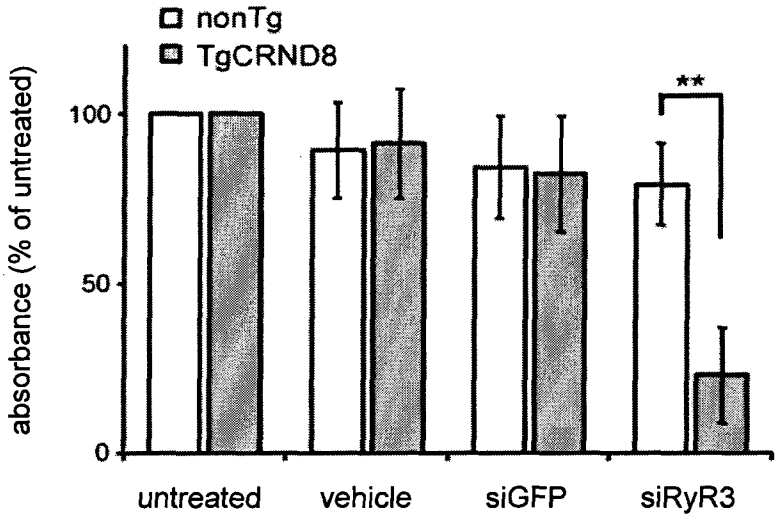

B. NeuN assay

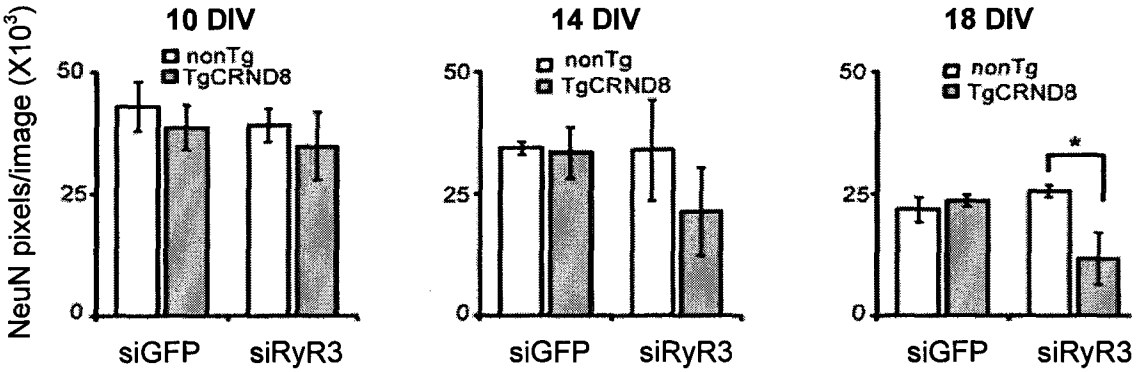

Figure 3.5. Knock-down of RyR3 selectively induces cell death in TgCRND8 neurons. A. Cell viability of Tg and cultures treated with siRNA directed to GFP (siGFP) and RyR3 (siRyR3) was determined with the MTT assay at 18 DIV. Absorbance readings for each genotype were normalized to the untreated condition. Means ± s.d. are shown. **B.** Quantification of neuronal number at different times (10, 14 and 18 days) in culture. TgCRND8 neurons treated with siRNA to RyR3 show a significant decrease in neuronal number at 18 DIV. means ± S.D. are shown for data obtained from 4 independent experiments. *$p<0.05$, **$p<0.01$; one-way ANOVA with Tukey's post-test.

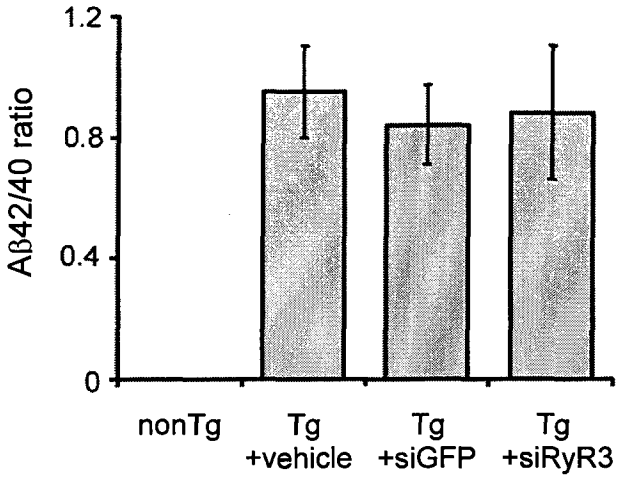

Figure 3.6. Knock-down of RyR3 does not affect the synthesis of Aβ42 in TgCRND8 neurons. ELISA for Aβ40 and Aβ42 shown as a ratio of Aβ42/40, in the culture media from TgCRND8 and cortical cultures at 18 DIV after treatment with siRyR3 or siGFP. Values are the mean and ± S.D. of 3 separate experiments.

3.5 DISCUSSION

The study of ryanodine receptors and their ability to alter intracellular Ca^{2+} levels has grown in popularity as their up-regulation is a consistent observation in FAD models, implying a fundamental role for RyRs in the development of the disease. We have identified an important downstream consequence of up-regulated RyR3 in TgCRND8 cortical neurons; namely maintenance of neuronal viability. Tg cortical cultures survived exposure to toxicants that model AD-related stressors, such as Glu, H_2O_2 and STS, to the same extent as nonTg cultures, despite having increased RyR3 levels and potential for increased Ca^{2+} release from ER (Supnet et al. 2006). In addition, Tg cultures survived long-term culture, or *in vitro* aging (Lesuisse et al. 2002), as well as nonTg cultures. Finally, suppression of RyR3 mRNA up-regulation in Tg neurons with siRNA caused significant neurotoxicity compared to nonTg after long-term culture (18 DIV) without affecting Aβ42 production. These findings highlight a novel and essential role for RyR3 in the neurobiology of AD.

A single mutation in APP, PS1 or PS2 is sufficient to trigger FAD humans, which is pathologically identical to sporadic or late-onset AD (Hardy & Selkoe 2002). Mice expressing mutations of APP recapitulate many aspects of AD pathology, for example Aβ plaque formation, dystrophic neurites, loss of synaptic densities, gliosis, cholinergic dysfunction, inflammation and oxidative stress (Bellucci et al. 2006; Chen et al. 2000; Dudal et al. 2004; Hsiao et al. 1996). In addition, both the Swedish (APP-KM670/671NL) and Indiana (APP-V717F) mutants have impaired reference and working memory and hippocampus-dependent object recognition (Dodart et al. 1999; Hsiao et al. 1996; Ognibene et al. 2005). TgCRND8 mice were designed by Chishti, M., et al. 2001 to contain both the Swedish and Indiana mutations, resulting in similar pathology (Woodhouse et al. 2007) and cognitive deficits in an accelerated time frame as mice

containing Swedish or Indiana mutations alone but (Chishti et al. 2001; Hyde et al. 2005). However, mutant APP mice do not produce AD-like neurofibrillary tangles or overt neurodegeneration. Results from this study implicate a role for RyR3 in neuroprotection and could explain the lack of neuronal loss in TgCRND8 mice, as our observations from the previous chapter showed increased RyR3 in the neocortex of adult Tg mice compared to littermate controls (Supnet et al. 2006). Interestingly, PS1-M146V and PS2N141I mice lacking neurodegeneration show increased RyR protein in adult brain homogenates and in both cases the mRNA profiles suggest that RyR3 was up-regulated (Chan et al. 2000; Lee et al. 2006). RyRs are also increased in the 3XTg-AD model that harbours APP-KM670/671NL, PS1-M146V and human tau-P301L (Stutzmann et al. 2006). What is common to these models is that they all produce high levels of Aβ resulting in an increased Aβ42/40 ratio and aggregation. Given that increased RyR3 is a direct result of Aβ exposure in TgCRND8 neurons (Supnet et al. 2006), RyR up-regulation could be a protective response to the neurotoxic effects of Aβ accumulation in these models.

The mechanism by which RyR3 up-regulation protects neurons from death in culture remains to be elucidated. Recent data on the function of RyR3 in neurons suggest an important role for RyR3 in modulating the excitability of the neuronal membrane. RyR3 knock-out mice demonstrate increased long-term potentiation (LTP), a correlate for learning and memory, after short or weak tetanus stimulation, suggesting a role for RyR3 in the depression of LTP or the excitability of hippocampal circuits (Balschun et al. 1999; Futatsugi et al. 1999). RyR3 mRNA was transiently increased in the mouse hippocampus 2 to 6 hr after kainic acid-induced status epilepticus, or hyper excited neurons (Mori et al. 2005). Finally, RyR3 triggered I_{sAHP} in hippocampal CA1 neurons; a distinct phase of AHP that could be involved in synaptic plasticity (van de

Vrede et al. 2007). These data suggest a role for RyR3 in the suppression of neuronal membrane excitability, which could affect how neuronal circuits are shaped or constructed, *in vivo*. TgCRND8 mice, as well as other mouse models of AD display changes in neuronal excitability (Del Vecchio et al. 2004; Palop et al. 2007) and structural and functional disruption of neuronal networks (Kuchibhotla et al. 2008). *In vitro*, RyR3 up-regulation may be a mechanism Tg neurons use to suppress the excitability elicited by Aβ exposure. Tg neurons that are unable to up-regulate RyR3 due to siRNA treatment could be more vulnerable to the excitotoxicity, oxidative stress and death related to Aβ exposure (Butterfield 2002). Because of synaptic proteins, such as synaptophysin, synapsin IIa, and α/β-synucleins, are all expressed at 15-20 DIV (Lesuisse & Martin 2002), it would be interesting to determine if a lack of RyR3 in Tg neurons leads to the aberrant formation of *in vitro* neuronal networks, which could potentially compromise the health of the culture.

Results of this study reveal a novel role for increased levels of RyRs in AD; specifically that RyR3 up-regulation affords neuroprotection *in vitro* in a model of AD. There are many studies that have shown the importance of dysregulated or altered cytosolic Ca^{2+} signalling in AD (Bezprozvanny et al. 2008) and that increased RyRs contribute to these changes in Ca^{2+} handling (Stutzmann et al. 2007; Supnet et al. 2006) but this is the first study to determine an effect of up-regulated RyRs on neuronal viability. Studies are required to further characterize RyR3 function in TgCRND8 mice as they display cognitive impairment in spite of having increased RyRs and little neurodegeneration. Furthermore, in human AD brain, RyR levels are increased in the hippocampus in post-mortem tissue of patients that show early cognitive impairment but not at later stages of the disease (Kelliher et al. 1999). This observation could be explained by the extensive neurodegeneration that occurs in the human condition. A

malfunction of RyR up-regulation itself or up-/down-stream regulators of RyR expression and function in human brain at the later stages of disease could also contribute to neuronal loss. Nevertheless, further study into RyR3 and its mechanism of neuroprotection will give insight into AD pathology and potential targets for therapeutic intervention.

4. RYANODINE RECEPTOR TYPE 3 - DEFICIENT TgCRND8 MICE HAVE A DECREASED SURVIVAL RATE COMPARED TO LITTERMATE CONTROLS

Some sections were published in: Charlene Supnet, Jeff Grant, Hong Kong, David Westaway and Michael Mayne, *$A\beta_{1-42}$ increases ryanodine receptor-3 expression and function in neurons of TgCRND8 mice.* J Biol Chem, 2006. **281**(50): p. 38440-7.

4.1 ABSTRACT

Several studies show that RyRs have increased expression and function in mouse models of AD. RyRs are thought to contribute to the dysregulation of cytosolic Ca^{2+}, an early and detectable occurrence in the pathophysiology of AD. Three isoforms of RyR exist in brain and RyR type 3 is increased in cortical neurons from the TgCRND8 model of AD. Data from preceding chapters show that up-regulation of RyR3 protein leads to changes in cytosolic Ca^{2+} handling and affords protection *in vitro* to cortical neurons from TgCRND8 mice. The objectives of this study were to characterise RyR up-regulation in different brain regions of TgCRND8 mice and to determine if RyR up-regulation was protective to adult TgCRND8 mice. Western blotting of brain tissue from 4 to 4.5 month old nonTg and TgCRND8 mice showed a significant increase in RyR3, but not RyR1 or 2, protein levels in the cortex and hippocampus of Tg mice compared to their nonTg littermates. 2 month old mice appeared to show a slight increase in RyR3 in the cortex and hippocampus as well but the difference was not statistically significant. Older mice did not have increased RyR3 expression. After knocking out RyR3 in TgCRND8 mice, their survival was drastically compromised. By 75 days (2.5 months), approximately 60% of Tg/RyR3$^{-/-}$ and 50% of Tg/RyR3$^{+/-}$ mice had died compared to 20% of Tg/RyR3$^{+/+}$. The survival of nonTg mice was not affected by RyR3 genotype. How premature death occurs in the mice is undetermined. Because RyR3 is implicated in the modulation of neuronal excitability and RyR3$^{-/-}$ mice display impaired depression of synaptic activity, it was hypothesized that Tg mice lacking RyR3 would be more prone to hyperexcitablitiy of neuronal networks and would potentially be more prone to severe

seizures. In fact, Tg mice lacking RyR3 display more severe seizure-like behaviour after administration of 40 mg/kg of pentylenetetrazole to induce seizure compared to nonTg lacking RyR3. These results support an important role for up-regulated RyR3 in the maintenance of TgCRND8 viability, possibly by attenuating brain hyperexcitability and severe seizures.

4.2 INTRODUCTION

Recent evidence suggests that RyRs could mediate the dysregulation of cytosolic Ca^{2+} signalling observed in AD. Kelliher and colleagues 1999 reported that post-mortem hippocampal brain specimens from AD patients with early cognitive decline had increased [^{3}H]ryanodine binding, suggestive of increased RyR protein levels (Kelliher et al. 1999). Increased RyR expression and function have also been observed in neurons from several mouse models of AD (Chan et al. 2000; Lee et al. 2006; Stutzmann et al. 2006; Supnet et al. 2006). Three isoforms of RyRs have been identified but isoform-specific expression has not been characterized in AD mice, including TgCRND8s.

Mice expressing mutations that cause FAD have been invaluable tools for studying the molecular mechanisms of AD. The first transgenic mouse models to show pathological hallmarks of AD and cognitive deficits contained single mutations of the human APP (Games et al. 1995b; Hsiao et al. 1996). For example, mice possessing the APP-V717F (Indiana) or APP-KM670/671NL (Swedish) mutation showed histological characteristics such as Aβ plaques, dystrophic neurites, loss of synaptic densities and gliosis by 8 to 11 months of age (Chen et al. 2000; Hsiao et al. 1996). In addition, both Indiana and Swedish mutants had impaired reference and working memory and hippocampus-dependent object recognition (Dodart et al. 1999; Hsiao et al. 1996; Ognibene et al. 2005). Such models were useful but not very practical because mice had to age for long periods before AD pathology was evident. TgCRND8 mice were designed by Chishti and colleagues 2001 to contain both the Indiana and Swedish mutations under the same hamster prion promoter as the popular Tg2567 model, resulting in robust overall Aβ production. The first Aβ plaques were detectable at 3 months of age and dense-cored plaques (Chishti et al. 2001; Janus et al. 2000b) with

increased inflammatory response were evident by 5 months of age (Chauhan et al. 2004). Plaque formation in TgCRND8 mice coincided with impaired spatial reference memory and working memory (Chishti et al. 2001; Janus 2004). However, FAD mutations do not produce AD-like neurofibrillary tangles or overt neurodegeneration. Nonetheless, mouse models containing FAD mutations are utilized in the study of the early stages of the disease prior to extensive neurodegeneration and for testing drug targets (Ashe 2005; Woodhouse et al. 2007).

The objectives of this study were to use Western blot analysis to determine if RyR levels are elevated in young, adult and aged brain tissue of TgCRND8 mice and if so, which isoform(s) was increased. Based on the *in vitro* data of the preceding chapters and published data that increased RyRs have been demonstrated in the brains of other models of AD (Stutzmann et al. 2006), it was hypothesized that RyR3 would be increased in TgCRND8 brain and that RyR3 would impact the survival of TgCRND8 mice. To determine if RyR3 affected TgCRND8 viability, RyR3 was knocked-out of TgCRND8 mice by crossing with $RyR3^{-/-}$ mice and survival was observed. The results of this study could reveal a more sophisticated profile of RyR up-regulation in AD and help determine if RyRs are a possible drug target.

4.3 MATERIALS AND METHODS

4.3.1 Animals

See Chapter 2, page 45 for TgCRND8 details. RyR3 knock-out ($RyR3^{-/-}$) mice were a gift from Dr. V. Sorrentino (University of Siena, Italy) and described previously (Bertocchini et al. 1997). Our stock was shipped from the College of Veterinary Medicine at Cornell University (Ithaca, NY). $RyR3^{-/-}$ mice were generated on a C57BL/6 background strain (Bertocchini et al. 1997).

4.3.2 Breeding and Genotyping of CRND8, $RyR3^{-/-}$ and TgCRND8/ $RyR3^{-/-}$ mice

Because the objective was to produce TgCRND8/$RyR3^{-/-}$ mice (see **Figure 4.1. A** for breeding strategy) and the appropriate genotypes for comparison, $RyR3^{-/-}$ were initially out-bred to the CRND8 background using nonTg mice. Once nonTgCRND8/$RyR3^{-/-}$ females were produced they were bred to Tg males to generate litters that were 1:1 for nonTg and Tg and all heterozygous for RyR3 ($RyR3^{+/-}$). This breeding was used to maintain the knock-out RyR3 allele on the CRND8 background. Tg/$RyR3^{+/-}$ and nonTg/$RyR3^{+/-}$ were bred to produce all the required genotypes (expected ratios in **Figure 4.1. A**). Four-week-old pups were weaned and genotyped for the human APP_{695} double mutation in Chapter 2, page 45. In addition, pups were genotyped for the wild-type ($RyR3^{+/+}$) and knock-out RyR3 allele by PCR. The sequences of the primers used for the detection of wild-type and knock-out RyR3 were (forward, 5' to 3' for both genotypes) GTC AGA GCA CAT CCC AAT CTC CTT, (reverse, 5' to 3' for wild-type) CCC TAA TGC CAC AGC TGT TTG TTC and (reverse, 5' to 3' for knock-out) GCT ACT TCC ATT TGT CAC GTC CTG (from Cornell University). The 350 and 450 base pair PCR fragments for wild-type and knock-out RyR3, respectively, were generated by 25 cycles of 94/60/72°C using the Bio-Rad iCycler and

A. Breeding strategy to generate TgCRND8/RyR3$^{-/-}$ mice

APP$^{-/-}$ = nonTg
APP$^{+/-}$= Tg or APP-KM670/671NL+V717F$^{+/-}$

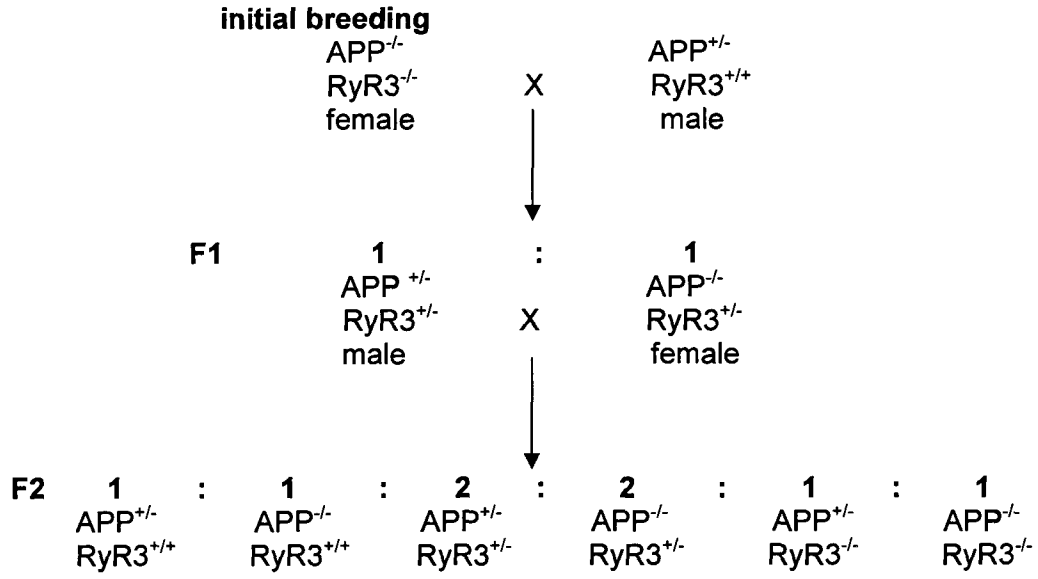

B. Genotyping

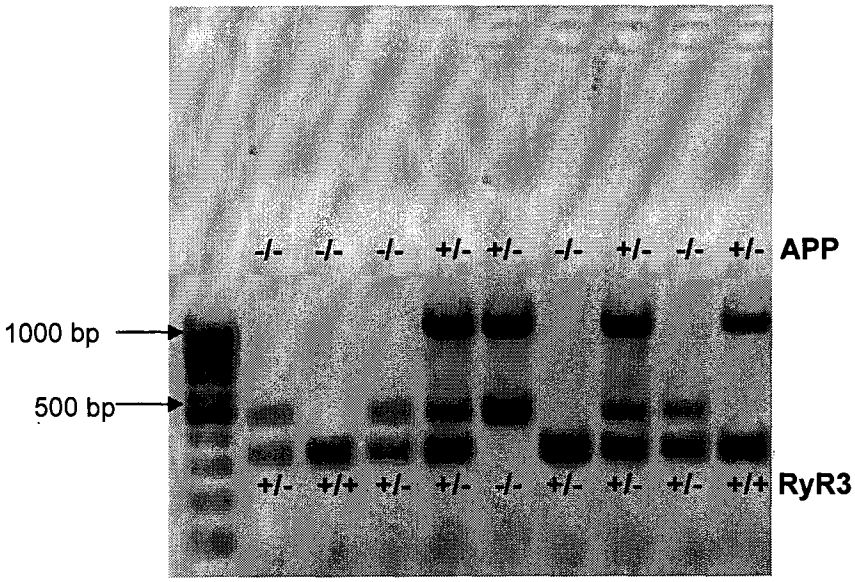

Figure 4.1. Generation of TgCRND8/RyR3$^{-/-}$ mice. A. Breeding strategy to generate the all genotypes required for comparison. **B.** Agarose gel with PCR products from genotyping of RyR3$^{-/-}$ bred with TgCRND8 mice. The first lane is a 100 base pair (bp) ladder. Each lane is genomic DNA amplified from tail from an individual mouse. APP$_{695}$-KM670/671NL+V717F$^{+/-}$ (Tg) is 1000 bp, RyR3$^{+/+}$ is 350 bp and RyR3$^{-/-}$ is 450 bp. RyR3$^{+/-}$ express both 350 and 450 bp fragments. Examples of each genotype are shown on the gel.

visualized on a 1.2% agarose gel stained with 0.4 μg/mL ethidium bromide (Invitrogen) under UV illumination (**Figure 4.1. B**). $RyR3^{+/-}$ generated both fragments. When breeding for timed-pregnancies, $nonTg/RyR3^{+/-}$ females were bred with $Tg/RyR3^{+/-}$ males to generate nonTg or Tg fetuses that were either $RyR3^{+/+}$, $RyR3^{+/-}$ or $RyR3^{-/-}$. Weights of adult mice were recorded 40 days after birth.

4.3.3 Western Blot Analysis for RyRs in CRND8 brain

Mice were raised to 2, 4 and 12 months in regular housing with minimal enrichment. Mice were anaesthetised with pentobarbital (Euthanyl) (Bimeda-MTC Animal Health Inc., Cambridge, ON) diluted in PBS (Sigma) to 60 mg/mL. Pentobarbital was administered by i.p. injection at 50 mg/kg. Once anaesthetised, mice were decapitated. Whole brains were extracted and dissected on wet ice into cerebellar, cortical, hippocampal and basal regions (the remainder of tissue after the removal of the cortex, hippocampus and brain stem). After dissection, tissue was immediately homogenized on ice with 400 μL of non-denaturing lysis buffer (see **Appendix A**). Microsome preparations of skeletal and heart muscle (see **Appendix B**) were used for RyR antibody positive controls. Samples were incubated on ice for 1 h, collected and centrifuged at 950 *g* to pellet insoluble proteins. 125 μg of soluble protein was loaded onto a 3-8% tris-acetate NuPAGE® Novex gradient gel (Invitrogen). Use of RyR isoform specific antibodies and densitometric analysis was carried out as in Chapter 2, page 51. The pixel density of RyR/actin was used to show total levels of protein over time.

4.3.4 Seizure induction in CRND8/RyR3 mice with pentylenetetrazole

Pentylenetertrazole (PTZ) is a non-competitive γ-aminobutyric acid ($GABA_A$) receptor antagonist (Huang et al. 2001) and is used to elicit seizure activity in models of

epilepsy (Loscher et al. 1991). A stock solution of PTZ (Sigma) was made in PBS and administered i.p. at 40 mg/kg to 6 week old mice. Animals were video-monitored for seizure-like activity for 20 min and seizure severity was graded based on the Racine scale (Racine 1972), where 0 = normal exploratory behavior, 1 = immobility, 2 = generalized spasm, tremble, or twitch, 3 = tail extension, 4 = forelimb clonus, 5 = generalized clonic activity, 6 = bouncing or running seizures, 7 = full tonic extension, 8 = death (Palop et al. 2007). All mice were euthanized with an i.p. injection of 50 mg/kg pentobarbital immediately after the experiment.

4.3.5 Statistical Analysis

Data were analysed using GraphPad Prism, version 3.02 (San Diego, CA). Paired t-test, one-way ANOVA with Tukey's post-test or two-way ANOVA with Bonferroni post-test was used to determine the affect of genotype and brain region on RyR expression and the possible interactions of each factor. All data are presented as mean ± S.E. Differences were considered significant at $p<0.05$.

4.4 RESULTS

4.4.1 RyR3 protein is increased in TgCRND8 brain

To determine regional changes in RyR TgCRND8 brain, lysates of different brain regions dissected from 2, 4 and 12 month old CRND8 mice were analyzed for RyR protein by western blot analysis using isoform specific antibodies (Rossi et al. 2002). RyR3 levels in 4 month old CRND8 brain were increased in the cortex of Tg mice approximately 2.7 ± 0.42 fold (n=14, ***p<0.001, two-way ANOVA, Bonferroni's post-test) as compared to nonTg, while RyR1 and RyR2 levels were unchanged (**Figure 4.2. B**). RyR3 levels were increased 1.9 ± 0.26 fold in the hippocampus as well (n=14, **p<0.01, two-way ANOVA, Bonferroni's post-test) but unchanged in the basal and cerebellar regions (**Figure 4.2. B**). Two-way ANOVA tests revealed that the differences in RyR3 expression were attributed to the genotype or was specific to the brain region, but that there was no interaction between the two factors. RyR3 levels in the cortex and hippocampus showed a trend towards an increase in expression in the 2 month old Tg animals, but was not a statistically significant difference, probably due to the low sample size (n=3 of each genotype, **Figure 4.2. A**). RyR expression in 12 month old Tg did not differ from nonTg (**Figure 4.2 C**). To determine if total levels of RyR protein increased over time in the regions of interest, namely cortical and hippocampus, the pixel density of the bands normalized to actin were graphed over time. In the cortex, a significant increase in total protein of RyR1 and RyR2 subtypes at 4 months compared to 2 or 12 months was discovered, **p<0.001 and ***p<0.001 compared with 2 or 12 month values (two-way ANOVA with Bonferroni's post-test) (**Figure 4.2. D**). A significant increase in total RyR3 protein was revealed at 4 months in T compared to N ($^{\#\#}p$<0.01, two-way ANOVA with Bonferroni's post-test). In the hippocampus, total protein of RyR1 was significantly decreased at 4 and 12 months compared to 2 months (*p<0.05, two-way ANOVA with Bonferroni's post-test) (**Figure 4.2. E**) and RyR2 total protein was

A. 2 month old

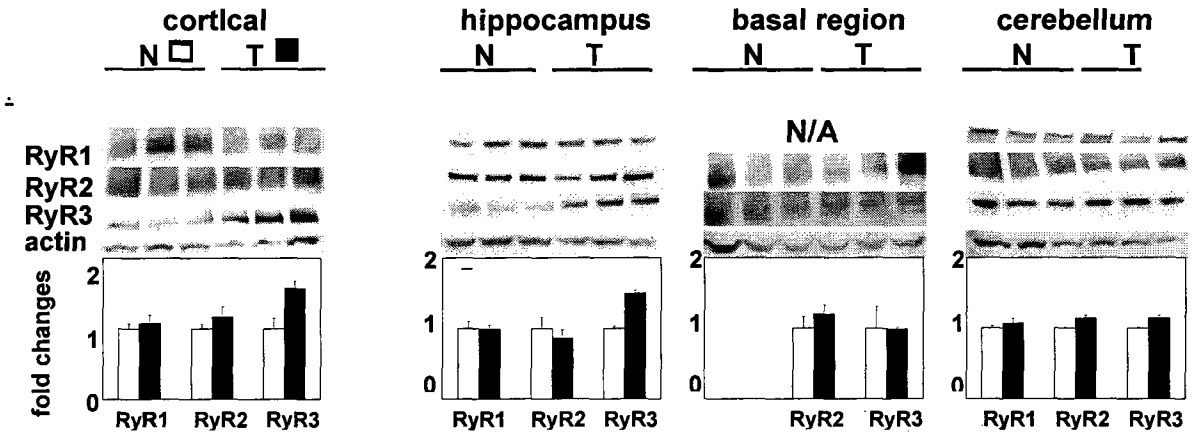

B. 4 month old

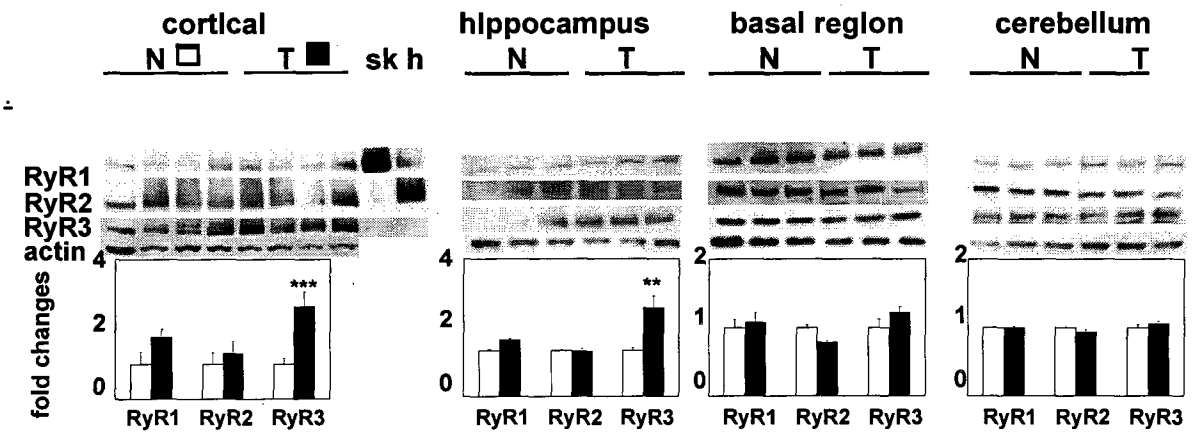

C. 12 month old

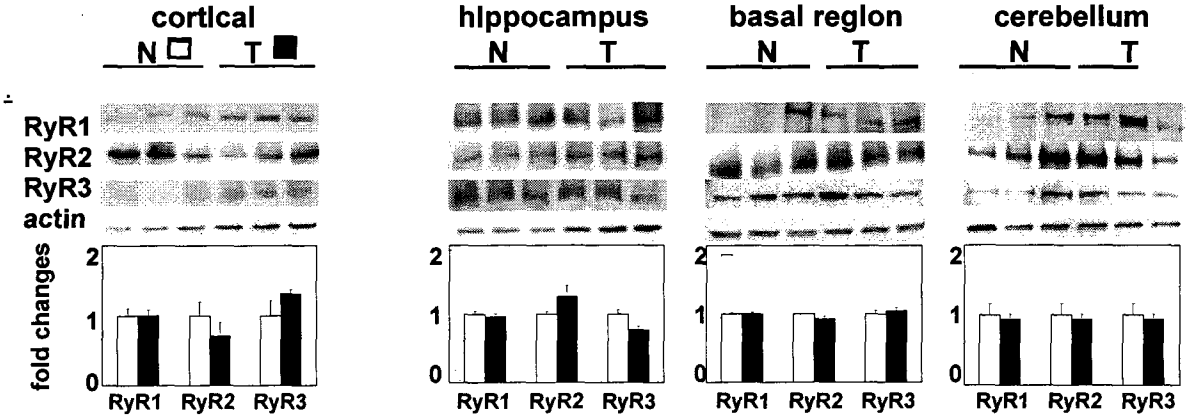

D. Levels of RyR in cortex

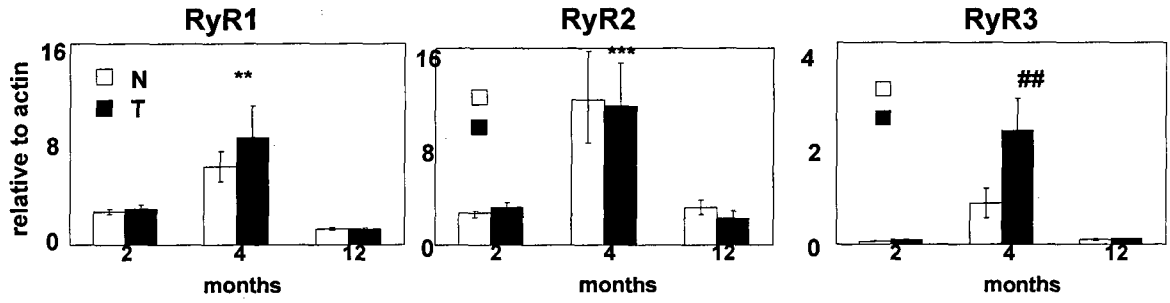

E. Levels of RyR in hippocampus

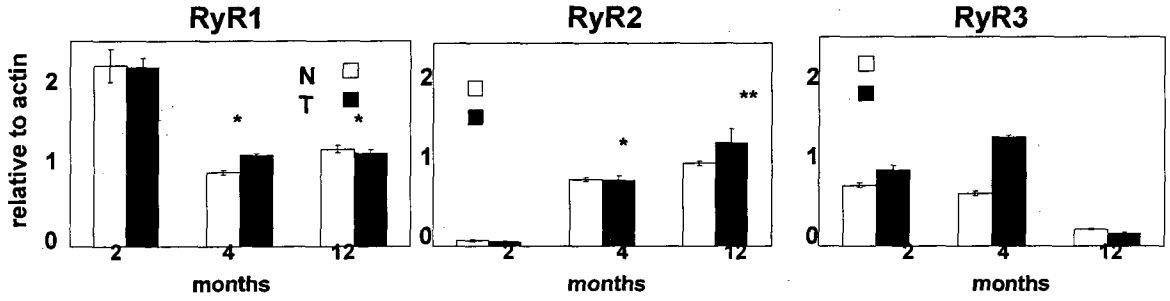

Figure 4.2. RyR protein levels in CRND8 brain over time. A. Immunoblots of brain tissue lysates from different regions of nonTg (N) and TgCRND8 (T) 2 month old mice for RyR1, 2 and 3. Expression levels were determined relative to actin and graphs represent the fold change compared to control (N). Blots represent 1 experiment with 3-4 samples of each genotype. **B.** Immunoblots of RyR proteins from different regions of N and T mice at 4 to 4.5 months. Skeletal (sk) and heart (h) muscle microsomes were used as positive controls for RyR1 and RyR2, respectively. Values are the mean and S.E. of fold changes in RyR levels from 4 separate experiments (3-4 brains of N and T were used for each experiment, n=14). ***$p<0.001$ and **$p<0.01$ compared with littermate control values (one-way ANOVA with Tukey's post-test). **C.** Immunoblots of RyR protein in brain from 12 month old CRND8 mice. Expression levels are expressed relative to actin and are compared to control (N). Blots represent 1 experiment with 3-4 samples of each genotype. **D.** Expression of the different RyR subtypes over time in cortex. **$p<0.001$ and ***$p<0.001$ compared with 2 or 12 month values (one-way ANOVA with Tukey's post-test). ##$p<0.01$ T compared to N at same time point. **E.** Expression of the different RyR subtypes over time in hippocampus. *$p<0.05$ and **$p<0.01$ compared with 2 month values (one-way ANOVA with Tukey's post-test).

increased at 4 and 12 months compared to 2 months (*p<0.05 and **p<0.01, two-way ANOVA with Bonferroni's post-test). Two-way ANOVA revealed that the differences in RyR expression were attributed to genotype and time, but that there was no interaction between the two factors. However, interpreting the total protein levels of RyR3 over time in the hippocampus is difficult as the two-way ANOVA revealed that there is a significant interaction between the affect of genotype and time (***p<0.001, two-way ANOVA with Bonferroni's post-test).

4.4.2 TgCRND8 mice expressing RyR3$^{+/-}$ and RyR3$^{-/-}$ are susceptible to premature death compared to littermates

Based on the observation that up-regulated RyR3 was neuroprotective in cortical cultures from embryonic TgCRND8, it was hypothesized that RyR3 would also affect neuronal function and survival of adult mice. To address this hypothesis, RyR3 expression was knocked out in TgCRND8 mice by crossing with RyR3$^{-/-}$ mice and offspring were raised in routine housing conditions. It was clear that by 1 to 2 months of age, Tg/RyR3$^{-/-}$ and Tg/RyR3$^{+/-}$ mice were more susceptible to spontaneous death compared to all other genotypes (**Figure 4.3.**). It was also observed that some neonates were being lost before they were old enough to be weaned and genotyped; within 4 weeks of birth. Only one Tg/RyR3$^{-/-}$ neonate was included in the data set as the genotypes of the others could not be confirmed. Tg/RyR3$^{+/+}$ mice show a trend towards susceptibility to spontaneous death, though it is not a statistically significant difference. The weights of the mice were recorded as an indicator of morbidity. Genotype did not contribute to the variances in weight and mice displayed typical gender differences, where females were lighter than males (**Figure 4.4.**). To further assess how the mice were dying, necropsies were performed on a few mice euthanized; one each of Tg/RyR3$^{-/-}$, Tg/RyR3$^{+/-}$, nonTg/RyR3$^{-/-}$ and nonTg/RyR$^{+/-}$. No gross morphological or

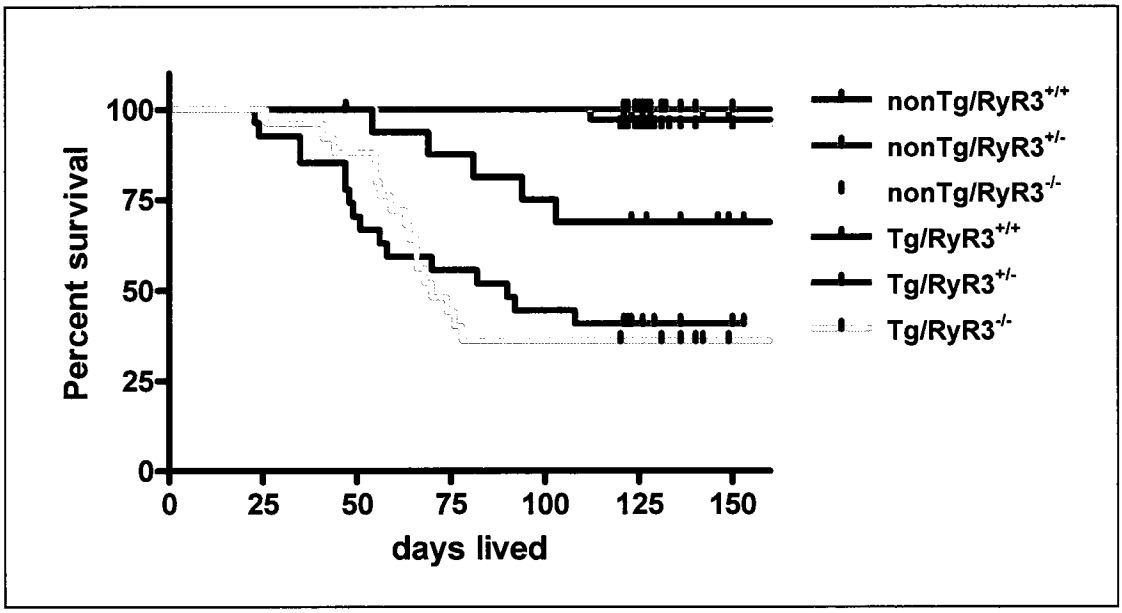

Figure 4.3. RyR3 protects TgCRND8 mice from premature, spontaneous death. The graph is a Kaplan-Meier survival curve showing the effect of reducing or knocking out RyR3 on the mortality of nonTg and TgCRND8 mice. Only mice genotyped and designated for this study were included in the analysis, n=200, one-way ANOVA and Tukey's post-test reveals that the probability of survival of both Tg/RyR3$^{+/-}$ and Tg/RyR3$^{-/-}$ are significantly lower than their nonTg counterparts, (p<0.001) and Tg/RyR3$^{+/+}$ (p<0.05 and p<0.01, respectively). Mice that died before 120 days were given a score of 1 and those that survived were given a score of 0 (indicated by ticks on the survival curve) on the Kaplan-Meier scale.

A. Weight of all CRND8/RyR3 mice at 40 days

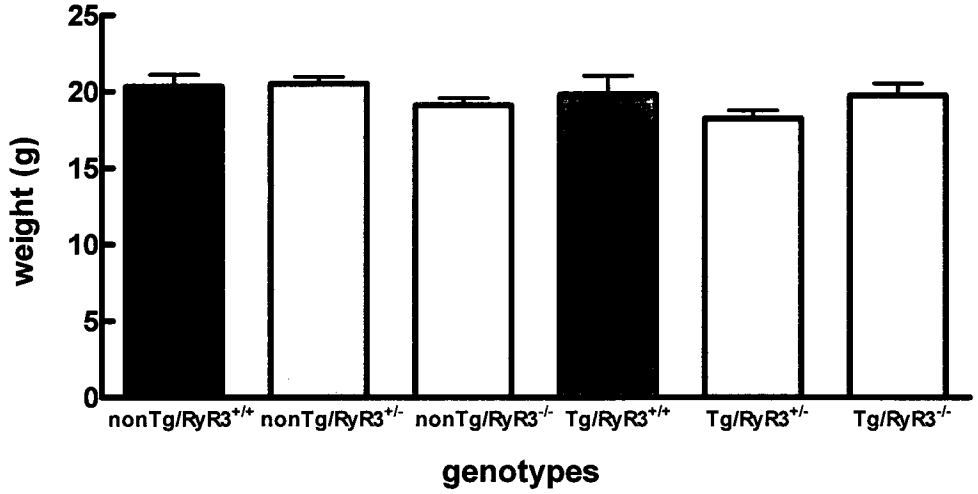

B. Weight of CRND8/RyR3 mice at 40 days by gender

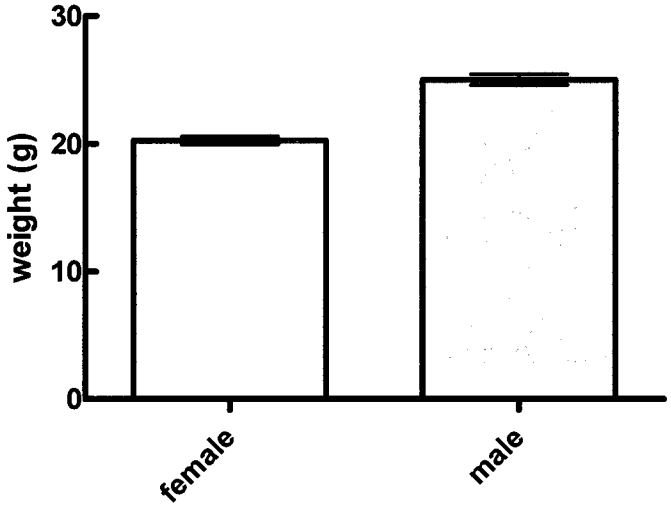

Figure 4.4. Average weight of CRND8/RyR3 mice. A. The graph shows the mean weight ± S.E. of CRND8/RyR3 mice at 40 days of age. There was no statistical difference between the different genotypes (n=11 to 29). **B.**The graph shows the mean weight ± S.E. of CRND8/RyR3 mice grouped by gender. Female mice (n=30) had significantly lower body weight compared to males (n=51) ***$p<0.001$, paired t-test.

histological abnormalities were found in any of the samples, including the central nervous system.

4.4.3 TgCRND8 mice expressing RyR3$^{+/-}$ and RyR3$^{-/-}$ have increased sensitivity to pharmacologically induced seizures

It is unclear how Tg mice lacking RyR3 are dying. RyR3 activation is implicated in the modulation of excitability of hippocampal neurons (van de Vrede et al. 2007) and RyR3 mRNA is up-regulated in the hippocampus of mice treated with kainic-acid to induce seizures, but they are not more susceptible to death (Mori et al. 2005). Given such data and that spontaneous seizure activity was observed in one Tg/RyR3$^{+/-}$ mouse, resulting in full tonic extension and death, it was hypothesized that Tg/RyR3$^{-/-}$ mice were more prone to hyperexcitability in the brain and severe seizures that could lead to death. To test the hypothesis, Tg/RyR3$^{-/-}$ mice and littermate controls were treated with 40 mg/kg of PTZ to induce seizures. Such experiments were performed at 6 weeks of age, a time point prior to the significant loss of mice from spontaneous death. After administration of PTZ, Tg/RyR3$^{-/-}$ mice (n=11) displayed more severe seizure activity compared to nonTg/RyR3$^{-/-}$

(n=9, $^{**}p<0.01$) and nonTg/RyR3$^{+/-}$ (n=12, $^{*}p<0.05$, one-way ANOVA with Tukey's post-test) (**Figure 4.5.**). Tg/RyR3$^{+/-}$ appeared to be sensitized to seizure activity compared to nonTg/RyR3$^{+/-}$ and nonTg/RyR3$^{-/-}$, although the difference was not statistically significant. Two Tg/RyR3$^{-/-}$mice and one Tg/RyR3$^{+/-}$ mouse died after PTZ treatment, while all nonTg/RyR3$^{-/-}$ and nonTg/RyR3$^{+/-}$ mice survived. These data suggest that TgCRND8

mice lacking RyR3 are susceptible to more severe seizures compared to nonTg mice lacking RyR3, which could sensitize them to spontaneous death.

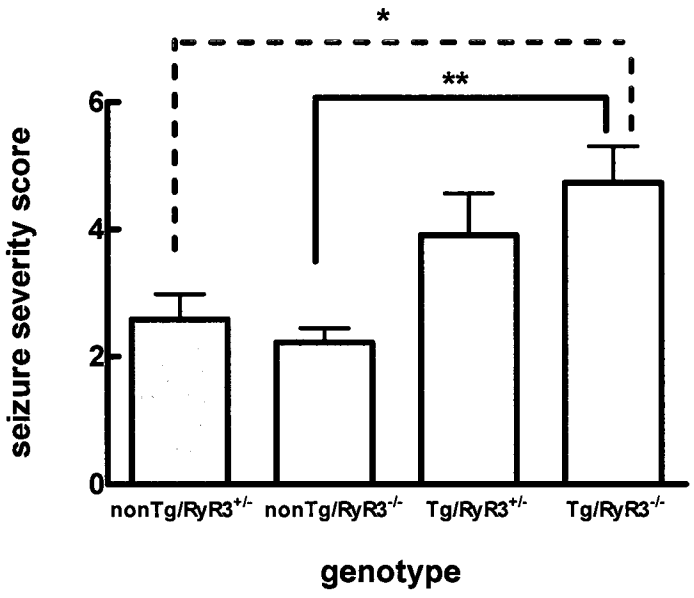

Figure 4.5. TgCRND8/RyR3$^{-/-}$ mice are more susceptible to PTZ-induced seizures. The graph shows the mean seizure severity score ± S.E. of male and female 6-week-old CRND8/RyR3 mice after the i.p. administration of 40 mg/kg PTZ. Tg/RyR3$^{-/-}$ (n=11) show increased severity of seizure activity compared to nonTg/RyR3$^{+/-}$ (n=12, *p<0.05) and nonTg/RyR3$^{-/-}$ (n=9, **p<0.01, one-way ANOVA with Tukey's post-test). Values are the mean maximum seizure severity score exhibited within 20 min of injection of PTZ.

4.5 DISCUSSION

The role of increased RyRs in AD has been investigated in several models. RyRs contribute to the altered intracellular Ca^{2+} signalling observed in neurons of FAD mutants and are thought to be key components of the dysregulation of neuronal Ca^{2+} homeostasis in AD. Following the *in vitro* observations of the previous chapters, this study has identified that the RyR3 is up-regulated in the cortex and hippocampus of TgCRND8 mice. RyR3 protein levels are increased at 4 months, when plaque formation is initiated and spatial learning impairments are evident. RyR3 protein levels may also be increased at 2 months of age, where there is no plaque formation or changes in cognition, therefore, RyR3 up-regulation might be present prior to amyloid plaque formation and impairments to cognitive functioning. Older mice did not show changes in expression of any of the RyRs. Total protein levels of RyR1, 2 and 3 were increased in 4 month old cortex. Total protein levels of RyR1 were decreased in the hippocampus, while protein levels of RyR2 were increased in a time-dependent manner. Total protein levels of RyR3 in the hippocampus appeared to be increased at 4 months, but was not significant due to the possible interaction between time and genotype on RyR3 protein levels. TgCRND8 mice that do not express $RyR3^{+/+}$ were more susceptible to spontaneous death, possibly by sensitization to severe seizures. These data highlight the importance of up-regulated RyR3 in TgCRND8 brain and a possible role in maintaining neuronal and animal viability in mouse models of AD.

It has been demonstrated that RyRs are increased in the brains of another model of AD, the 3XTg-AD, and that expression levels of RyRs areincreased in mice at 6 weeks and 18 months of age, but not at 6 months (Stutzmann et al. 2006). Stutzmann and colleagues 2006 were able to show that increased RyRs were responsible for the exaggerated intracellular Ca^{2+} response to IP_3 in 3XTg-AD hippocampal neurons in organotypic brain slices. Furthermore, they determined that IP_3-mediated

hyperpolarizations of the membrane in Tg mice were greater than in nonTg mice, demonstrating an increased coupling efficiency between intracellular Ca^{2+} and K^+ channel regulation, and emphasizes a role for increased RyRs in the lifelong dysregulation of cytosolic Ca^{2+} in AD (Stutzmann et al. 2006). 3XTg-AD mice express APP-K670N/M671L, PS1-M146V and tau-P301L in an attempt to recapitulate AD neuropathology. When the APP and tau mutations were bred out of the line, the PS1-M146V and 3XTg-AD were identical regarding RyR up-regulation and increased cytosolic Ca^{2+} response to IP_3 (Stutzmann et al. 2006). RyR up-regulation was not observed in mice expressing APP-K670N/M671L or tau-P301L alone (Stutzmann et al. 2006). TgCRND8 mice express both APP-K670N/M671L and APP-V717F and have increased RyR3 levels (Supnet et al. 2006). Moreover, cortical neurons from TgCRND8 mice demonstrate increased cytosolic Ca^{2+} responses mediated by up-regulated RyR3 (Supnet et al. 2006). If RyR up-regulation is due to the exposure of neurons to Aβ42, as in TgCRND8, then why is there a discrepancy in RyR expression between the different AD mutants which all produce high levels of Aβ42? One possibility is that the amount and rate at which Aβ is produced can affect the expression levels of RyR, where TgCRND8 mice produce higher levels of Aβ compared to mice containing single APP mutations (Chishti et al. 2001). It would also be interesting and important to further characterize which isoform of RyR is up-regulated in 3XTg-AD mice and determine which RyR is involved in the exaggerated IP_3-mediated Ca^{2+} signaling, as different isoforms have different roles in neurophysiology and AHPs (van de Vrede et al. 2007).

The mechanism by which RyR3 contributes to the survival of TgCRND8 is not known. Unlike $RyR1^{-/-}$ and $RyR2^{-/-}$ mice, that die early in development, $RyR3^{-/-}$ mice do not exhibit increased susceptibility to death. In the whole animal, a lack of RyR3 appears rather benign. $RyR3^{-/-}$ mice have normal growth and reproduction (Bertocchini et al.

1997; Takeshima et al. 1996). Skeletal muscle from newborns demonstrates impaired contraction, where electrically or caffeine stimulated contractions are depressed (Bertocchini et al. 1997). The effect is lost in adult mice, with the exception of the diaphragm and soleus muscle, which could be explained by compensation of function by RyR1. Adult $RyR3^{-/-}$ mice displayed increased locomotor activity, impaired learning and memory and abnormal electrophysiological properties of hippocampal neurons (Balschun et al. 1999; Futatsugi et al. 1999; Shimuta et al. 2001; Takeshima et al. 1996). Because of their role in the modulation of neural circuits and in the survival of TgCRND8 neurons in primary cortical cultures, perhaps knocking out RyR3 in TgCRND8 mice makes them more vulnerable to death due to their lack of ability to deal with the increased excitability of neurons in response to Aβ (Mattson et al. 1992; Ye et al. 2004).

Altering RyR3 expression by either $RyR3^{+/-}$ or $RyR3^{-/-}$ changes the survival of Tg mice but not nonTg mice. When first characterized, $RyR3^{+/-}$ did not show any phenotypic difference compared to $RyR3^{+/+}$ and microsomes from $RyR3^{+/-}$ diaphragm muscle expressed similar protein levels of RyR3 compared to $RyR3^{+/+}$. Therefore, a dosage effect of the heterozygous genotype on RyR3 function was not determined in muscle (Bertocchini et al. 1997). However, in another RyR3 knock-out model generated by Futatsugi and colleagues 1999, they demonstrated a dosage effect of $RyR3^{+/+}$, $RyR3^{+/-}$ and $RyR3^{-/-}$ on RyR3 expression in microsomes from the cerebrum, including the hippocampus, and determined that RyR3 expression was almost undetectable in $RyR3^{+/-}$ compared to $RyR3^{+/+}$ (Futatsugi et al. 1999). Thus, $RyR3^{+/-}$ mice were excluded from neurophysiological testing as well as learning and memory tests. If expression of RyR3 is initially suppressed by the $RyR3^{+/-}$ genotype, then up-regulation due to Aβ exposure in Tg mice could also be lessened and may be insufficient to afford the same protection as

$RyR3^{+/+}$. Such a scenario could explain why $Tg/RyR3^{+/-}$ and $Tg/RyR3^{-/-}$ mice are both susceptible to spontaneous death.

It is unclear how $Tg/RyR3^{-/-}$ mice were dying. Necropsies from a small sample size did not indicate any abnormalities in the central nervous system or in any other areas of the body of Tg mice lacking RyR3. Spontaneous seizure-like activity was observed in one $Tg/RyR3^{+/-}$ mouse that resulted in death and Tg mice lacking RyR3 exhibit increased seizure severity compared to nonTg mice lacking RyR3 after PTZ-induced seizure. Given the role of RyR3-mediated Ca^{2+} release in the generation of slow afterhyperpolarization currents and suppression of neuronal membrane excitability, such an observation is logical. Lack of RyR3 in Tg mice could therefore sensitize them to hyperexcitability and severe seizure activity. Others have shown that Tg AD mice, including TgCRND8, show decreased seizure threshold compared to littermates after treatment with PTZ or kainic acid (Del Vecchio et al. 2004; Roberson et al. 2007). Such data are consistent with the observation that AD patients show a high prevalence of seizure-like activity (Palop et al. 2009a). Perhaps up-regulation of RyR3 is in response to the increased excitability of neurons exposed to Aβ42 in an effort to attenuate hyperexcitability of the neurons, decreasing the severity of seizures and potentially decreasing the likelihood of death in AD mice. Interestingly, RyR3 mRNA is transiently up-regulated in mouse brain, the hippocampal CA3 region and striatum, following kainic acid-induced seizures (Mori et al. 2005). Prevention of hyperexcitability could be a mechanism by which up-regulated RyR3 affords protection to Tg mice, perhaps by moderating the increased excitability observed in TgCRND8 mice (Del Vecchio et al. 2004) to prevent full tonic-clonic seizures and death. Further studies in Tg mice lacking RyR3 are required to physiologically characterize the seizure-like activity observed and to determine if lack of RyR3 in Tg mice alters neuronal circuitry. A full characterization of the $Tg/RyR3^{-/-}$ mouse is necessary and could provide insight as to how the mice are

dying. Histological (brain morphology, Aβ plaque load, neuronal densities in the hippocampus, Timm's stain for aberrant axonal or dendritic branching), electrophysiological (synaptic transmission, LTP, LTD) and behavioural (spatial learning and working memory tasks, basal seizure-like activity) features of the Tg/RyR3$^{-/-}$ mice compared to TgCRND8 could provide further insight to the mechanism of protection afforded by RyR3. In addition, the study of Tg mice lacking RyR3 which do not experience premature spontaneous death could provide insight into further protective mechanisms. While AD patients typically do not die from seizures, it would still be important to identify how neurons can be protected as neurodegeneration is a major concern in clinical AD.

5.GENERAL DISCUSSION

5.1 SUMMARY OF MAJOR FINDINGS

Along with the accumulation of Aβ42 peptide in the brain, changes to intracellular Ca^{2+} handling in neurons is a prominent feature of AD. Recent evidence suggests that Ca^{2+} release channels on the ER, the RyRs, could contribute to the alterations of intracellular Ca^{2+} signalling in AD. The study of RyRs ability to alter intracellular Ca^{2+} levels has grown in popularity as their up-regulation is a consistent observation in FAD models, implying a fundamental role for RyRs in the development of the disease. The objectives of this thesis were to determine if and where RyRs were up-regulated in the brains of TgCRND8 mice, how RyRs were being up-regulated, their contribution to intracellular Ca^{2+} signalling in neurons and how they affected neuronal physiology in TgCRND8 neurons.

The studies outlined here have identified a key role for RyR3 in altering the cytosolic Ca^{2+} homeostasis of neurons from TgCRND8 mice. The *in vitro* studies demonstrate that Aβ42 peptide, regardless of the source (endogenous or synthetic), increased mRNA and protein levels of RyR3, but not RyR1 or RyR2. As a direct consequence, Tg neurons had exaggerated cytosolic Ca^{2+} responses to ryanodine and to glutamate, which can trigger CICR from RyR stores (Arundine & Tymianski 2003; Clodfelter et al. 2002; Emptage et al. 1999; LaFerla 2002; Linn & Gafka 2001). After knock-down of RyR3 mRNA and protein levels by siRNA, Ca^{2+} imaging experiments confirmed that the RyR3 pools represented the majority of the glutamate and ryanodine-induced increase in cytosolic Ca^{2+} in Tg neurons. In addition, RyR3 levels were increased *in vivo* in the cortex and hippocampus of TgCRND8 mice, areas of the brain affected in AD, which suggests an important role for RyR3 in disease progression.

Studies designed to determine the downstream consequences of up-regulated RyR3 in TgCRND8 cortical neurons revealed that RyR3 was important for the

maintenance of neuronal viability. Tg cultures survived exposure to toxicants that model AD-related stressors, such as Glu, H_2O_2 and STS, to the same extent as nonTg cultures, despite having increased RyR3 levels and function (Supnet et al. 2006). Tg cultures also survived long-term culture, or *in vitro* aging (Lesuisse & Martin 2002), as well as nonTg cultures. However, suppression of RyR3 mRNA up-regulation in Tg neurons with siRNA caused significant neurotoxicity compared to nonTg after long-term culture (18 DIV) without affecting Aβ42 production. Finally, Tg mice lacking wild-type RyR3 were significantly more susceptible to pharmacologically-induced seizures and premature, spontaneous death compared to littermates, possibly by increased brain excitability. Taken together, the data suggests that up-regulation of RyR3 is a protective mechanism to combat the increased excitability due to Aβ42 accumulation in TgCRND8 brain and is important for the viability of Tg mice.

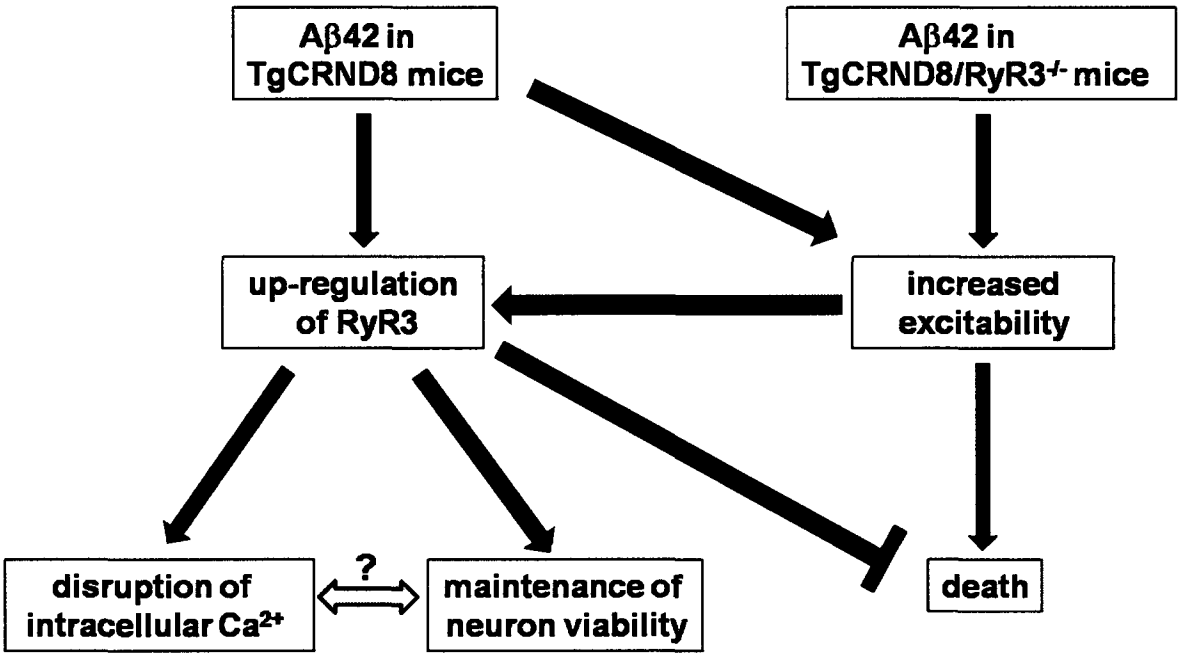

Figure 5.1 Role of up-regulated RyR3 in TgCRND8 mice

Illustration of how RyR3 is involved in Ca^{2+} handling neuronal viability and TgCRND8 health. Black arrows depict thesis results and red arrows show how RyR3 might afford

protection to TgCRND8 mice. Blue arrow indicates the unknown relationship between increases in intracellular Ca^{2+} and viability of TgCRND8 neurons.

5.2 POTENTIAL SIGNALLING MECHANISMS INVOLVED IN RYR3 UP-REGULATION

It has been demonstrated *in vitro* that after 18-24 h of exposure, Aβ42 can specifically up-regulate RyR3 mRNA and protein levels in cortical neurons from C57Bl/6 or nonTgCRND8 mice, without affecting the expression levels of other RyRs, IP_3R or SERCA (Supnet et al. 2006). However, the cell signalling mechanisms utilized by Aβ42 to increase the expression of RyR3 are still unknown. The identification of such mechanisms could be important for the development of therapeutics if RyR3 is in fact proven to be essential for the survival of neurons in AD.

It is known that Aβ forms Ca^{2+} channels in lipid bilayers and the neuronal plasma membrane (Arispe et al. 2007) and leads to rapid and sustained increases in $[Ca^{2+}]_{cyto}$ (Arispe et al. 2007). Ca^{2+} influx and increased $[Ca^{2+}]_{cyto}$ can activate cell signalling pathways important for gene regulation. For example, cyclic AMP/Ca^{2+} response element binding protein (CREB) induces the transrcription of several neuronal genes, including those that are important for LTP and synaptic plasticity (West et al. 2001). CREB transcription of genes related to synaptic plasticity requires phosphorylation by the Ca^{2+}-sensitive extracellular signal-regulated kinase (ERK) pathway, which can be activated by Ca^{2+} influx through NMDA receptors (Klann et al. 1999). To investigate the specificity of the transcriptional regulation of RyR3 by Aβ treatment and whether Ca^{2+} influx alone was sufficient to induce the up-regulation of RyR3, cortical neurons were treated with ionomycin and glutamate. The data showed that neither treatment was sufficient to up-regulate RyR3 (Figure 2.3, page 57). Ca^{2+} released from intracellular stores can elevate $[Ca^{2+}]_{cyto}$ and activate the ERK pathway and downstream phosphorylation of CREB in N2a cells and hippocampal neurons (Kemmerling et al.

2007). The use of an ERK inhibitor prior to treatment with Aβ42 or or treatment of TgCRND8 neurons would demonstrate the involvement of the ERK pathway in the up-regulation of RyR3. Because high levels of Aβ can increase excitability in hippocampal neurons of AD mice (Palop et al. 2007), it would also be interesting to determine if increased synaptic activity itself could signal the compensatory up-regulation of RyR3.

There is very little known about how RyR3 transcription is controlled and its promoter has yet to be identified. Giannini and colleagues had demonstrated that porcine transforming growth factor (TGF)β isoform 1 could up-regulate the gene expression of a caffeine insensitive RyR, later characterized as RyR3, in mink lung epithelial cells (Giannini et al. 1992). TGFβs are pleiotropic cytokines with important neuroprotective functions (Flanders et al. 1998; Unsicker et al. 2002), observations that align with the possible neuroprotection afforded by the up-regulation of RyR3. A deficiency in TGFβ signalling in cultured neurons and adult brain from hAPP transgenic mice resulted in increased levels of secreted Aβ, BACE, Aβ accumulation, loss of dendrites and neurodegeneration (Tesseur et al. 2006). It has been observed that increased levels of TGFβ are present in brains of AD patients and overproduction of TGFβ1 in astrocytes of hAPP mice reduces overall Aβ accumulation (Wyss-Coray et al. 2001). However, it has also been demonstrated that TGFβ overexpression causes cerebrovascular fibrosis and amyloidosis (Ueberham et al. 2005; Wyss-Coray et al. 2001; Wyss-Coray et al. 1997) and therefore has been implicated in a condition associated with AD, cerebral amyloid angiopathy (Grammas et al. 2002). It was recently reported that 12 month old TgCRND8 mice had increased levels of TGFβ1 in cortical brain regions and that TGFβ1 signalling was induced by treatment with 5 μM of synthetic, oligomeric Aβ42, contributing to neurotoxicity in TgCRND8 primary cortical cultures (Salins et al. 2008). Preliminary studies show that TGFβ1 treatment of nonTg

cortical neurons up-regulated the mRNA levels of RyR1, RyR2 and RyR3 as detected by quantitative RT-PCR (data not shown). Perhaps the regulation of a specific RyR depends on which receptor TGFβ receptor, of which there are two present in neurons, is activated. Further studies are needed to identify how TGFβ and its potential to regulate RyR gene expression confer neuroprotection in AD.

Another approach is to identify which cell signalling pathway(s) are activated in neurons after Aβ treatment to help determine which may be involved in the up-regulation of RyR3. Aβ42 can trigger a plethora of signalling pathways that alter gene regulation, such as mitogen-activated protein kinase (MAPK), ERK1/2, CREB and c-jun N-terminal kinase (JNK) (Ma et al. 2007; Smith et al. 2006; Zhao et al. 2002). Also, the activation of particular pathways depends on the concentration of Aβ, which Aβ assembly is used and how long the neurons are treated must be considered as the end result, either detrimental (apoptosis) or protective (RyR3 up-regulation), is dependent on the initial stressor.

Aβ treatment and subsequent increases in $[Ca^{2+}]_{cyto}$ can cause excessive Ca^{2+} flux into mt and increase ROS production (Brustovetsky et al. 2003). Recent reports show that RyRs mediate the induction of LTP in hippocampal neurons by ROS (Serrano et al. 2004) and functional RyR3 in particular is required for superoxide-induced activation of ERK and LTP (Huddleston et al. 2008). Because RyRs are sensitive to redox modification by ROS and reactive nitrogen species and can undergo *S*-glutathionylation (Hidalgo et al. 2007), increased expression of RyR3 and function by Aβ could be a link between modulation of cytosolic Ca^{2+} and oxidative stress. Interestingly, microarray analysis revealed that in cortical cultures from NF-E2 p45-related factor 2 (Nrf2) knock-out mice, mRNA levels of proteins involved in Ca^{2+} handling, including RyR3, were decreased compared to littermate controls (Lee et al. 2003), but protein

levels of RyR3 were never confirmed in the cultures. Nrf2 is a transcription factor that binds the anti-oxidant response element (ARE) and up-regulates the expression of phase II anti-oxidant enzymes which are important for the protection of primary cortical neurons in culture against oxidative stressors such as rotenone or H_2O_2. Preliminary data revealed that cortical neurons treated with *tert*-butyl hydroquinone (*t*-BHQ), an inducer of ARE, did not demonstrate up-regulation of RyR3 (data not shown). However, cortical cells from $RyR3^{-/-}$ mice were more susceptible to 20 μM H_2O_2 treatment compared to $RyR3^{+/+}$ and $RyR3^{-/-}$ neurons could not be protected from H_2O_2-induced toxicity by *t*-BHQ to the same extent as it protected $RyR3^{+/+}$ neurons (data not shown). Given that TgCRND8 neurons have up-regulated RyR3 and are no more susceptible to H_2O_2 compared to nonTg, it is alluring to consider that RyR3 may be involved in the cellular response to oxidative stress. However, further studies are required to elucidate a role for RyR3 in anti-oxidant mechanisms.

5.3 POSSIBLE MECHANISMS OF PROTECTION BY RYR3 UP-REGULATION

How can up-regulation of RyR3, and the potential to release more Ca^{2+} from the ER afford protection in TgCRND8 neurons? As proposed by the "Ca^{2+} hypothesis of aging and AD", such dysregulation of Ca^{2+} handling triggers the neuronal dysfunction and eventually death observed in AD. The data presented here suggests that in addition to contributing to dysregulated ER Ca^{2+} signalling, RyR3 modulates the neuronal hyperexcitability, possibly due to Aβ42 accumulation, in TgCRND8 mice.

While there is the potential for increased Ca^{2+} release from ER stores through increased expression of RyR3, other aspects of neuronal Ca^{2+} handling, which are compromised in mutant PS models of AD, are unchanged in TgCRND8 neurons. Basal Ca^{2+} levels, Ca^{2+} responses to high K^+ and NMDA and capacitative Ca^{2+} entry responses

of TgCRND8 neurons were all comparible to nonTg responses (data not shown). Perhaps the up-regulation of RyR3 is responsible for the maintainance of global Ca^{2+} responses, preventing large increases in $[Ca^{2+}]_{cyto}$ that can lead to the activation of apoptotic processes. This does not rule out the increased function or recruitment of RyRs in spatially restricted areas of the neuron during activation, such as at the synapse, which results in functional synaptic transmission (Chakroborty et al. 2009).

It has been demonstrated that high levels of Aβ in the brain can cause epileptiform activity in cortical and hippocampal networks and are linked to cognitive deficits in Tg mouse models of AD (Palop et al. 2009b). TgCRND8 mice show slightly decreased seizure threshold, increased seizure severity (Del Vecchio et al. 2004) and cognitive deficits compared to nonTg (Chishti et al. 2001; Lovasic et al. 2005). Furthermore, pre-plaque TgCRND8 mice display presynaptic depression of basal synaptic transmission in hippocampal CA1 by BK channels, known to be activated in epilepsy (Ye et al. 2008). Given the role of RyR3 in controlling *I*sAHP in hippocampal CA1 neurons (van de Vrede et al. 2007), increased RyR3 expression and increased cytosolic Ca^{2+} could mediate the activation of BK channels to modulate neuronal excitability. If so, blockade of BK channels with specific inhibitors, such as iberiotoxin, should sensitize TgCRND8 neurons to hyperexcitability and death in culture similar to siRyR3 treatment or increased synaptic transmission in CA1. Similarly, it would be expected that TgCRND8/RyR3$^{-/-}$ would display hyperexcitability in hippocampal circuits, particularly in CA1 neurons, possibly showing increased or aberrant synaptic transmission. It has also been demonstrated that mutations linked to CPVT result in "leaky" RyR2 due to decreased binding of calstabin2 (Lehnart et al. 2008). Mice harbouring this mutation exhibited spontaneous generalized tonic-clonic seizures, exercise-induced ventricular arrhythmias and sudden cardiac death. A dominant-negative splice variant of RyR3 is known to negatively regulated Ca^{2+} release from RyR2

in smooth muscle cells (Dabertrand 2006), perhaps knocking-out RyR3 in TgCRND8 mice abolishes the RyR3 modulation of RyR2 activity, causing Ca^{2+} leak from RyR2 and decreasing seizure threshold. While modulation of excitability may be the mechanism of neuroprotection afforded by up-regulated RyR3 in TgCRND8 mice, the resulting depression of synaptic transmission could ultimately contribute to the cognitive deficits observed.

Seizures related to dementia and AD were first reported in 1986 (Hauser et al. 1986) and were thought to be a result of the neurodegeneration that occurs in the later stages of the disease. More recent data have demonstrated that seizures may accompany the onset of AD and can occur at the time of diagnosis prior to extensive neurodegeneration (Lozsadi et al. 2006). Epileptiform activity could indicate plasticity in neuronal networks as a result of injury or loss of neurons. Mild epileptic activity can trigger endogenous protective cell signalling pathways, such as ERK, the phosphatidylinositol 3 kinase (PI3K)-Akt pathway and glycogen synthase kinase (GSK) β3 inhibition, to protect neurons from death after subsequent seizures, termed epileptic preconditioning (Soriano et al. 2006). RyR3 could be involved in similar protective cell signalling pathways in TgCRND8 mice and afford protection in addition to its Ca^{2+} handling function.

5.4 FUTURE EXPERIMENTS AND THE ROLE OF RYR3 IN AD

RyR3 appears to be important for the survival of TgCRND8 neurons and mice, which has been demonstrated by decreasing or knocking-out the expression of the protein. A rescue experiment showing that Tg neurons with RyR3 knock-down can be protected by over-expression of RyR3, perhaps by co-transfection with an RyR3-expressing plasmid, would demonstrate a more convincing role for RyR3 in

neuroprotection. Similarly, the survival of TgCRND8/RyR3$^{-/-}$ mice brain should be restored after replacing the expression of RyR3 in neurons. Lentiviral constructs could be used to express RyR3 in TgCRND8/RyR3$^{-/-}$ cortical and hippocampal neurons *in vivo* to prevent premature spontaneous death (Jakobsson et al. 2003; Naldini et al. 1996). It would also be interesting to determine if RyR3 contributes to changes in cytosolic Ca^{2+} regulation in cortical neurons *in vivo* as it does *in vitro* (Kuchibhotla et al. 2008) and if neuroprotective mechanisms such as ERK and PI3K-Akt pathway activation or GSK β3 pathway inhibition are compromised as a result. Such experiments could provide a more definitive link between RyR3-mediated changes in Ca^{2+} and neuronal function and viability in TgCRND8.

The impact of RyR3 in clinical AD is not known. It has been demonstrated that [^{3}H]Ry binding is increased in autopsy brain of AD patients compared to non-demented controls, suggesting an up-regulation of RyR in clinical AD (Kelliher et al. 1999). Given the potential role for RyR3 in neuroprotection, it would be advantageous to determine whether or not RyR3 is up-regulated in AD brain. Therapeutics that target RyR3 up-regulation might positively impact the neurodegeneration observed in AD. Combining such therapeutics with drugs that enhance cognitive performance, such as ChEIs, could prove an effective regimen to combat the symptoms of and stop the progression of AD.

REFERENCES

2008 Alzheimer's disease facts and figures. Alzheimers Dement 2008; 4 (2):110-33.

Aisen PS, Gauthier S, Vellas B et al. Alzhemed: a potential treatment for Alzheimer's disease. Curr Alzheimer Res 2007; 4 (4):473-8.

Akita T, Kuba K. Functional triads consisting of ryanodine receptors, Ca(2+) channels, and Ca(2+)-activated K(+) channels in bullfrog sympathetic neurons. Plastic modulation of action potential. J Gen Physiol 2000; 116 (5):697-720.

Aley PK, Murray HJ, Boyle JP et al. Hypoxia stimulates Ca2+ release from intracellular stores in astrocytes via cyclic ADP ribose-mediated activation of ryanodine receptors. Cell Calcium 2006; 39 (1):95-100.

The Alzheimer Society of Canada. 1997-2009.

Antos CL, Frey N, Marx SO et al. Dilated cardiomyopathy and sudden death resulting from constitutive activation of protein kinase a. Circ Res 2001; 89 (11):997-1004.

APA. Diagnostic criteria from DSM-IV / American Psychiatric Association.: Washington, D.C. : The Association, c1994.; 1994.

Arai H, Lee VM, Messinger ML et al. Expression patterns of beta-amyloid precursor protein (beta-APP) in neural and nonneural human tissues from Alzheimer's disease and control subjects. Ann Neurol 1991; 30 (5):686-93.

Arendash GW, King DL, Gordon MN et al. Progressive, age-related behavioral impairments in transgenic mice carrying both mutant amyloid precursor protein and presenilin-1 transgenes. Brain Res 2001; 891 (1-2):42-53.

Arispe N, Diaz JC, Simakova O. Abeta ion channels. Prospects for treating Alzheimer's disease with Abeta channel blockers. Biochim Biophys Acta 2007; 1768 (8):1952-65.

Arispe N, Rojas E, Pollard HB. Alzheimer disease amyloid beta protein forms calcium channels in bilayer membranes: blockade by tromethamine and aluminum. Proc Natl Acad Sci U S A 1993; 90 (2):567-71.

Arrasate M, Mitra S, Schweitzer ES et al. Inclusion body formation reduces levels of mutant huntingtin and the risk of neuronal death. Nature 2004; 431 (7010):805-10.

Arundine M, Tymianski M. Molecular mechanisms of calcium-dependent neurodegeneration in excitotoxicity. Cell Calcium 2003; 34 (4-5):325-37.

Ashe KH. Mechanisms of memory loss in Abeta and tau mouse models. Biochem Soc Trans 2005; 33 (Pt 4):591-4.

Augustine GJ, Neher E. Neuronal Ca2+ signalling takes the local route. Curr Opin Neurobiol 1992; 2 (3):302-7.

Avila G, O'Brien JJ, Dirksen RT. Excitation--contraction uncoupling by a human central core disease mutation in the ryanodine receptor. Proc Natl Acad Sci U S A 2001; 98 (7):4215-20.

Ball MJ. Topographic distribution of neurofibrillary tangles and granulovacuolar degeneration in hippocampal cortex of aging and demented patients. A quantitative study. Acta Neuropathol 1978; 42 (2):73-80.

Ballard C, Day S, Sharp S et al. Neuropsychiatric symptoms in dementia: importance and treatment considerations. Int Rev Psychiatry 2008; 20 (4):396-404.

Balschun D, Wolfer DP, Bertocchini F et al. Deletion of the ryanodine receptor type 3 (RyR3) impairs forms of synaptic plasticity and spatial learning. Embo J 1999; 18 (19):5264-73.

Barger SW, Fiscus RR, Ruth P et al. Role of cyclic GMP in the regulation of neuronal calcium and survival by secreted forms of beta-amyloid precursor. J Neurochem 1995; 64 (5):2087-96.

Barnes MP. Medical management of spasticity in stroke. Age Ageing 2001; 30 Suppl 1:13-6.

Bellucci A, Luccarini I, Scali C et al. Cholinergic dysfunction, neuronal damage and axonal loss in TgCRND8 mice. Neurobiol Dis 2006; 23 (2):260-72.
Bennett MR. The early history of the synapse: from Plato to Sherrington. Brain Res Bull 1999; 50 (2):95-118.
Berridge MJ. Neuronal calcium signaling. Neuron 1998; 21 (1):13-26.
Berridge MJ. The versatility and complexity of calcium signalling. Novartis Found Symp 2001; 239:52-64; discussion -7, 150-9.
Berridge MJ, Bootman MD, Lipp P. Calcium--a life and death signal. Nature 1998; 395 (6703):645-8.
Berridge MV, Tan AS. Characterization of the cellular reduction of 3-(4,5-dimethylthiazol-2-yl)-2,5-diphenyltetrazolium bromide (MTT): subcellular localization, substrate dependence, and involvement of mitochondrial electron transport in MTT reduction. Arch Biochem Biophys 1993; 303 (2):474-82.
Bertocchini F, Ovitt CE, Conti A et al. Requirement for the ryanodine receptor type 3 for efficient contraction in neonatal skeletal muscles. Embo J 1997; 16 (23):6956-63.
Bezprozvanny I, Mattson MP. Neuronal calcium mishandling and the pathogenesis of Alzheimer's disease. Trends Neurosci 2008; 31 (9):454-63.
Bidasee KR, Besch HR, Jr. Structure-function relationships among ryanodine derivatives. Pyridyl ryanodine definitively separates activation potency from high affinity. J Biol Chem 1998; 273 (20):12176-86.
Blaustein MP, Ratzlaff RW, Schweitzer ES. Calcium buffering in presynaptic nerve terminals. II. Kinetic properties of the nonmitochondrial Ca sequestration mechanism. J Gen Physiol 1978; 72 (1):43-66.
Blessed G, Tomlinson BE, Roth M. The association between quantitative measures of dementia and of senile change in the cerebral grey matter of elderly subjects. Br J Psychiatry 1968; 114 (512):797-811.
Bliss TV, Lomo T. Long-lasting potentiation of synaptic transmission in the dentate area of the anaesthetized rabbit following stimulation of the perforant path. J Physiol 1973; 232 (2):331-56.
Borchelt DR, Thinakaran G, Eckman CB et al. Familial Alzheimer's disease-linked presenilin 1 variants elevate Abeta1-42/1-40 ratio in vitro and in vivo. Neuron 1996; 17 (5):1005-13.
Borghi R, Pellegrini L, Lacana E et al. Neuronal apoptosis is accompanied by amyloid beta-protein accumulation in the endoplasmic reticulum. J Alzheimers Dis 2002; 4 (1):31-7.
Bouchard R, Pattarini R, Geiger JD. Presence and functional significance of presynaptic ryanodine receptors. Prog Neurobiol 2003; 69 (6):391-418.
Braak H, Braak E. Neuropathological stageing of Alzheimer-related changes. Acta Neuropathol 1991; 82 (4):239-59.
Brillantes AB, Ondrias K, Scott A et al. Stabilization of calcium release channel (ryanodine receptor) function by FK506-binding protein. Cell 1994; 77 (4):513-23.
Brustovetsky N, Brustovetsky T, Purl KJ et al. Increased susceptibility of striatal mitochondria to calcium-induced permeability transition. J Neurosci 2003; 23 (12):4858-67.
Brzyska M, Elbaum D. Dysregulation of calcium in Alzheimer's disease. Acta Neurobiol Exp (Wars) 2003; 63 (3):171-83.
Buck E, Zimanyi I, Abramson JJ et al. Ryanodine stabilizes multiple conformational states of the skeletal muscle calcium release channel. J Biol Chem 1992; 267 (33):23560-7.

Butterfield DA. Amyloid beta-peptide (1-42)-induced oxidative stress and neurotoxicity: implications for neurodegeneration in Alzheimer's disease brain. A review. Free Radic Res 2002; 36 (12):1307-13.
Buttini M, Masliah E, Barbour R et al. Beta-amyloid immunotherapy prevents synaptic degeneration in a mouse model of Alzheimer's disease. J Neurosci 2005; 25 (40):9096-101.
Buxbaum JD, Ruefli AA, Parker CA et al. Calcium regulates processing of the Alzheimer amyloid protein precursor in a protein kinase C-independent manner. Proc Natl Acad Sci U S A 1994; 91 (10):4489-93.
Callaway C, Seryshev A, Wang JP et al. Localization of the high and low affinity [3H]ryanodine binding sites on the skeletal muscle Ca2+ release channel. J Biol Chem 1994; 269 (22):15876-84.
Campbell LW, Hao SY, Thibault O et al. Aging changes in voltage-gated calcium currents in hippocampal CA1 neurons. J Neurosci 1996; 16 (19):6286-95.
Canevari L, Abramov AY, Duchen MR. Toxicity of amyloid beta peptide: tales of calcium, mitochondria, and oxidative stress. Neurochem Res 2004; 29 (3):637-50.
Cao X, Sudhof TC. A transcriptionally [correction of transcriptively] active complex of APP with Fe65 and histone acetyltransferase Tip60. Science 2001; 293 (5527):115-20.
Carter AG, Vogt KE, Foster KA et al. Assessing the role of calcium-induced calcium release in short-term presynaptic plasticity at excitatory central synapses. J Neurosci 2002; 22 (1):21-8.
Chakroborty S, Goussakov I, Miller MB et al. Deviant ryanodine receptor-mediated calcium release resets synaptic homeostasis in presymptomatic 3xTg-AD mice. J Neurosci 2009; 29 (30):9458-70.
Chan SL, Mayne M, Holden CP et al. Presenilin-1 mutations increase levels of ryanodine receptors and calcium release in PC12 cells and cortical neurons. J Biol Chem 2000; 275 (24):18195-200.
Chauhan NB, Siegel GJ, Lichtor T. Effect of age on the duration and extent of amyloid plaque reduction and microglial activation after injection of anti-Abeta antibody into the third ventricle of TgCRND8 mice. J Neurosci Res 2004; 78 (5):732-41.
Chen G, Chen KS, Knox J et al. A learning deficit related to age and beta-amyloid plaques in a mouse model of Alzheimer's disease. Nature 2000; 408 (6815):975-9.
Chen SR, MacLennan DH. Identification of calmodulin-, Ca(2+)-, and ruthenium red-binding domains in the Ca2+ release channel (ryanodine receptor) of rabbit skeletal muscle sarcoplasmic reticulum. J Biol Chem 1994; 269 (36):22698-704.
Chishti MA, Yang DS, Janus C et al. Early-onset amyloid deposition and cognitive deficits in transgenic mice expressing a double mutant form of amyloid precursor protein 695. J Biol Chem 2001; 276 (24):21562-70.
Chu A, Diaz-Munoz M, Hawkes MJ et al. Ryanodine as a probe for the functional state of the skeletal muscle sarcoplasmic reticulum calcium release channel. Mol Pharmacol 1990a; 37 (5):735-41.
Chu A, Sumbilla C, Inesi G et al. Specific association of calmodulin-dependent protein kinase and related substrates with the junctional sarcoplasmic reticulum of skeletal muscle. Biochemistry 1990b; 29 (25):5899-905.
Citron M, Oltersdorf T, Haass C et al. Mutation of the beta-amyloid precursor protein in familial Alzheimer's disease increases beta-protein production. Nature 1992; 360 (6405):672-4.
Citron M, Westaway D, Xia W et al. Mutant presenilins of Alzheimer's disease increase production of 42-residue amyloid beta-protein in both transfected cells and transgenic mice. Nat Med 1997; 3 (1):67-72.

Clark LN, Poorkaj P, Wszolek Z et al. Pathogenic implications of mutations in the tau gene in pallido-ponto-nigral degeneration and related neurodegenerative disorders linked to chromosome 17. Proc Natl Acad Sci U S A 1998; 95 (22):13103-7.
Cleary JP, Walsh DM, Hofmeister JJ et al. Natural oligomers of the amyloid-beta protein specifically disrupt cognitive function. Nat Neurosci 2005; 8 (1):79-84.
Clementi E, Riccio M, Sciorati C et al. The type 2 ryanodine receptor of neurosecretory PC12 cells is activated by cyclic ADP-ribose. Role of the nitric oxide/cGMP pathway. J Biol Chem 1996; 271 (30):17739-45.
Clinical trials.
Clodfelter GV, Porter NM, Landfield PW et al. Sustained Ca(2+)-induced Ca(2+)-release underlies the post-glutamate lethal Ca(2+) plateau in older cultured hippocampal neurons. Eur J Pharmacol 2002; 447 (2-3):189-200.
Collins JH. Sequence analysis of the ryanodine receptor: possible association with a 12K, FK506-binding immunophilin/protein kinase C inhibitor. Biochem Biophys Res Commun 1991; 178 (3):1288-90.
Corder EH, Saunders AM, Strittmatter WJ et al. Gene dose of apolipoprotein E type 4 allele and the risk of Alzheimer's disease in late onset families. Science 1993; 261 (5123):921-3.
Courtney C, Farrell D, Gray R et al. Long-term donepezil treatment in 565 patients with Alzheimer's disease (AD2000): randomised double-blind trial. Lancet 2004; 363 (9427):2105-15.
Cruts M, Van Broeckhoven C. Molecular genetics of Alzheimer's disease. Ann Med 1998; 30 (6):560-5.
Cummings JL. Alzheimer's disease. N Engl J Med 2004; 351 (1):56-67.
Dabertrand F, Morel JL, Sorrentino V et al. Modulation of calcium signalling by dominant negative splice variant of ryanodine receptor subtype 3 in native smooth muscle cells. Cell Calcium 2006; 40 (1):11-21.
de Leon MJ, Mosconi L, Blennow K et al. Imaging and CSF studies in the preclinical diagnosis of Alzheimer's disease. Ann N Y Acad Sci 2007; 1097:114-45.
De Strooper B. Aph-1, Pen-2, and Nicastrin with Presenilin generate an active gamma-Secretase complex. Neuron 2003; 38 (1):9-12.
De Strooper B, Annaert W, Cupers P et al. A presenilin-1-dependent gamma-secretase-like protease mediates release of Notch intracellular domain [see comments]. Nature 1999; 398 (6727):518-22.
De Strooper B, Saftig P, Craessaerts K et al. Deficiency of presenilin-1 inhibits the normal cleavage of amyloid precursor protein [see comments]. Nature 1998; 391 (6665):387-90.
Del Vecchio RA, Gold LH, Novick SJ et al. Increased seizure threshold and severity in young transgenic CRND8 mice. Neurosci Lett 2004; 367 (2):164-7.
Denizot F, Lang R. Rapid colorimetric assay for cell growth and survival. Modifications to the tetrazolium dye procedure giving improved sensitivity and reliability. J Immunol Methods 1986; 89 (2):271-7.
Dettling M, Sander T, Weber M et al. Mutation analysis of the ryanodine receptor gene isoform 3 (RYR3) in recurrent neuroleptic malignant syndrome. J Clin Psychopharmacol 2004; 24 (4):471-3.
Disterhoft JF, Oh MM. Pharmacological and molecular enhancement of learning in aging and Alzheimer's disease. J Physiol Paris 2006; 99 (2-3):180-92.
Disterhoft JF, Thompson LT, Moyer JR, Jr. et al. Calcium-dependent afterhyperpolarization and learning in young and aging hippocampus. Life Sci 1996; 59 (5-6):413-20.

Dodart JC, Bales KR, Gannon KS et al. Immunization reverses memory deficits without reducing brain Abeta burden in Alzheimer's disease model. Nat Neurosci 2002; 5 (5):452-7.
Dodart JC, Mathis C, Saura J et al. Neuroanatomical abnormalities in behaviorally characterized APP(V717F) transgenic mice. Neurobiol Dis 2000; 7 (2):71-85.
Dodart JC, Meziane H, Mathis C et al. Behavioral disturbances in transgenic mice overexpressing the V717F beta-amyloid precursor protein. Behav Neurosci 1999; 113 (5):982-90.
Dreses-Werringloer U, Lambert JC, Vingtdeux V et al. A polymorphism in CALHM1 influences Ca2+ homeostasis, Abeta levels, and Alzheimer's disease risk. Cell 2008; 133 (7):1149-61.
Du GG, Sandhu B, Khanna VK et al. Topology of the Ca2+ release channel of skeletal muscle sarcoplasmic reticulum (RyR1). Proc Natl Acad Sci U S A 2002; 99 (26):16725-30.
Duchen MR. Mitochondria and calcium: from cell signalling to cell death. J Physiol 2000; 529 Pt 1:57-68.
Dudal S, Krzywkowski P, Paquette J et al. Inflammation occurs early during the Abeta deposition process in TgCRND8 mice. Neurobiol Aging 2004; 25 (7):861-71.
Duff K, Eckman C, Zehr C et al. Increased amyloid-beta42(43) in brains of mice expressing mutant presenilin 1. Nature 1996; 383 (6602):710-3.
Dulhunty AF. Excitation-contraction coupling from the 1950s into the new millennium. Clin Exp Pharmacol Physiol 2006; 33 (9):763-72.
Ekerot CF, Kano M. Long-term depression of parallel fibre synapses following stimulation of climbing fibres. Brain Res 1985; 342 (2):357-60.
El-Hayek R, Saiki Y, Yamamoto T et al. A postulated role of the near amino-terminal domain of the ryanodine receptor in the regulation of the sarcoplasmic reticulum Ca(2+) channel. J Biol Chem 1999; 274 (47):33341-7.
Ellis KO, Castellion AW, Honkomp LJ et al. Dantrolene, a direct acting skeletal muscle relaxant. J Pharm Sci 1973; 62 (6):948-51.
Emilsson L, Saetre P, Jazin E. Alzheimer's disease: mRNA expression profiles of multiple patients show alterations of genes involved with calcium signaling. Neurobiol Dis 2006; 21 (3):618-25.
Empson RM, Galione A. Cyclic ADP-ribose enhances coupling between voltage-gated Ca2+ entry and intracellular Ca2+ release. J Biol Chem 1997; 272 (34):20967-70.
Emptage N, Bliss TV, Fine A. Single synaptic events evoke NMDA receptor-mediated release of calcium from internal stores in hippocampal dendritic spines. Neuron 1999; 22 (1):115-24.
Emptage NJ, Reid CA, Fine A. Calcium stores in hippocampal synaptic boutons mediate short-term plasticity, store-operated Ca2+ entry, and spontaneous transmitter release. Neuron 2001; 29 (1):197-208.
Etcheberrigaray R, Hirashima N, Nee L et al. Calcium responses in fibroblasts from asymptomatic members of Alzheimer's disease families. Neurobiol Dis 1998a; 5 (1):37-45.
Etcheberrigaray R, Hirashima N, Nee L et al. Calcium responses in fibroblasts from asymptomatic members of Alzheimer's disease families. Neurobiol Dis 1998b; 5 (1):37-45.
Feldman HH, Schmitt FA, Olin JT. Activities of daily living in moderate-to-severe Alzheimer disease: an analysis of the treatment effects of memantine in patients receiving stable donepezil treatment. Alzheimer Dis Assoc Disord 2006; 20 (4):263-8.

Ferguson DG, Schwartz HW, Franzini-Armstrong C. Subunit structure of junctional feet in triads of skeletal muscle: a freeze-drying, rotary-shadowing study. J Cell Biol 1984; 99 (5):1735-42.
Flanders KC, Ren RF, Lippa CF. Transforming growth factor-betas in neurodegenerative disease. Prog Neurobiol 1998; 54 (1):71-85.
Flewellen EH, Nelson TE, Jones WP et al. Dantrolene dose response in awake man: implications for management of malignant hyperthermia. Anesthesiology 1983; 59 (4):275-80.
Forette F, Seux ML, Staessen JA et al. The prevention of dementia with antihypertensive treatment: new evidence from the Systolic Hypertension in Europe (Syst-Eur) study. Arch Intern Med 2002; 162 (18):2046-52.
Franzini-Armstrong C, Protasi F, Ramesh V. Shape, size, and distribution of Ca(2+) release units and couplons in skeletal and cardiac muscles. Biophys J 1999; 77 (3):1528-39.
Friel DD, Tsien RW. A caffeine- and ryanodine-sensitive Ca2+ store in bullfrog sympathetic neurones modulates effects of Ca2+ entry on [Ca2+]i. J Physiol 1992; 450:217-46.
Fruen BR, Mickelson JR, Louis CF. Dantrolene inhibition of sarcoplasmic reticulum Ca2+ release by direct and specific action at skeletal muscle ryanodine receptors. J Biol Chem 1997; 272 (43):26965-71.
Fuentes O, Valdivia C, Vaughan D et al. Calcium-dependent block of ryanodine receptor channel of swine skeletal muscle by direct binding of calmodulin. Cell Calcium 1994; 15 (4):305-16.
Futatsugi A, Kato K, Ogura H et al. Facilitation of NMDAR-independent LTP and spatial learning in mutant mice lacking ryanodine receptor type 3. Neuron 1999; 24 (3):701-13.
Futatsugi A, Kuwajima G, Mikoshiba K. Tissue-specific and developmentally regulated alternative splicing in mouse skeletal muscle ryanodine receptor mRNA. Biochem J 1995; 305 (Pt 2):373-8.
Gaiarsa JL, Caillard O, Ben-Ari Y. Long-term plasticity at GABAergic and glycinergic synapses: mechanisms and functional significance. Trends Neurosci 2002; 25 (11):564-70.
Galeotti N, Quattrone A, Vivoli E et al. Different involvement of type 1, 2, and 3 ryanodine receptors in memory processes. Learn Mem 2008; 15 (5):315-23.
Games D, Adams D, Alessandrini R et al. Alzheimer-type neuropathology in transgenic mice overexpressing V717F beta-amyloid precursor protein. Nature 1995a; 373 (6514):523-7.
Games D, Adams D, Alessandrini R et al. Alzheimer-type neuropathology in transgenic mice overexpressing V717F beta-amyloid precursor protein [see comments]. Nature 1995b; 373 (6514):523-7.
Gelinas DS, DaSilva K, Fenili D et al. Immunotherapy for Alzheimer's disease. Proc Natl Acad Sci U S A 2004; 101 Suppl 2:14657-62.
Genazzani AA, Carafoli E, Guerini D. Calcineurin controls inositol 1,4,5-trisphosphate type 1 receptor expression in neurons. Proc Natl Acad Sci U S A 1999; 96 (10):5797-801.
Ghosh A, Greenberg ME. Calcium signaling in neurons: molecular mechanisms and cellular consequences. Science 1995; 268 (5208):239-47.
Giacobini E. Cholinesterase inhibitors: new roles and therapeutic alternatives. Pharmacol Res 2004; 50 (4):433-40.
Giannini G, Clementi E, Ceci R et al. Expression of a ryanodine receptor-Ca2+ channel that is regulated by TGF-beta. Science 1992; 257 (5066):91-4.

Giannini G, Conti A, Mammarella S et al. The ryanodine receptor/calcium channel genes are widely and differentially expressed in murine brain and peripheral tissues. J Cell Biol 1995; 128 (5):893-904.
Gibson GE, Vestling M, Zhang H et al. Abnormalities in Alzheimer's disease fibroblasts bearing the APP670/671 mutation. Neurobiol Aging 1997; 18 (6):573-80.
Gillian CM, Heffron JJ, Lehane M et al. Analysis of expression of the human ryanodine receptor gene in malignant hyperthermia skeletal muscle tissue. Biochem Soc Trans 1991; 19 (1):46S.
Glazner GW, Chan SL, Lu C et al. Caspase-mediated degradation of AMPA receptor subunits: a mechanism for preventing excitotoxic necrosis and ensuring apoptosis. J Neurosci 2000; 20 (10):3641-9.
Glenner GG, Wong CW. Alzheimer's disease: initial report of the purification and characterization of a novel cerebrovascular amyloid protein. Biochem Biophys Res Commun 1984; 120 (3):885-90.
Goate A, Chartier-Harlin MC, Mullan M et al. Segregation of a missense mutation in the amyloid precursor protein gene with familial Alzheimer's disease. Nature 1991; 349 (6311):704-6.
Golde TE, Estus S, Usiak M et al. Expression of beta amyloid protein precursor mRNAs: recognition of a novel alternatively spliced form and quantitation in Alzheimer's disease using PCR. Neuron 1990; 4 (2):253-67.
Goodman Y, Mattson MP. Secreted forms of beta-amyloid precursor protein protect hippocampal neurons against amyloid beta-peptide-induced oxidative injury. Exp Neurol 1994; 128 (1):1-12.
Gotz J, Chen F, van Dorpe J et al. Formation of neurofibrillary tangles in P301l tau transgenic mice induced by Abeta 42 fibrils. Science 2001; 293 (5534):1491-5.
Grammas P, Ovase R. Cerebrovascular transforming growth factor-beta contributes to inflammation in the Alzheimer's disease brain. Am J Pathol 2002; 160 (5):1583-7.
Green KN, Demuro A, Akbari Y et al. SERCA pump activity is physiologically regulated by presenilin and regulates amyloid beta production. J Cell Biol 2008; 181 (7):1107-16.
Greene JD, Baddeley AD, Hodges JR. Analysis of the episodic memory deficit in early Alzheimer's disease: evidence from the doors and people test. Neuropsychologia 1996; 34 (6):537-51.
Grogan H, Hopkins PM. Heat stroke: implications for critical care and anaesthesia. Br J Anaesth 2002; 88 (5):700-7.
Guis S, Figarella-Branger D, Monnier N et al. Multiminicore disease in a family susceptible to malignant hyperthermia: histology, in vitro contracture tests, and genetic characterization. Arch Neurol 2004; 61 (1):106-13.
Guo Q, Fu W, Sopher BL et al. Increased vulnerability of hippocampal neurons to excitotoxic necrosis in presenilin-1 mutant knock-in mice. Nat Med 1999; 5 (1):101-6.
Guo Q, Sopher BL, Furukawa K et al. Alzheimer's presenilin mutation sensitizes neural cells to apoptosis induced by trophic factor withdrawal and amyloid beta-peptide: involvement of calcium and oxyradicals. J Neurosci 1997; 17 (11):4212-22.
Gyorke I, Hester N, Jones LR et al. The role of calsequestrin, triadin, and junctin in conferring cardiac ryanodine receptor responsiveness to luminal calcium. Biophys J 2004; 86 (4):2121-8.
Haass C, Lemere CA, Capell A et al. The Swedish mutation causes early-onset Alzheimer's disease by beta-secretase cleavage within the secretory pathway. Nat Med 1995; 1 (12):1291-6.
Haass C, Selkoe DJ. Soluble protein oligomers in neurodegeneration: lessons from the Alzheimer's amyloid beta-peptide. Nat Rev Mol Cell Biol 2007; 8 (2):101-12.

Hajnoczky G, Csordas G, Yi M. Old players in a new role: mitochondria-associated membranes, VDAC, and ryanodine receptors as contributors to calcium signal propagation from endoplasmic reticulum to the mitochondria. Cell Calcium 2002; 32 (5-6):363-77.
Hakamata Y, Nakai J, Takeshima H et al. Primary structure and distribution of a novel ryanodine receptor/calcium release channel from rabbit brain. FEBS Lett 1992; 312 (2-3):229-35.
Hardy J. A hundred years of Alzheimer's disease research. Neuron 2006; 52 (1):3-13.
Hardy J, Selkoe DJ. The amyloid hypothesis of Alzheimer's disease: progress and problems on the road to therapeutics. Science 2002; 297 (5580):353-6.
Hardy JA, Higgins GA. Alzheimer's disease: the amyloid cascade hypothesis. Science 1992; 256 (5054):184-5.
Harteneck C, Plant TD, Schultz G. From worm to man: three subfamilies of TRP channels. Trends Neurosci 2000; 23 (4):159-66.
Hashimoto M, Kazui H, Matsumoto K et al. Does donepezil treatment slow the progression of hippocampal atrophy in patients with Alzheimer's disease? Am J Psychiatry 2005; 162 (4):676-82.
Hauser WA, Morris ML, Heston LL et al. Seizures and myoclonus in patients with Alzheimer's disease. Neurology 1986; 36 (9):1226-30.
Hemond P, Jaffe DB. Caloric restriction prevents aging-associated changes in spike-mediated Ca2+ accumulation and the slow afterhyperpolarization in hippocampal CA1 pyramidal neurons. Neuroscience 2005; 135 (2):413-20.
Henze DA, McMahon DB, Harris KM et al. Giant miniature EPSCs at the hippocampal mossy fiber to CA3 pyramidal cell synapse are monoquantal. J Neurophysiol 2002; 87 (1):15-29.
Hernandez-Cruz A, Diaz-Munoz M, Gomez-Chavarin M et al. Properties of the ryanodine-sensitive release channels that underlie caffeine-induced Ca2+ mobilization from intracellular stores in mammalian sympathetic neurons. Eur J Neurosci 1995; 7 (8):1684-99.
Hidalgo C, Carrasco MA, Munoz P et al. A role for reactive oxygen/nitrogen species and iron on neuronal synaptic plasticity. Antioxid Redox Signal 2007; 9 (2):245-55.
Holcomb L, Gordon MN, McGowan E et al. Accelerated Alzheimer-type phenotype in transgenic mice carrying both mutant amyloid precursor protein and presenilin 1 transgenes. Nat Med 1998; 4 (1):97-100.
Holcomb LA, Gordon MN, Jantzen P et al. Behavioral changes in transgenic mice expressing both amyloid precursor protein and presenilin-1 mutations: lack of association with amyloid deposits. Behav Genet 1999; 29 (3):177-85.
Hsiao K, Chapman P, Nilsen S et al. Correlative memory deficits, Abeta elevation, and amyloid plaques in transgenic mice. Science 1996; 274 (5284):99-102.
Huang RQ, Bell-Horner CL, Dibas MI et al. Pentylenetetrazole-induced inhibition of recombinant gamma-aminobutyric acid type A (GABA(A)) receptors: mechanism and site of action. J Pharmacol Exp Ther 2001; 298 (3):986-95.
Huang X, Atwood CS, Hartshorn MA et al. The A beta peptide of Alzheimer's disease directly produces hydrogen peroxide through metal ion reduction. Biochemistry 1999; 38 (24):7609-16.
Huddleston AT, Tang W, Takeshima H et al. Superoxide-induced potentiation in the hippocampus requires activation of ryanodine receptor type 3 and ERK. J Neurophysiol 2008; 99 (3):1565-71.
Hui CS, Besch HR, Jr., Bidasee KR. Effects of ryanoids on spontaneous and depolarization-evoked calcium release events in frog muscle. Biophys J 2004; 87 (1):243-55.

Hutton M, Lendon CL, Rizzu P et al. Association of missense and 5'-splice-site mutations in tau with the inherited dementia FTDP-17. Nature 1998; 393 (6686):702-5.
Hux MJ, O'Brien BJ, Iskedjian M et al. Relation between severity of Alzheimer's disease and costs of caring. Cmaj 1998; 159 (5):457-65.
Hyde LA, Kazdoba TM, Grilli M et al. Age-progressing cognitive impairments and neuropathology in transgenic CRND8 mice. Behav Brain Res 2005; 160 (2):344-55.
Ikemoto N, Yamamoto T. Regulation of calcium release by interdomain interaction within ryanodine receptors. Front Biosci 2002; 7:d671-83.
Ikonomovic MD, Klunk WE, Abrahamson EE et al. Post-mortem correlates of in vivo PiB-PET amyloid imaging in a typical case of Alzheimer's disease. Brain 2008; 131 (Pt 6):1630-45.
The incidence of dementia in Canada. The Canadian Study of Health and Aging Working Group. Neurology 2000; 55:66-73.
Irizarry MC, Soriano F, McNamara M et al. Abeta deposition is associated with neuropil changes, but not with overt neuronal loss in the human amyloid precursor protein V717F (PDAPP) transgenic mouse. J Neurosci 1997; 17 (18):7053-9.
Ito E, Oka K, Etcheberrigaray R et al. Internal Ca2+ mobilization is altered in fibroblasts from patients with Alzheimer disease. Proc Natl Acad Sci U S A 1994; 91 (2):534-8.
Jakobsson J, Ericson C, Jansson M et al. Targeted transgene expression in rat brain using lentiviral vectors. J Neurosci Res 2003; 73 (6):876-85.
Janus C. Search strategies used by APP transgenic mice during navigation in the Morris water maze. Learn Mem 2004; 11 (3):337-46.
Janus C, D'Amelio S, Amitay O et al. Spatial learning in transgenic mice expressing human presenilin 1 (PS1) transgenes. Neurobiol Aging 2000a; 21 (4):541-9.
Janus C, Pearson J, McLaurin J et al. A beta peptide immunization reduces behavioural impairment and plaques in a model of Alzheimer's disease. Nature 2000b; 408 (6815):979-82.
Jarvis CR, Lilge L, Vipond GJ et al. Interpretation of intrinsic optical signals and calcein fluorescence during acute excitotoxic insult in the hippocampal slice. Neuroimage 1999; 10 (4):357-72.
Jenden DJ, Fairhurst AS. The pharmacology of ryanodine. Pharmacol Rev 1969; 21 (1):1-25.
Jiang D, Xiao B, Li X et al. Smooth muscle tissues express a major dominant negative splice variant of the type 3 Ca2+ release channel (ryanodine receptor). J Biol Chem 2003; 278 (7):4763-9.
Jolas T, Zhang XS, Zhang Q et al. Long-term potentiation is increased in the CA1 area of the hippocampus of APP(swe/ind) CRND8 mice. Neurobiol Dis 2002; 11 (3):394-409.
Jurkat-Rott K, Lerche H, Lehmann-Horn F. Skeletal muscle channelopathies. J Neurol 2002; 249 (11):1493-502.
Jurkat-Rott K, McCarthy T, Lehmann-Horn F. Genetics and pathogenesis of malignant hyperthermia. Muscle Nerve 2000; 23 (1):4-17.
Kakizawa S, Kishimoto Y, Hashimoto K et al. Junctophilin-mediated channel crosstalk essential for cerebellar synaptic plasticity. Embo J 2007; 26 (7):1924-33.
Kamal A, Almenar-Queralt A, LeBalnc J et al. Kinesin-mediated axonal transport of a membrance compartment containing beta-secretase and presenilin-1 requires APP. Nature 2001; 414:643-8.
Kawakami M, Okabe E. Superoxide anion radical-triggered Ca2+ release from cardiac sarcoplasmic reticulum through ryanodine receptor Ca2+ channel. Mol Pharmacol 1998; 53 (3):497-503.

Kelliher M, Fastbom J, Cowburn RF et al. Alterations in the ryanodine receptor calcium release channel correlate with Alzheimer's disease neurofibrillary and beta-amyloid pathologies. Neuroscience 1999; 92 (2):499-513.
Kemmerling U, Munoz P, Muller M et al. Calcium release by ryanodine receptors mediates hydrogen peroxide-induced activation of ERK and CREB phosphorylation in N2a cells and hippocampal neurons. Cell Calcium 2007; 41 (5):491-502.
Ketel WB, Kolb ME. Long-term treatment with dantrolene sodium of stroke patients with spasticity limiting the return of function. Curr Med Res Opin 1984; 9 (3):161-9.
Khachaturian ZS. Calcium, membranes, aging, and Alzheimer's disease. Introduction and overview. Ann N Y Acad Sci 1989; 568:1-4.
Khachaturian ZS. Diagnosis of Alzheimer's disease: two-decades of progress. J Alzheimers Dis 2006; 9 (3 Suppl):409-15.
Khachaturian ZS. Hypothesis on the regulation of cytosol calcium concentration and the aging brain. Neurobiol Aging 1987; 8 (4):345-6.
Kim HS, Park CH, Cha SH et al. Carboxyl-terminal fragment of Alzheimer's APP destabilizes calcium homeostasis and renders neuronal cells vulnerable to excitotoxicity. Faseb J 2000; 14 (11):1508-17.
Kim S, Yun HM, Baik JH et al. Functional Interaction of Neuronal Cav1.3 L-type Calcium Channel with Ryanodine Receptor Type 2 in the Rat Hippocampus. J Biol Chem 2007; 282 (45):32877-89.
Klann E, Thiels E. Modulation of protein kinases and protein phosphatases by reactive oxygen species: implications for hippocampal synaptic plasticity. Prog Neuropsychopharmacol Biol Psychiatry 1999; 23 (3):359-76.
Klunk WE, Engler H, Nordberg A et al. Imaging brain amyloid in Alzheimer's disease with Pittsburgh Compound-B. Ann Neurol 2004; 55 (3):306-19.
Knopman DS, DeKosky ST, Cummings JL et al. Practice parameter: diagnosis of dementia (an evidence-based review). Report of the Quality Standards Subcommittee of the American Academy of Neurology. Neurology 2001; 56 (9):1143-53.
Kokjohn TA, Roher AE. Antibody responses, amyloid-beta peptide remnants and clinical effects of AN-1792 immunization in patients with AD in an interrupted trial. CNS Neurol Disord Drug Targets 2009; 8 (2):88-97.
Krishnan KR, Charles HC, Doraiswamy PM et al. Randomized, placebo-controlled trial of the effects of donepezil on neuronal markers and hippocampal volumes in Alzheimer's disease. Am J Psychiatry 2003; 160 (11):2003-11.
Kuchibhotla KV, Goldman ST, Lattarulo CR et al. Abeta plaques lead to aberrant regulation of calcium homeostasis in vivo resulting in structural and functional disruption of neuronal networks. Neuron 2008; 59 (2):214-25.
Kunerth S, Langhorst MF, Schwarzmann N et al. Amplification and propagation of pacemaker Ca2+ signals by cyclic ADP-ribose and the type 3 ryanodine receptor in T cells. J Cell Sci 2004; 117 (Pt 10):2141-9.
Kuwajima G, Futatsugi A, Niinobe M et al. Two types of ryanodine receptors in mouse brain: skeletal muscle type exclusively in Purkinje cells and cardiac muscle type in various neurons. Neuron 1992; 9 (6):1133-42.
LaFerla FM. Calcium dyshomeostasis and intracellular signalling in Alzheimer's disease. Nat Rev Neurosci 2002; 3 (11):862-72.
Lai FA, Misra M, Xu L et al. The ryanodine receptor-Ca2+ release channel complex of skeletal muscle sarcoplasmic reticulum. Evidence for a cooperatively coupled, negatively charged homotetramer. J Biol Chem 1989; 264 (28):16776-85.
Laitinen PJ, Brown KM, Piippo K et al. Mutations of the cardiac ryanodine receptor (RyR2) gene in familial polymorphic ventricular tachycardia. Circulation 2001; 103 (4):485-90.

Lam E, Martin MM, Timerman AP et al. A novel FK506 binding protein can mediate the immunosuppressive effects of FK506 and is associated with the cardiac ryanodine receptor. J Biol Chem 1995; 270 (44):26511-22.
Lambert MP, Barlow AK, Chromy BA et al. Diffusible, nonfibrillar ligands derived from Abeta1-42 are potent central nervous system neurotoxins. Proc Natl Acad Sci U S A 1998; 95 (11):6448-53.
Lanctot KL, Herrmann N, Yau KK et al. Efficacy and safety of cholinesterase inhibitors in Alzheimer's disease: a meta-analysis. Cmaj 2003; 169 (6):557-64.
Landfield PW. 'Increased calcium-current' hypothesis of brain aging. Neurobiol Aging 1987; 8 (4):346-7.
Landfield PW, editor Mechanisms of altered neural function during aging. Amsterdam, The Netherlands: Elsevier; 1983. 51-7 p. (G WH; T J editors. Aging Brain).
Landfield PW, Pitler TA. Prolonged Ca2+-dependent afterhyperpolarizations in hippocampal neurons of aged rats. Science 1984; 226 (4678):1089-92.
Larson J, Lynch G, Games D et al. Alterations in synaptic transmission and long-term potentiation in hippocampal slices from young and aged PDAPP mice. Brain Res 1999; 840 (1-2):23-35.
Laver DR, Baynes TM, Dulhunty AF. Magnesium inhibition of ryanodine-receptor calcium channels: evidence for two independent mechanisms. J Membr Biol 1997; 156 (3):213-29.
Lee G, Pollard HB, Arispe N. Annexin 5 and apolipoprotein E2 protect against Alzheimer's amyloid-beta-peptide cytotoxicity by competitive inhibition at a common phosphatidylserine interaction site. Peptides 2002; 23 (7):1249-63.
Lee JM, Shih AY, Murphy TH et al. NF-E2-related factor-2 mediates neuroprotection against mitochondrial complex I inhibitors and increased concentrations of intracellular calcium in primary cortical neurons. J Biol Chem 2003; 278 (39):37948-56.
Lee SY, Hwang DY, Kim YK et al. PS2 mutation increases neuronal cell vulnerability to neurotoxicants through activation of caspase-3 by enhancing of ryanodine receptor-mediated calcium release. Faseb J 2006; 20 (1):151-3.
Lehnart SE, Mongillo M, Bellinger A et al. Leaky Ca2+ release channel/ryanodine receptor 2 causes seizures and sudden cardiac death in mice. J Clin Invest 2008; 118 (6):2230-45.
Lehnart SE, Wehrens XH, Laitinen PJ et al. Sudden death in familial polymorphic ventricular tachycardia associated with calcium release channel (ryanodine receptor) leak. Circulation 2004; 109 (25):3208-14.
Leissring MA, Akbari Y, Fanger CM et al. Capacitative calcium entry deficits and elevated luminal calcium content in mutant presenilin-1 knockin mice. J Cell Biol 2000; 149 (4):793-8.
Leissring MA, Parker I, LaFerla FM. Presenilin-2 mutations modulate amplitude and kinetics of inositol 1, 4,5-trisphosphate-mediated calcium signals. J Biol Chem 1999a; 274 (46):32535-8.
Leissring MA, Paul BA, Parker I et al. Alzheimer's presenilin-1 mutation potentiates inositol 1,4,5- trisphosphate-mediated calcium signaling in Xenopus oocytes. J Neurochem 1999b; 72 (3):1061-8.
Lesne S, Koh MT, Kotilinek L et al. A specific amyloid-beta protein assembly in the brain impairs memory. Nature 2006; 440 (7082):352-7.
Lesuisse C, Martin LJ. Long-term culture of mouse cortical neurons as a model for neuronal development, aging, and death. J Neurobiol 2002; 51 (1):9-23.
Levy-Lahad E, Wasco W, Poorkaj P et al. Candidate gene for the chromosome 1 familial Alzheimer's disease locus. Science 1995; 269 (5226):973-7.

Lewis J, Dickson DW, Lin WL et al. Enhanced neurofibrillary degeneration in transgenic mice expressing mutant tau and APP. Science 2001; 293 (5534):1487-91.
Lilienfeld S, Parys W. Galantamine: additional benefits to patients with Alzheimer's disease. Dement Geriatr Cogn Disord 2000; 11 Suppl 1:19-27.
Lim GP, Yang F, Chu T et al. Ibuprofen suppresses plaque pathology and inflammation in a mouse model for Alzheimer's disease. J Neurosci 2000; 20 (15):5709-14.
Linn CL, Gafka AC. Modulation of a voltage-gated calcium channel linked to activation of glutamate receptors and calcium-induced calcium release in the catfish retina. J Physiol 2001; 535 (Pt 1):47-63.
Lipton SA. Pathologically-activated therapeutics for neuroprotection: mechanism of NMDA receptor block by memantine and S-nitrosylation. Curr Drug Targets 2007; 8 (5):621-32.
Liu Z, Zhang J, Li P et al. Three-dimensional reconstruction of the recombinant type 2 ryanodine receptor and localization of its divergent region 1. J Biol Chem 2002; 277 (48):46712-9.
Liu Z, Zhang J, Wang R et al. Location of divergent region 2 on the three-dimensional structure of cardiac muscle ryanodine receptor/calcium release channel. J Mol Biol 2004; 338 (3):533-45.
Lokuta AJ, Meyers MB, Sander PR et al. Modulation of cardiac ryanodine receptors by sorcin. J Biol Chem 1997; 272 (40):25333-8.
Lopez-Arrieta JM, Birks J. Nimodipine for primary degenerative, mixed and vascular dementia. Cochrane Database Syst Rev 2002; (3):CD000147.
Lopez AD, Mathers CD, Ezzati M et al. Global and regional burden of disease and risk factors, 2001: systematic analysis of population health data. Lancet 2006; 367 (9524):1747-57.
Loscher W, Honack D, Fassbender CP et al. The role of technical, biological and pharmacological factors in the laboratory evaluation of anticonvulsant drugs. III. Pentylenetetrazole seizure models. Epilepsy Res 1991; 8 (3):171-89.
Lovasic L, Bauschke H, Janus C. Working memory impairment in a transgenic amyloid precursor protein TgCRND8 mouse model of Alzheimer's disease. Genes Brain Behav 2005; 4 (3):197-208.
Lozsadi DA, Larner AJ. Prevalence and causes of seizures at the time of diagnosis of probable Alzheimer's disease. Dement Geriatr Cogn Disord 2006; 22 (2):121-4.
Lu T, Pan Y, Kao SY et al. Gene regulation and DNA damage in the ageing human brain. Nature 2004; 429 (6994):883-91.
Ma J. Block by ruthenium red of the ryanodine-activated calcium release channel of skeletal muscle. J Gen Physiol 1993; 102 (6):1031-56.
Ma J, Fill M, Knudson CM et al. Ryanodine receptor of skeletal muscle is a gap junction-type channel. Science 1988; 242 (4875):99-102.
Ma QL, Harris-White ME, Ubeda OJ et al. Evidence of Abeta- and transgene-dependent defects in ERK-CREB signaling in Alzheimer's models. J Neurochem 2007; 103 (4):1594-607.
MacLennan DH, Duff C, Zorzato F et al. Ryanodine receptor gene is a candidate for predisposition to malignant hyperthermia. Nature 1990; 343 (6258):559-61.
MacLennan DH, Phillips MS. Malignant hyperthermia. Science 1992; 256 (5058):789-94.
Mahley RW. Apolipoprotein E: cholesterol transport protein with expanding role in cell biology. Science 1988; 240 (4852):622-30.
Marambaud P, Shioi J, Serban G et al. A presenilin-1/gamma-secretase cleavage releases the E-cadherin intracellular domain and regulates disassembly of adherens junctions. Embo J 2002; 21 (8):1948-56.

Mark RJ, Hensley K, Butterfield DA et al. Amyloid beta-peptide impairs ion-motive ATPase activities: evidence for a role in loss of neuronal Ca2+ homeostasis and cell death. J Neurosci 1995; 15 (9):6239-49.
Marks AR, Priori S, Memmi M et al. Involvement of the cardiac ryanodine receptor/calcium release channel in catecholaminergic polymorphic ventricular tachycardia. J Cell Physiol 2002; 190 (1):1-6.
Marks AR, Tempst P, Hwang KS et al. Molecular cloning and characterization of the ryanodine receptor/junctional channel complex cDNA from skeletal muscle sarcoplasmic reticulum. Proc Natl Acad Sci U S A 1989; 86 (22):8683-7.
Marx SO, Reiken S, Hisamatsu Y et al. Phosphorylation-dependent regulation of ryanodine receptors: a novel role for leucine/isoleucine zippers. J Cell Biol 2001; 153 (4):699-708.
Marx SO, Reiken S, Hisamatsu Y et al. PKA phosphorylation dissociates FKBP12.6 from the calcium release channel (ryanodine receptor): defective regulation in failing hearts. Cell 2000; 101 (4):365-76.
Maryon EB, Coronado R, Anderson P. unc-68 encodes a ryanodine receptor involved in regulating C. elegans body-wall muscle contraction. J Cell Biol 1996; 134 (4):885-93.
Marziali G, Rossi D, Giannini G et al. cDNA cloning reveals a tissue specific expression of alternatively spliced transcripts of the ryanodine receptor type 3 (RyR3) calcium release channel. FEBS Lett 1996; 394 (1):76-82.
Masliah E, Sisk A, Mallory M et al. Comparison of neurodegenerative pathology in transgenic mice overexpressing V717F beta-amyloid precursor protein and Alzheimer's disease. J Neurosci 1996; 16 (18):5795-811.
Masters CL, Simms G, Weinman NA et al. Amyloid plaque core protein in Alzheimer disease and Down syndrome. Proc Natl Acad Sci U S A 1985; 82 (12):4245-9.
Mastrangelo MA, Bowers WJ. Detailed immunohistochemical characterization of temporal and spatial progression of Alzheimer's disease-related pathologies in male triple-transgenic mice. BMC Neurosci 2008; 9:81.
Mattei MG, Giannini G, Moscatelli F et al. Chromosomal localization of murine ryanodine receptor genes RYR1, RYR2, and RYR3 by in situ hybridization. Genomics 1994; 22 (1):202-4.
Mattson MP. Free radicals and disruption of neuronal ion homeostasis in AD: a role for amyloid beta-peptide? Neurobiol Aging 1995; 16 (4):679-82; discussion 83.
Mattson MP, Cheng B, Davis D et al. beta-Amyloid peptides destabilize calcium homeostasis and render human cortical neurons vulnerable to excitotoxicity. J Neurosci 1992; 12 (2):376-89.
Mattson MP, Gary DS, Chan SL et al. Perturbed endoplasmic reticulum function, synaptic apoptosis and the pathogenesis of Alzheimer's disease. Biochem Soc Symp 2001; 67:151-62.
Mattson MP, LaFerla FM, Chan SL et al. Calcium signaling in the ER: its role in neuronal plasticity and neurodegenerative disorders. Trends Neurosci 2000; 23 (5):222-9.
Mayne M, Moffatt T, Kong H et al. CYFIP2 is highly abundant in CD4+ cells from multiple sclerosis patients and is involved in T cell adhesion. Eur J Immunol 2004; 34 (4):1217-27.
Mbebi C, See V, Mercken L et al. Amyloid precursor protein family-induced neuronal death is mediated by impairment of the neuroprotective calcium/calmodulin protein kinase IV-dependent signaling pathway. J Biol Chem 2002; 277 (23):20979-90.
McCarthy TV, Healy JM, Heffron JJ et al. Localization of the malignant hyperthermia susceptibility locus to human chromosome 19q12-13.2. Nature 1990; 343 (6258):562-4.
McKhann G, Drachman D, Folstein M et al. Clinical diagnosis of Alzheimer's disease: report of the NINCDS-ADRDA Work Group under the auspices of Department of Health

and Human Services Task Force on Alzheimer's Disease. Neurology 1984; 34 (7):939-44.
McPherson PS, Campbell KP. Characterization of the major brain form of the ryanodine receptor/Ca2+ release channel. J Biol Chem 1993; 268 (26):19785-90.
Meissner G. Ryanodine activation and inhibition of the Ca2+ release channel of sarcoplasmic reticulum. J Biol Chem 1986; 261 (14):6300-6.
Meissner G. Ryanodine receptor/Ca2+ release channels and their regulation by endogenous effectors. Annu Rev Physiol 1994; 56:485-508.
Meissner G, el-Hashem A. Ryanodine as a functional probe of the skeletal muscle sarcoplasmic reticulum Ca2+ release channel. Mol Cell Biochem 1992; 114 (1-2):119-23.
Meissner G, Henderson JS. Rapid calcium release from cardiac sarcoplasmic reticulum vesicles is dependent on Ca2+ and is modulated by Mg2+, adenine nucleotide, and calmodulin. J Biol Chem 1987; 262 (7):3065-73.
Memory Pharmaceuticals.
The Merck manual of diagnosis and therapy. 18th ed. MH BEERS; M ROBERT S. PORTER; M THOMAS V. JONES, MPH et al., editors. Whitehouse Station, NJ: Merck Research Laboratories, Division of Merck & Co., Inc.; 2006. (MH BEERS; M ROBERT S. PORTER; M THOMAS V. JONES, MPH et al. editors).
Mirra SS, Heyman A, McKeel D et al. The Consortium to Establish a Registry for Alzheimer's Disease (CERAD). Part II. Standardization of the neuropathologic assessment of Alzheimer's disease. Neurology 1991; 41 (4):479-86.
Miyatake R, Furukawa A, Matsushita M et al. Tissue-specific alternative splicing of mouse brain type ryanodine receptor/calcium release channel mRNA. FEBS Lett 1996; 395 (2-3):123-6.
Mori F, Fukaya M, Abe H et al. Developmental changes in expression of the three ryanodine receptor mRNAs in the mouse brain. Neurosci Lett 2000; 285 (1):57-60.
Mori F, Okada M, Tomiyama M et al. Effects of ryanodine receptor activation on neurotransmitter release and neuronal cell death following kainic acid-induced status epilepticus. Epilepsy Res 2005; 65 (1-2):59-70.
Morrissette J, Heisermann G, Cleary J et al. Cyclic ADP-ribose induced Ca2+ release in rabbit skeletal muscle sarcoplasmic reticulum. FEBS Lett 1993; 330 (3):270-4.
Mosmann T. Rapid colorimetric assay for cellular growth and survival: application to proliferation and cytotoxicity assays. J Immunol Methods 1983; 65 (1-2):55-63.
Moyer JR, Jr., Thompson LT, Black JP et al. Nimodipine increases excitability of rabbit CA1 pyramidal neurons in an age- and concentration-dependent manner. J Neurophysiol 1992; 68 (6):2100-9.
Nabauer M, Callewaert G, Cleemann L et al. Regulation of calcium release is gated by calcium current, not gating charge, in cardiac myocytes. Science 1989; 244 (4906):800-3.
Nagy Z, Esiri MM, Jobst KA et al. Relative roles of plaques and tangles in the dementia of Alzheimer's disease: correlations using three sets of neuropathological criteria. Dementia 1995; 6 (1):21-31.
Nakai J, Imagawa T, Hakamat Y et al. Primary structure and functional expression from cDNA of the cardiac ryanodine receptor/calcium release channel. FEBS Lett 1990; 271 (1-2):169-77.
Nakajima M, Miura M, Aosaki T et al. Deficiency of presenilin-1 increases calcium-dependent vulnerability of neurons to oxidative stress in vitro. J Neurochem 2001; 78 (4):807-14.

Naldini L, Blomer U, Gage FH et al. Efficient transfer, integration, and sustained long-term expression of the transgene in adult rat brains injected with a lentiviral vector. Proc Natl Acad Sci U S A 1996; 93 (21):11382-8.
Nelson O, Tu H, Lei T et al. Familial Alzheimer disease-linked mutations specifically disrupt Ca2+ leak function of presenilin 1. J Clin Invest 2007; 117 (5):1230-9.
Nelson TJ, Zhao WQ, Yuan S et al. Calexcitin interaction with neuronal ryanodine receptors. Biochem J 1999; 341 (Pt 2):423-33.
Ni CY, Murphy MP, Golde TE et al. gamma -Secretase cleavage and nuclear localization of ErbB-4 receptor tyrosine kinase. Science 2001; 294 (5549):2179-81.
Nimmrich V, Grimm C, Draguhn A et al. Amyloid beta oligomers (A beta(1-42) globulomer) suppress spontaneous synaptic activity by inhibition of P/Q-type calcium currents. J Neurosci 2008; 28 (4):788-97.
Nishiyama M, Hong K, Mikoshiba K et al. Calcium stores regulate the polarity and input specificity of synaptic modification. Nature 2000; 408 (6812):584-8.
Northover BJ. Effects of pretreatment with caffeine or ryanodine on the myocardial response to simulated ischaemia. Br J Pharmacol 1991; 103 (1):1225-9.
O'Neill C, Cowburn RF, Bonkale WL et al. Dysfunctional intracellular calcium homoeostasis: a central cause of neurodegeneration in Alzheimer's disease. Biochem Soc Symp 2001; 67:177-94.
Oddo S, Caccamo A, Cheng D et al. Genetically augmenting tau levels does not modulate the onset or progression of Abeta pathology in transgenic mice. J Neurochem 2007; 102 (4):1053-63.
Oddo S, Caccamo A, Kitazawa M et al. Amyloid deposition precedes tangle formation in a triple transgenic model of Alzheimer's disease. Neurobiol Aging 2003a; 24 (8):1063-70.
Oddo S, Caccamo A, Shepherd JD et al. Triple-transgenic model of Alzheimer's disease with plaques and tangles: intracellular Abeta and synaptic dysfunction. Neuron 2003b; 39 (3):409-21.
Oddo S, Caccamo A, Tseng B et al. Blocking Abeta42 accumulation delays the onset and progression of tau pathology via the C terminus of heat shock protein70-interacting protein: a mechanistic link between Abeta and tau pathology. J Neurosci 2008; 28 (47):12163-75.
Oddo S, Vasilevko V, Caccamo A et al. Reduction of soluble Abeta and tau, but not soluble Abeta alone, ameliorates cognitive decline in transgenic mice with plaques and tangles. J Biol Chem 2006; 281 (51):39413-23.
Ogawa Y. Role of ryanodine receptors. Crit Rev Biochem Mol Biol 1994; 29 (4):229-74.
Ogawa Y, Kurebayashi N, Murayama T. Putative roles of type 3 ryanodine receptor isoforms (RyR3). Trends Cardiovasc Med 2000; 10 (2):65-70.
Ognibene E, Middei S, Daniele S et al. Aspects of spatial memory and behavioral disinhibition in Tg2576 transgenic mice as a model of Alzheimer's disease. Behav Brain Res 2005; 156 (2):225-32.
Okamoto T, Takeda S, Giambarella U et al. Intrinsic signaling function of APP as a novel target of three V642 mutations linked to familial Alzheimer's disease. Embo J 1996; 15 (15):3769-77.
Otsu K, Fujii J, Periasamy M et al. Chromosome mapping of five human cardiac and skeletal muscle sarcoplasmic reticulum protein genes. Genomics 1993; 17 (2):507-9.
Otsu K, Willard HF, Khanna VK et al. Molecular cloning of cDNA encoding the Ca2+ release channel (ryanodine receptor) of rabbit cardiac muscle sarcoplasmic reticulum. J Biol Chem 1990; 265 (23):13472-83.
Ottini L, Marziali G, Conti A et al. Alpha and beta isoforms of ryanodine receptor from chicken skeletal muscle are the homologues of mammalian RyR1 and RyR3. Biochem J 1996; 315 (Pt 1):207-16.

Ouardouz M, Nikolaeva MA, Coderre E et al. Depolarization-induced Ca2+ release in ischemic spinal cord white matter involves L-type Ca2+ channel activation of ryanodine receptors. Neuron 2003; 40 (1):53-63.
Oyamada H, Murayama T, Takagi T et al. Primary structure and distribution of ryanodine-binding protein isoforms of the bullfrog skeletal muscle. J Biol Chem 1994; 269 (25):17206-14.
Palop JJ, Chin J, Roberson ED et al. Aberrant excitatory neuronal activity and compensatory remodeling of inhibitory hippocampal circuits in mouse models of Alzheimer's disease. Neuron 2007; 55 (5):697-711.
Palop JJ, Mucke L. Epilepsy and Cognitive Impairments in Alzheimer Disease. Arch Neurol 2009a.
Palop JJ, Mucke L. Epilepsy and cognitive impairments in Alzheimer disease. Arch Neurol 2009b; 66 (4):435-40.
Papadopoulos NG, Dedoussis GV, Spanakos G et al. An improved fluorescence assay for the determination of lymphocyte-mediated cytotoxicity using flow cytometry. J Immunol Methods 1994; 177 (1-2):101-11.
Parness J, Palnitkar SS. Identification of dantrolene binding sites in porcine skeletal muscle sarcoplasmic reticulum. J Biol Chem 1995; 270 (31):18465-72.
Paschen W. Role of calcium in neuronal cell injury: which subcellular compartment is involved? Brain Res Bull 2000; 53 (4):409-13.
Patel JR, Coronado R, Moss RL. Cardiac sarcoplasmic reticulum phosphorylation increases Ca2+ release induced by flash photolysis of nitr-5. Circ Res 1995; 77 (5):943-9.
Patterson C, Gauthier S. Canadian consensus conference on dementia: two years later. Can J Neurol Sci 2001; 28 Suppl 1:S1-2.
Perez CF, Mukherjee S, Allen PD. Amino acids 1-1,680 of ryanodine receptor type 1 hold critical determinants of skeletal type for excitation-contraction coupling. Role of divergence domain D2. J Biol Chem 2003; 278 (41):39644-52.
Pessah IN, Stambuk RA, Casida JE. Ca2+-activated ryanodine binding: mechanisms of sensitivity and intensity modulation by Mg2+, caffeine, and adenine nucleotides. Mol Pharmacol 1987; 31 (3):232-8.
Pessah IN, Waterhouse AL, Casida JE. The calcium-ryanodine receptor complex of skeletal and cardiac muscle. Biochem Biophys Res Commun 1985; 128 (1):449-56.
Pessah IN, Zimanyi I. Characterization of multiple [3H]ryanodine binding sites on the Ca2+ release channel of sarcoplasmic reticulum from skeletal and cardiac muscle: evidence for a sequential mechanism in ryanodine action. Mol Pharmacol 1991; 39 (5):679-89.
Petersen RC, Smith GE, Waring SC et al. Mild cognitive impairment: clinical characterization and outcome. Arch Neurol 1999; 56 (3):303-8.
Phillips HJ, Terryberry JE. Counting actively metabolizing tissue cultured cells. Exp Cell Res 1957; 13 (2):341-7.
Pierrot N, Ghisdal P, Caumont AS et al. Intraneuronal amyloid-beta1-42 production triggered by sustained increase of cytosolic calcium concentration induces neuronal death. J Neurochem 2004; 88 (5):1140-50.
Pillon B, Deweer B, Agid Y et al. Explicit memory in Alzheimer's, Huntington's, and Parkinson's diseases. Arch Neurol 1993; 50 (4):374-9.
Plank B, Wyskovsky W, Hohenegger M et al. Inhibition of calcium release from skeletal muscle sarcoplasmic reticulum by calmodulin. Biochim Biophys Acta 1988; 938 (1):79-88.
Poirier J. Evidence that the clinical effects of cholinesterase inhibitors are related to potency and targeting of action. Int J Clin Pract Suppl 2002; (127):6-19.

Porsteinsson AP, Grossberg GT, Mintzer J et al. Memantine treatment in patients with mild to moderate Alzheimer's disease already receiving a cholinesterase inhibitor: a randomized, double-blind, placebo-controlled trial. Curr Alzheimer Res 2008; 5 (1):83-9.
Postma AV, Denjoy I, Kamblock J et al. Catecholaminergic polymorphic ventricular tachycardia: RYR2 mutations, bradycardia, and follow up of the patients. J Med Genet 2005; 42 (11):863-70.
Querfurth HW, Jiang J, Geiger JD et al. Caffeine stimulates amyloid beta-peptide release from beta-amyloid precursor protein-transfected HEK293 cells. J Neurochem 1997; 69 (4):1580-91.
Querfurth HW, Selkoe DJ. Calcium ionophore increases amyloid beta peptide production by cultured cells. Biochemistry 1994; 33 (15):4550-61.
Racine RJ. Modification of seizure activity by electrical stimulation. II. Motor seizure. Electroencephalogr Clin Neurophysiol 1972; 32 (3):281-94.
Rademakers R, Cruts M, Van Broeckhoven C. Genetics of early-onset Alzheimer dementia. ScientificWorldJournal 2003; 3:497-519.
Rascol O, Potier B, Lamour Y et al. Effects of calcium channel agonist and antagonists on calcium-dependent events in CA1 hippocampal neurons. Fundam Clin Pharmacol 1991; 5 (4):299-317.
Reisberg B, Ferris SH, de Leon MJ et al. The Global Deterioration Scale for assessment of primary degenerative dementia. Am J Psychiatry 1982; 139 (9):1136-9.
Reyes M, Stanton PK. Induction of hippocampal long-term depression requires release of Ca2+ from separate presynaptic and postsynaptic intracellular stores. J Neurosci 1996; 16 (19):5951-60.
Roberson ED, Scearce-Levie K, Palop JJ et al. Reducing endogenous tau ameliorates amyloid beta-induced deficits in an Alzheimer's disease mouse model. Science 2007; 316 (5825):750-4.
Rogaev EI, Sherrington R, Rogaeva EA et al. Familial Alzheimer's disease in kindreds with missense mutations in a gene on chromosome 1 related to the Alzheimer's disease type 3 gene. Nature 1995; 376 (6543):775-8.
Rogawski MA, Wenk GL. The neuropharmacological basis for the use of memantine in the treatment of Alzheimer's disease. CNS Drug Rev 2003; 9 (3):275-308.
Rohra DK, Saito SY, Ohizumi Y. Functional role of ryanodine-sensitive Ca2+ stores in acidic pH-induced contraction in Wistar Kyoto rat aorta. Life Sci 2003; 72 (11):1259-69.
Rossi D, Simeoni I, Micheli M et al. RyR1 and RyR3 isoforms provide distinct intracellular Ca2+ signals in HEK 293 cells. J Cell Sci 2002; 115 (Pt 12):2497-504.
Rueffert H, Olthoff D, Deutrich C et al. A new mutation in the skeletal ryanodine receptor gene (RYR1) is potentially causative of malignant hyperthermia, central core disease, and severe skeletal malformation. Am J Med Genet A 2004; 124A (3):248-54.
Sadowski M, Pankiewicz J, Scholtzova H et al. Amyloid-beta deposition is associated with decreased hippocampal glucose metabolism and spatial memory impairment in APP/PS1 mice. J Neuropathol Exp Neurol 2004; 63 (5):418-28.
Sah P, Faber ES. Channels underlying neuronal calcium-activated potassium currents. Prog Neurobiol 2002; 66 (5):345-53.
Salins P, He Y, Olson K et al. TGF-beta1 is increased in a transgenic mouse model of familial Alzheimer's disease and causes neuronal apoptosis. Neurosci Lett 2008; 430 (1):81-6.
Santacruz KS, Swagerty D. Early diagnosis of dementia. Am Fam Physician 2001; 63 (4):703-13, 17-8.
Saunders AM, Strittmatter WJ, Schmechel D et al. Association of apolipoprotein E allele epsilon 4 with late-onset familial and sporadic Alzheimer's disease. Neurology 1993; 43 (8):1467-72.

Savic N, Sciancalepore M. Intracellular calcium stores modulate miniature GABA-mediated synaptic currents in neonatal rat hippocampal neurons. Eur J Neurosci 1998; 10 (11):3379-86.
Scheuner D, Eckman C, Jensen M et al. Secreted amyloid beta-protein similar to that in the senile plaques of Alzheimer's disease is increased in vivo by the presenilin 1 and 2 and APP mutations linked to familial Alzheimer's disease. Nat Med 1996; 2 (8):864-70.
Schmidt CJ, Kehne JH. Neurotoxicity of MDMA: neurochemical effects. Ann N Y Acad Sci 1990; 600:665-80; discussion 80-1.
Schmitt FA, van Dyck CH, Wichems CH et al. Cognitive response to memantine in moderate to severe Alzheimer disease patients already receiving donepezil: an exploratory reanalysis. Alzheimer Dis Assoc Disord 2006; 20 (4):255-62.
Seiler S, Wegener AD, Whang DD et al. High molecular weight proteins in cardiac and skeletal muscle junctional sarcoplasmic reticulum vesicles bind calmodulin, are phosphorylated, and are degraded by Ca2+-activated protease. J Biol Chem 1984; 259 (13):8550-7.
Seilheimer B, Bohrmann B, Bondolfi L et al. The toxicity of the Alzheimer's beta-amyloid peptide correlates with a distinct fiber morphology. J Struct Biol 1997; 119 (1):59-71.
Selkoe DJ. Presenilin, Notch, and the genesis and treatment of Alzheimer's disease. Proc Natl Acad Sci U S A 2001; 98 (20):11039-41.
Serrano F, Klann E. Reactive oxygen species and synaptic plasticity in the aging hippocampus. Ageing Res Rev 2004; 3 (4):431-43.
Shah M, Haylett DG. Ca(2+) channels involved in the generation of the slow afterhyperpolarization in cultured rat hippocampal pyramidal neurons. J Neurophysiol 2000; 83 (5):2554-61.
Shamoo AE, Thompson TR, Campbell KP et al. Mechanism of action of "ruthenium red" compounds on Ca2+ ionophore from sarcoplasmic reticulum (Ca2+ + Mg2+)- adenosine triphosphatase and lipid bilayer. J Biol Chem 1975; 250 (20):8289-91.
Shankar GM, Li S, Mehta TH et al. Amyloid-beta protein dimers isolated directly from Alzheimer's brains impair synaptic plasticity and memory. Nat Med 2008; 14 (8):837-42.
Sherrington R, Rogaev EI, Liang Y et al. Cloning of a gene bearing missense mutations in early-onset familial Alzheimer's disease [see comments]. Nature 1995; 375 (6534):754-60.
Shimuta M, Yoshikawa M, Fukaya M et al. Postsynaptic modulation of AMPA receptor-mediated synaptic responses and LTP by the type 3 ryanodine receptor. Mol Cell Neurosci 2001; 17 (5):921-30.
Shinozaki Y, Sato Y, Koizumi S et al. Retinoic acids acting through retinoid receptors protect hippocampal neurons from oxygen-glucose deprivation-mediated cell death by inhibition of c-jun-N-terminal kinase and p38 mitogen-activated protein kinase. Neuroscience 2007; 147 (1):153-63.
Shmigol A, Kirischuk S, Kostyuk P et al. Different properties of caffeine-sensitive Ca2+ stores in peripheral and central mammalian neurones. Pflugers Arch 1994; 426 (1-2):174-6.
Shuaib A, Paasuke RT, Brownell KW. Central core disease. Clinical features in 13 patients. Medicine (Baltimore) 1987; 66 (5):389-96.
Silverman DH, Small GW, Chang CY et al. Positron emission tomography in evaluation of dementia: Regional brain metabolism and long-term outcome. Jama 2001; 286 (17):2120-7.
Simkus CR, Stricker C. The contribution of intracellular calcium stores to mEPSCs recorded in layer II neurones of rat barrel cortex. J Physiol 2002; 545 (Pt 2):521-35.
Smith IF, Hitt B, Green KN et al. Enhanced caffeine-induced Ca2+ release in the 3xTg-AD mouse model of Alzheimer's disease. J Neurochem 2005; 94 (6):1711-8.

Smith JS, Imagawa T, Ma J et al. Purified ryanodine receptor from rabbit skeletal muscle is the calcium-release channel of sarcoplasmic reticulum. J Gen Physiol 1988; 92 (1):1-26.
Smith MA, Hirai K, Hsiao K et al. Amyloid-beta deposition in Alzheimer transgenic mice is associated with oxidative stress. J Neurochem 1998; 70 (5):2212-5.
Smith WW, Gorospe M, Kusiak JW. Signaling mechanisms underlying Abeta toxicity: potential therapeutic targets for Alzheimer's disease. CNS Neurol Disord Drug Targets 2006; 5 (3):355-61.
Soriano FX, Papadia S, Hofmann F et al. Preconditioning doses of NMDA promote neuroprotection by enhancing neuronal excitability. J Neurosci 2006; 26 (17):4509-18.
Sorrentino V, Giannini G, Malzac P et al. Localization of a novel ryanodine receptor gene (RYR3) to human chromosome 15q14-q15 by in situ hybridization. Genomics 1993a; 18 (1):163-5.
Sorrentino V, Rizzuto R. Molecular genetics of Ca(2+) stores and intracellular Ca(2+) signalling. Trends Pharmacol Sci 2001; 22 (9):459-64.
Sorrentino V, Volpe P. Ryanodine receptors: how many, where and why? Trends Pharmacol Sci 1993b; 14 (3):98-103.
Spires TL, Meyer-Luehmann M, Stern EA et al. Dendritic spine abnormalities in amyloid precursor protein transgenic mice demonstrated by gene transfer and intravital multiphoton microscopy. J Neurosci 2005; 25 (31):7278-87.
Statistics Canada.
Steiner H. The catalytic core of gamma-secretase: presenilin revisited. Curr Alzheimer Res 2008; 5 (2):147-57.
Stutzmann GE. Calcium dysregulation, IP3 signaling, and Alzheimer's disease. Neuroscientist 2005; 11 (2):110-5.
Stutzmann GE, Caccamo A, LaFerla FM et al. Dysregulated IP3 signaling in cortical neurons of knock-in mice expressing an Alzheimer's-linked mutation in presenilin1 results in exaggerated Ca2+ signals and altered membrane excitability. J Neurosci 2004; 24 (2):508-13.
Stutzmann GE, Smith I, Caccamo A et al. Enhanced ryanodine receptor recruitment contributes to Ca2+ disruptions in young, adult, and aged Alzheimer's disease mice. J Neurosci 2006; 26 (19):5180-9.
Stutzmann GE, Smith I, Caccamo A et al. Enhanced ryanodine-mediated calcium release in mutant PS1-expressing Alzheimer's mouse models. Ann N Y Acad Sci 2007; 1097:265-77.
Suko J, Maurer-Fogy I, Plank B et al. Phosphorylation of serine 2843 in ryanodine receptor-calcium release channel of skeletal muscle by cAMP-, cGMP- and CaM-dependent protein kinase. Biochim Biophys Acta 1993; 1175 (2):193-206.
Supnet C, Grant J, Kong H et al. Amyloid-beta-(1-42) increases ryanodine receptor-3 expression and function in neurons of TgCRND8 mice. J Biol Chem 2006; 281 (50):38440-7.
Sutko JL, Airey JA. Ryanodine receptor Ca2+ release channels: does diversity in form equal diversity in function? Physiol Rev 1996; 76 (4):1027-71.
Takasawa S, Akiyama T, Nata K et al. Cyclic ADP-ribose and inositol 1,4,5-trisphosphate as alternate second messengers for intracellular Ca2+ mobilization in normal and diabetic beta-cells. J Biol Chem 1998; 273 (5):2497-500.
Takeshima H, Iino M, Takekura H et al. Excitation-contraction uncoupling and muscular degeneration in mice lacking functional skeletal muscle ryanodine-receptor gene. Nature 1994a; 369 (6481):556-9.
Takeshima H, Ikemoto T, Nishi M et al. Generation and characterization of mutant mice lacking ryanodine receptor type 3. J Biol Chem 1996; 271 (33):19649-52.

Takeshima H, Komazaki S, Hirose K et al. Embryonic lethality and abnormal cardiac myocytes in mice lacking ryanodine receptor type 2. Embo J 1998; 17 (12):3309-16.
Takeshima H, Komazaki S, Nishi M et al. Junctophilins: a novel family of junctional membrane complex proteins. Mol Cell 2000; 6 (1):11-22.
Takeshima H, Nishi M, Iwabe N et al. Isolation and characterization of a gene for a ryanodine receptor/calcium release channel in Drosophila melanogaster. FEBS Lett 1994b; 337 (1):81-7.
Takeshima H, Nishimura S, Matsumoto T et al. Primary structure and expression from complementary DNA of skeletal muscle ryanodine receptor. Nature 1989; 339 (6224):439-45.
Takeshima H, Yamazawa T, Ikemoto T et al. Ca(2+)-induced Ca2+ release in myocytes from dyspedic mice lacking the type-1 ryanodine receptor. Embo J 1995; 14 (13):2999-3006.
Tanabe M, Gahwiler BH, Gerber U. L-Type Ca2+ channels mediate the slow Ca2+-dependent afterhyperpolarization current in rat CA3 pyramidal cells in vitro. J Neurophysiol 1998; 80 (5):2268-73.
Taratuto AL. Congenital myopathies and related disorders. Curr Opin Neurol 2002; 15 (5):553-61.
Tariot PN, Farlow MR, Grossberg GT et al. Memantine treatment in patients with moderate to severe Alzheimer disease already receiving donepezil: a randomized controlled trial. Jama 2004; 291 (3):317-24.
Tekirian TL, Saido TC, Markesbery WR et al. N-terminal heterogeneity of parenchymal and cerebrovascular Abeta deposits. J Neuropathol Exp Neurol 1998; 57 (1):76-94.
Terentyev D, Viatchenko-Karpinski S, Valdivia HH et al. Luminal Ca2+ controls termination and refractory behavior of Ca2+-induced Ca2+ release in cardiac myocytes. Circ Res 2002; 91 (5):414-20.
Tesseur I, Zou K, Esposito L et al. Deficiency in neuronal TGF-beta signaling promotes neurodegeneration and Alzheimer's pathology. J Clin Invest 2006; 116 (11):3060-9.
Thibault O, Hadley R, Landfield PW. Elevated postsynaptic [Ca2+]i and L-type calcium channel activity in aged hippocampal neurons: relationship to impaired synaptic plasticity. J Neurosci 2001; 21 (24):9744-56.
Thibault O, Landfield PW. Increase in single L-type calcium channels in hippocampal neurons during aging. Science 1996; 272 (5264):1017-20.
Tollefson GD. Short-term effects of the calcium channel blocker nimodipine (Bay-e-9736) in the management of primary degenerative dementia. Biol Psychiatry 1990; 27 (10):1133-42.
Tu H, Nelson O, Bezprozvanny A et al. Presenilins form ER Ca2+ leak channels, a function disrupted by familial Alzheimer's disease-linked mutations. Cell 2006; 126 (5):981-93.
Ueberham U, Ueberham E, Bruckner MK et al. Inducible neuronal expression of transgenic TGF-beta1 in vivo: dissection of short-term and long-term effects. Eur J Neurosci 2005; 22 (1):50-64.
Unni VK, Zakharenko SS, Zablow L et al. Calcium release from presynaptic ryanodine-sensitive stores is required for long-term depression at hippocampal CA3-CA3 pyramidal neuron synapses. J Neurosci 2004; 24 (43):9612-22.
Unsicker K, Krieglstein K. TGF-betas and their roles in the regulation of neuron survival. Adv Exp Med Biol 2002; 513:353-74.
Van Broeckhoven C, Backhovens H, Cruts M et al. APOE genotype does not modulate age of onset in families with chromosome 14 encoded Alzheimer's disease. Neurosci Lett 1994; 169 (1-2):179-80.

van de Vrede Y, Fossier P, Baux G et al. Control of IsAHP in mouse hippocampus CA1 pyramidal neurons by RyR3-mediated calcium-induced calcium release. Pflugers Arch 2007; 455 (2):297-308.
van Duijn CM, de Knijff P, Cruts M et al. Apolipoprotein E4 allele in a population-based study of early-onset Alzheimer's disease. Nat Genet 1994; 7 (1):74-8.
Vanterpool CK, Vanterpool EA, Pearce WJ et al. Advancing age alters the expression of the ryanodine receptor 3 isoform in adult rat superior cervical ganglia. J Appl Physiol 2006; 101 (2):392-400.
Vassar R, Bennett BD, Babu-Khan S et al. Beta-secretase cleavage of Alzheimer's amyloid precursor protein by the transmembrane aspartic protease BACE. Science 1999; 286 (5440):735-41.
Vazquez-Martinez O, Canedo-Merino R, Diaz-Munoz M et al. Biochemical characterization, distribution and phylogenetic analysis of Drosophila melanogaster ryanodine and IP3 receptors, and thapsigargin-sensitive Ca2+ ATPase. J Cell Sci 2003; 116 (Pt 12):2483-94.
Verkhratsky A. The endoplasmic reticulem and neuronal calcium signaling. Cell Calcium 2002; 32:393-404.
Verkhratsky AJ, Petersen OH. Neuronal calcium stores. Cell Calcium 1998; 24 (5-6):333-43.
Walker LC, Ibegbu CC, Todd CW et al. Emerging prospects for the disease-modifying treatment of Alzheimer's disease. Biochem Pharmacol 2005; 69 (7):1001-8.
Walsh DM, Hartley DM, Kusumoto Y et al. Amyloid beta-protein fibrillogenesis. Structure and biological activity of protofibrillar intermediates. J Biol Chem 1999; 274 (36):25945-52.
Walsh DM, Klyubin I, Fadeeva JV et al. Naturally secreted oligomers of amyloid beta protein potently inhibit hippocampal long-term potentiation in vivo. Nature 2002; 416 (6880):535-9.
Wang J, Best PM. Inactivation of the sarcoplasmic reticulum calcium channel by protein kinase. Nature 1992; 359 (6397):739-41.
Wang SY, Winka L, Langer GA. Role of calcium current and sarcoplasmic reticulum calcium release in control of myocardial contraction in rat and rabbit myocytes. J Mol Cell Cardiol 1993; 25 (11):1339-47.
Wang X, Seed B. A PCR primer bank for quantitative gene expression analysis. Nucleic Acids Res 2003; 31 (24):e154.
Wang YX, Zheng YM, Mei QB et al. FKBP12.6 and cADPR regulation of Ca2+ release in smooth muscle cells. Am J Physiol Cell Physiol 2004; 286 (3):C538-46.
Watkins PB, Zimmerman HJ, Knapp MJ et al. Hepatotoxic effects of tacrine administration in patients with Alzheimer's disease. Jama 1994; 271 (13):992-8.
Webb C, Williams V. Ecstasy intoxication: appreciation of complications and the role of dantrolene. Anaesthesia 1993; 48 (6):542-3.
Wehrens XH, Lehnart SE, Huang F et al. FKBP12.6 deficiency and defective calcium release channel (ryanodine receptor) function linked to exercise-induced sudden cardiac death. Cell 2003; 113 (7):829-40.
West AE, Chen WG, Dalva MB et al. Calcium regulation of neuronal gene expression. Proc Natl Acad Sci U S A 2001; 98 (20):11024-31.
Westerman MA, Cooper-Blacketer D, Mariash A et al. The relationship between Abeta and memory in the Tg2576 mouse model of Alzheimer's disease. J Neurosci 2002; 22 (5):1858-67.
Williams DR, Lees AJ. Progressive supranuclear palsy: clinicopathological concepts and diagnostic challenges. Lancet Neurol 2009; 8 (3):270-9.

Williams M. Progress in Alzheimer's disease drug discovery: an update. Curr Opin Investig Drugs 2009; 10 (1):23-34.
Wisniewski T, Ghiso J, Frangione B. Peptides homologous to the amyloid protein of Alzheimer's disease containing a glutamine for glutamic acid substitution have accelerated amyloid fibril formation. Biochem Biophys Res Commun 1991; 179 (3):1247-54.
Wolfe MS, Xia W, Ostaszewski BL et al. Two transmembrane aspartates in presenilin-1 required for presenilin endoproteolysis and gamma-secretase activity. Nature 1999; 398 (6727):513-7.
Woodhouse A, Vickers JC, Adlard PA et al. Dystrophic neurites in TgCRND8 and Tg2576 mice mimic human pathological brain aging. Neurobiol Aging 2007.
Wyss-Coray T, Lin C, Yan F et al. TGF-beta1 promotes microglial amyloid-beta clearance and reduces plaque burden in transgenic mice. Nat Med 2001; 7 (5):612-8.
Wyss-Coray T, Masliah E, Mallory M et al. Amyloidogenic role of cytokine TGF-beta1 in transgenic mice and in Alzheimer's disease. Nature 1997; 389 (6651):603-6.
Xu L, Eu JP, Meissner G et al. Activation of the cardiac calcium release channel (ryanodine receptor) by poly-S-nitrosylation. Science 1998; 279 (5348):234-7.
Yamaguchi N, Xu L, Pasek DA et al. Calmodulin regulation and identification of calmodulin binding region of type-3 ryanodine receptor calcium release channel. Biochemistry 2005; 44 (45):15074-81.
Yang HC, Reedy MM, Burke CL et al. Calmodulin interaction with the skeletal muscle sarcoplasmic reticulum calcium channel protein. Biochemistry 1994; 33 (2):518-25.
Yang T, Riehl J, Esteve E et al. Pharmacologic and functional characterization of malignant hyperthermia in the R163C RyR1 knock-in mouse. Anesthesiology 2006; 105 (6):1164-75.
Ye C, Walsh DM, Selkoe DJ et al. Amyloid beta-protein induced electrophysiological changes are dependent on aggregation state: N-methyl-D-aspartate (NMDA) versus non-NMDA receptor/channel activation. Neurosci Lett 2004; 366 (3):320-5.
Ye H, Jalini S, Mylvaganam S et al. Activation of large-conductance Ca(2+)-activated K(+) channels depresses basal synaptic transmission in the hippocampal CA1 area in APP (swe/ind) TgCRND8 mice. Neurobiol Aging 2008.
Yoo AS, Cheng I, Chung S et al. Presenilin-mediated modulation of capacitative calcium entry. Neuron 2000; 27 (3):561-72.
Zarka A, Shoshan-Barmatz V. Characterization and photoaffinity labeling of the ATP binding site of the ryanodine receptor from skeletal muscle. Eur J Biochem 1993; 213 (1):147-54.
Zhang G, Teggatz EG, Zhang AY et al. Cyclic ADP ribose-mediated Ca2+ signaling in mediating endothelial nitric oxide production in bovine coronary arteries. Am J Physiol Heart Circ Physiol 2006; 290 (3):H1172-81.
Zhang J, Liu Z, Masumiya H et al. Three-dimensional localization of divergent region 3 of the ryanodine receptor to the clamp-shaped structures adjacent to the FKBP binding sites. J Biol Chem 2003; 278 (16):14211-8.
Zhang Y, Chen HS, Khanna VK et al. A mutation in the human ryanodine receptor gene associated with central core disease. Nat Genet 1993; 5 (1):46-50.
Zhao F, Li P, Chen SR et al. Dantrolene inhibition of ryanodine receptor Ca2+ release channels. Molecular mechanism and isoform selectivity. J Biol Chem 2001; 276 (17):13810-6.
Zhao W, Meiri N, Xu H et al. Spatial learning induced changes in expression of the ryanodine type II receptor in the rat hippocampus. Faseb J 2000; 14 (2):290-300.

Zhao WQ, Ravindranath L, Mohamed AS et al. MAP kinase signaling cascade dysfunction specific to Alzheimer's disease in fibroblasts. Neurobiol Dis 2002; 11 (1):166-83.
Zheng H, Jiang M, Trumbauer ME et al. Mice deficient for the amyloid precursor protein gene. Ann N Y Acad Sci 1996; 777:421-6.
Zhu Y, Nosek TM. Ruthenium red affects the contractile apparatus but not sarcoplasmic reticulum Ca2+ release of skinned papillary muscle. Pflugers Arch 1992; 420 (3-4):255-8.
Zimanyi I, Buck E, Abramson JJ et al. Ryanodine induces persistent inactivation of the Ca2+ release channel from skeletal muscle sarcoplasmic reticulum. Mol Pharmacol 1992; 42 (6):1049-57.
Zimanyi I, Pessah IN. Comparison of [3H]ryanodine receptors and Ca++ release from rat cardiac and rabbit skeletal muscle sarcoplasmic reticulum. J Pharmacol Exp Ther 1991a; 256 (3):938-46.
Zimanyi I, Pessah IN. Pharmacological characterization of the specific binding of [3H]ryanodine to rat brain microsomal membranes. Brain Res 1991b; 561 (2):181-91.
Zorzato F, Fujii J, Otsu K et al. Molecular cloning of cDNA encoding human and rabbit forms of the Ca2+ release channel (ryanodine receptor) of skeletal muscle sarcoplasmic reticulum. J Biol Chem 1990; 265 (4):2244-56.
Zucchi R, Ronca-Testoni S. The sarcoplasmic reticulum Ca2+ channel/ryanodine receptor: modulation by endogenous effectors, drugs and disease states. Pharmacol Rev 1997; 49 (1):1-51.

APPENDIX A. Buffer and reagent components

All chemicals from Fisher Scientific unless otherwise indicated

Glu

1 M L-glutamic acid in d_2H_2O
pH 7.3 with NaOH
sterilize using 0.22 μm filter

HEPES-Triton buffer

20 mM HEPES (Sigma), pH 7.4
300 mM sucrose (Sigma)
50 mM NaCl
3 mM $MgCl_2$,
0.5% Triton X-100

Locke's buffer

154 mM NaCl
3.6 mM $NaHCO_3$
5.6 mM KCl
1 mM MgCl2
5 mM glucose
2.3 mM $CaCl_2$
pH 7.2

Neurobasal with 10% fetal bovine serum

Neurobasal medium (Invitrogen)
5 mM HEPES
1 mM L-glutamine
25 μg/mL gentamycin reagent solution (Invitrogen)
10 mL B27 supplement (Invitrogen)
10% fetal bovine serum (Hyclone)

Non-denaturing lysis buffer

25 mM Tris.HCl, pH 7.4
50 mM HEPES, pH 7.4
137 mM NaCl
1% CHAPS
2.5 mM dithiothreitol

TBS (10X)

1 M Tris.HCl, pH 7.4
5 M NaCl
Dilute to 1X before use

APPENDIX B. Detailed methodologies

All chemicals from Fisher Scientific unless otherwise indicated

1. Primary cortical neuron preparation

Materials:

ice
1 large & 2 superfine forceps (Fine Science Instruments, North Vancouver, BC)
scissors (Fine Science Instruments)
1.7 mL tubes (VWR)
12-well plates (VWR)
petri dishes (VWR)
pipettes (VWR)
15 mL Falcon tubes (VWR)
beaker with 70% ethanol
beaker with ddH_2O
dissecting microscope (Zeiss)
Trypsin, 0.25% in HBSS (Hyclone), warm
HBSS (Hyclone) with 5 mM HEPES and 25 mg/mL gentamycin reagent solution (Invitrogen)
fetal bovine serum (Hyclone)
1000 μL pipette tips, with ends cut off
Neurobasal (Invitrogen) with 10% fetal bovine serum
Trypan blue dye (Invitrogen)
hemocytometer (VWR)

Method:

1. Place 0.25% trypsin and HBSS 37°C water bath. Place Neurobasal with 10% fetal bovine serum at RT.
2. Number 1.7 mL tubes and the wells of two 12-well plates if expecting Tg fetuses. Cortical tissue must be kept separate until genotyped.
3. Pour placenta and media into Petri dish, keeping everything on ice. Open the embryonic sacs & remove fetuses using large forceps & scissors. Remove a limb for genotyping and place in labelled 1.7 mL tube. Remove the head & place in labelled well of 12-well plate.
4. Place superfine forceps in the eyes to anchor the head. Use the scissors at the back and cut through the skull along the midsagittal plane to the nose. Use the blunt edges of the scissors to tease out the brain, which is whiter in color than the skull.
5. Put a Petri dish with HBSS under the dissecting microscope. Transfer brain to dish. Under the microscope remove meninges and olfactory bulbs.
6. Separate the hemispheres from each other. Unfold the flap that is the cortex from the rest of the brain and use forceps to cut out tissue. Place the cortices from one brain into a well in a new 12-well plate containing HBSS (appropriately numbered).
7. Once genotyping is complete (or if dissecting a non-transgenic), place the dissected cortices in a 15 mL tube, 3 brains per tube. Allow tissue to settle and aspirate off the HBSS.
8. Add 1 mL of warm trypsin to each tube. Shake tube to mix and incubate at 37°C for 10-15 min.

9. Add 200 μL of fetal bovine serum to inhibit the trypsin. Shake the tube to mix and leave at room temperature for a few minutes. Aspirate off media.
10. In the hood, use 1000 μL pipette tip to triturate, use ~15 strokes gently, should have very little tissue. If so, try 5 more.
11. Wait 5 min for larger pieces of tissue to settle, aspirate supernatant into a new tube with 2-3 mL of Neurobasal with fetal bovine serum. Cortices from like genotypes can be combined into a single tube.
12. Count cells stained with trypan blue using a hemocytometer.
13. Day 0 - Plate cortical cells in Neurobasal with fetal bovine serum
14. Day 1 - change media to Neurobasal without fetal bovine serum

Note: If keeping cells long-term (> 5 days in culture), change media every 3 days. Take half of the conditioned media, filter using 0.22 μm pore size, add the same amount of new media and replace.

2. poly-D-Lysine coating procedure

Materials:

poly-D-Lysine, 5 mg bottle (Sigma)
d_2H_20

Method:

1. Add 30 mL of d_2H_2O to 1 bottle of poly-D-Lysine. Swirl 5-10 times.
2. Pour contents into a 100 mL bottle.
3. Repeat steps 1&2. The final concentration is 83 μg/mL. Store at 4°C.
4. poly-D-Lysine can be used twice and then discarded.
5. Add 2 mL of poly-D-Lysine solution to each well of a 6-well plate. For 96-well plate, use 70 μL/well. Coverslips can be added to wells for coating. Incubate overnight at room temperature or at 4°C.
6. Remove poly-D-Lysine, save or discard.
7. Wash each well twice with d_2H_2O.
8. Place plates in the hood to dry and UV for 15 min to sterilize. Plates can be used immediately or stored at 4°C for up to 4 weeks.

3. Brain Microsome Preparation

Materials:

Homogenization buffer
- 10 mM HEPES, pH 7.4
- 350 mM sucrose
- 5 mM EDTA
- protease inhibitor tablet (Roche Diagnostics, 1 per 10mL of buffer)

Dounce glass-glass homogenizer (Kontes Glass Company, Vineland, NJ)
1% CHAPS lysis buffer
- 1% CHAPS
- 25 mM Tris.HCl, pH 7.4
- 50 mM HEPES
- 137 mM NaCl
- 2.5 mM dithiothreitol

protease inhibitor tablet (Roche Diagnostics, 1 per 10mL of buffer)
1.24 M sucrose
5 M NaCl
ice
bench-top centrifuge
high speed, refrigerated centrifuges
BioRad *Dc* Protein Assay

Note: all buffers and instruments are iced before use and all steps are performed on ice.

Method:

1. Harvest brain tissue and dissect out cortices, hippocampi, and basal regions. Combine 6 brains.
2. Add 9X the volume of the tissue of homogenization buffer. Use 4 strokes of the loose fitting pestle (A) and 6 strokes of the tight fitting pestle (B).
3. Centrifuge homogenate at 2000 *g* for 10 min at 4°C.
4. Centrifuge the supernatant at 100000 *g* for 1 h at 4°C.
5. Resuspend the pellet in 100 μL 1%CHAPS lysis buffer. Ice for 1h.
6. Remove insoluble materials by centrifugation in the microcentrifuge for at 3000 rpm for 15 min at 4°C. Collect the supernatant.
7. Add 1.24 M sucrose to obtain a final concentration of 300 mM. Add 5 M NaCl to obtain a final concentration of 400 mM.
8. Perform protein quantification of preparations using the BioRad *Dc* Protein Assay as per manufacturer's instructions. Load 20-50 μg of protein per well on a NuPAGE for RyR detection.

4. Muscle microsome preparation

Materials:

Homogenization buffer
- 20 mM Tris.HCl, pH 7.4
- 1 mM EDTA
- Protease Inhibitor tablet (Roche Diagnostics, 1per 10 mL of buffer)

Resuspension buffer
- 20 mM Tris.HCl, pH 7.4
- 1 mM EDTA
- 600 mM KCl
- protease inhibitor tablet (Roche Diagnostics, 1per 10 mL of buffer)

PBS (Sigma)
liquid N_2 or dry ice
mortar and pestle
Teflon-glass motor-driven homogenizer
1% CHAPS lysis buffer
- 1% CHAPS
- 25 mM Tris.HCl, pH 7.4
- 50 mM HEPES
- 137 mM NaCl
- 2.5 mM dithiothreitol
- Protease Inhibitor tablet (Roche Diagnostics, 1 per 10mL of buffer)

1.24 M sucrose
5 M NaCl

ice
bench-top centrifuge
high speed, refrigerated centrifuges
BioRad *Dc* Protein Assay

Note: all buffers and instruments are iced before use and all steps are performed on ice.

Method:

1. Harvest heart or skeletal muscle. Rinse with ice-cold PBS. Freeze immediately with liquid N_2 or dry ice.
2. Add liquid N_2 to tissue and powder frozen tissue with mortar and pestle. Suspend the powder in 1 mL of homogenization buffer.
3. Bring volume to 10 mL with homogenization buffer and homogenize using Teflon-glass homogenizer using 4X10 strokes at 500 rpm.
4. Centrifuge at 1000 *g* for 10 min at 4°C to pellet nuclei and debris. Save supernatant.
5. Homogenize the pellet and repeat step 4. Combine the supernatants.
6. Centrifuge supernatants at 40000 *g* for 10 min at 4°C. Discard supernatant. Resuspend the pellet in resuspension buffer, ice for 10 min.
7. Centrifuge resuspension at 40000g for 10min @ 4°C. Resuspend the pellet in homogenization buffer.
8. Repeat step 7 twice to remove KCl.
9. Resuspend the pellet in 100 µL of 1% CHAPS lysis buffer. Ice for 1 h.
10. Remove insoluble materials by centrifugation in the microcentrifuge for at 3000 rpm for 15 min at 4°C. Collect the supernatant.
11. Add 1.24 M sucrose to obtain a final concentration of 300 mM. Add 5 M NaCl to obtain a final concentration of 400 mM.
12. Perform protein quantification of preparations using the BioRad *Dc* Protein Assay as per manufacturer's instructions. Load 20-50 µg of protein per well on a NuPAGE for RyR detection.

APPENDIX C. Determining Aβ treatment parameters

OBJECTIVE

To determine the concentration and incubation time for the induction of RyR gene expression in primary cortical neurons by Aβ42 treatment.

METHOD

See Chapter 2, page 49-51 for details.

RESULTS

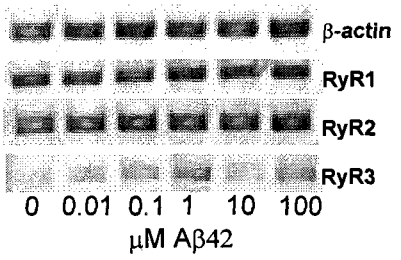

Figure 1. Induction of RyR3 mRNA by Aβ42 treatment. Primary cortical neurons from C57BL/6 were treated with varying concentrations of Aβ42 peptide for 18 h on 6 DIV. Cell were collected and RT-PCR was performed for the RyR mRNA levels. PCR products run on 1.2% agarose gel and visualized with ethidium bromide stain. Gel is representative of n=2.

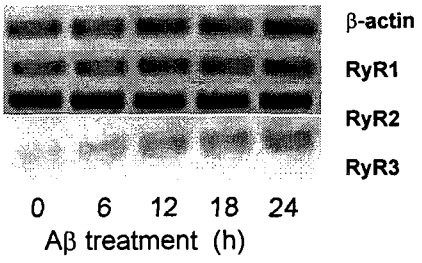

Figure 2. Induction of RyR3 mRNA by 1 μM Aβ42 treatment over time. Primary cortical neurons fom C57BL/6 mice were treated with 1μM Aβ42 peptide for varying

times on 6 DIV. Cell were collected and RT-PCR was performed for the RyR mRNA levels. PCR products run on 1.2% agarose gel and visualized with ethidium bromide stain. Gel is representative of n=2.

CONCLUSION

A concentration of 1 μM Aβ42 is sufficient to up-regulate RyR3 mRNA expression in primary cortical neurons after 18 h of incubation. While RyR3 appears to be significantly up-regulated at 12 h, an incubation time of 18 h will be used for subsequent experiments as induction of RyR3 mRNA does not appear to be significantly different than 12 h and the 18 h time point is more practical.